The effect of scale on the relative importance of climatic and biotic variables influencing methane fluxes from an Arctic wet sedge meadow

by

Emma Riley

A thesis submitted to the Faculty of Graduate and Postdoctoral Affairs in partial fulfillment of the requirements for the degree of

Master of Science

in

Geography

Carleton University
Ottawa, Ontario

Abstract

Methane fluxes (F_{CH4}) from an Arctic wet sedge meadow at Daring Lake, NT, Canada were examined during the growing seasons of 2008-2017 over several temporal and spatial scales. The largest methane emissions (seasonal averages of 118 - 277 mg CH_4 m^{-2} d^{-1}) were recorded at the plot scale mid-summer using manual chamber methods and were associated with wetter locations with more sedges. Plot-scale F_{CH4} were negligible where shrubby peat soils were raised above the water table. Ecosystem-scale F_{CH4} measured on a quasi-continuous basis employing an eddy covariance technique were roughly 50% of plot-scale F_{CH4}. Moisture, temperature and vegetation-related variables explained up to 80% of temporal F_{CH4} variability ($p<0.001$). Both magnitudes of F_{CH4} and relationships with driving variables were not consistent between scales and measurement techniques, demonstrating both the importance of scale in deducing all processes influencing F_{CH4} variability and the difficulties in upscaling F_{CH4} at this heterogeneous wetland.

Acknowledgements

I would like to thank the many people who supported and guided me throughout my thesis, without whom it surely would not have been possible. I would like to thank my supervisor, Elyn Humphreys, as her knowledge, enthusiasm and strength were both inspiring and contagious throughout the process. I acknowledge her patience and generosity towards all her students, including myself. I was truly blessed to have such a great role model during these last two years of growth and development. I would also like to thank my friends, family and especially my partner, Shane, for relentless encouragement and support.

During the field season I had many different field/research assistants and everyone was eager to lend a hand. Thanks to Caitlyn Proctor, Janelle Nitsizo, Shannon Petrie, Liam Case, Zhalanni Drygeese, Jody Zoe and numerous others at the Daring Lake Tundra Ecosystem Research Station (TERS). Thanks to Karin Clark, Steve Matthews and the TERS staff for a life changing experience that has inspired me to continue research in the North. Thanks to Mike Treberg for building custom equipment and laboratory guidance. Thanks to Dr. Klaus-Holger Knorr and Svenja Agethen for the analysis of porewater CH_4 and CO_2 concentrations and stable isotope signatures.

This research would not have been possible without many funding sources, including: Canadian Foundation for Climate and Atmospheric Sciences, Natural Science and Engineering Council, International Polar year – Government of Canada, Northern Science Training Program, Polar Continental shelf project, Canada Foundation for Innovation, Ontario Innovation Trust and generous awards and scholarships from the Department of Geography, Carleton University.

Table of Contents

Abstract ..... **i**

Acknowledgements ..... **ii**

Table of Contents ..... **iii**

List of Tables ..... **v**

List of Figures ..... **vii**

List of Abbreviations and Symbols ..... **ix**

1 Chapter: Introduction **1**

2 Chapter: Background **5**

2.1 Carbon budgets 5

2.2 Arctic wetlands 6

2.3 Methane fluxes 9

2.3.1 CH_4 production 12

2.3.2 CH_4 consumption 14

2.3.3 CH_4 transport 15

2.4 Scale dependence 16

2.5 Methods of measuring F_{CH4} 17

2.6 Methods to assess other factors influencing F_{CH4} 20

3 Chapter: Methods **24**

3.1 Site description 25

3.2 Chamber measurements 32

3.3 Eddy covariance measurements 36

3.4 Environmental variables 37

3.5 Porewater sampling 38

3.5.1 Dissolved Organic Carbon 38

3.5.2 Dissolved CH_4 and $\delta^{13}C$ 39

3.6 Vegetation survey 39

3.7 Data Analysis 40

4 Chapter: Results **43**

4.1 Spatial variability in F_{CH4} 43

4.2 EC footprint analysis 52

4.3 Temporal variability 56
4.3.1 Diel patterns 56
4.3.2 Seasonal patterns 60
4.3.3 Interannual trends 65
4.4 DOC, TN, SUVA 66
4.5 CH_4 and CO_2 isotope signatures 70
4.6 Source CO_2 and CH_4 isotope signatures 73
5 Chapter: Discussion 75
5.1 Comparison to other wetland and Arctic sites 75
5.2 Environmental variables influencing spatial and temporal F_{CH4} variability 76
5.3 Microform as an integrated set of explanatory environmental variables 83
5.4 Differences between and limitations of plot and ecosystem-scale F_{CH4} measurement methods 86
6 Chapter: Conclusion 89
Appendices 91
Appendix A 91
References 96

List of Tables

Table 1. Mean, median and ranges for F_{CH4} from wetlands, bogs, fens and wet sedge meadows. Units are converted to mg CH_4 m^{-2} d^{-1} and rounded to the nearest mg for comparisons across multiple datasets including the current study. 11

Table 2. Chamber F_{CH4}, vegetation and environmental characteristics classified by lawn, tussock, collapse scar and palsa microform. Median and/or mean ± 1 standard error are from 8 sampling days during the 2017 growing season and 5 collars each for lawn and tussock microforms and 3 collars each for collapse scars and palsas. Over the 9 years, 408, 404, 63, and 63 F_{CH4} measurements were used to compute means for the lawn, tussock, collapse scar, and palsa microforms, respectively. 45

Table 3. Linear mixed effect models describing significant spatial and temporal trends in F_{CH4} both among and between lawn, tussock, collapse scar and palsa plots. T_5 and T_{10} are 5 and 10 cm soil temperatures, VWC is soil moisture, TD is thaw depth, %Carex is the percent cover of Carex/Eriophorum *spp*., WT is water table, and lawn, tussock and collapse scars are referred to in equations as the fixed effects of each microform. Collar is set as a random effect in each model with the exception of the model for the 2017 seasonal means where microform was not set as a fixed effect in order to highlight abiotic and biotic variable effects. 48

Table 4. Differences in F_{CH4} and climatic variables including air temperature, friction velocity (u_*), vapour pressure (VP), net radiation (Q*) and water table depth (WT) based on source area relative to the EC tower with corresponding standard error. Median F_{CH4} values are noted before mean values. Significant differences ($p < 0.05$) in variables among source areas were determined using an ANOVA and Tukey HSD post-hoc test and are noted by different subscript letters within a column. 55

Table 5. Linear regression equations for daytime (8:00-17:00) EC F_{CH4} and for 24 hr values July 10-11, 2017, coinciding with the dates with 24 hr chamber F_{CH4}. T_{air}, T_5, T_{10}, T_{20} are air, 5, 10 and 20-cm soil temperature, respectively, VP is vapour pressure, Q* is net radiation and u_* is friction velocity. 58

Table 6. Linear regressions and mixed effect models for mean daily EC F_{CH4} and chamber F_{CH4}, respectively across multiple growing seasons. MEMs were performed using collar as a random effect from 2008-2017 and year when all years were combined. T_{air}, T_5, T_{10}, T_{20} are air, 5, 10 and 20-cm soil temperature, respectively, VWC is soil moisture, WT is water table depth, VP is vapour pressure, Q* is net radiation, u_* is friction velocity, TD is thaw depth, %Carex is percent cover of *Carex/Eriophorum* spp. and m is microform. 62

Table 7. Dissolved CH_4 concentrations and $\delta^{13}C$ values for CH_4 and CO_2 from porewater samples from 5 cm to a maximum depth of 40 cm from the peat surface. Standard error (SE) is listed for measurements with more than 1 replicate plot for the corresponding date. 72

Table 8. The importance of several abiotic and biotic variables in driving variation in chamber (plot-scale) and EC (ecosystem) F_{CH4}, represented by the occurrence of significant coefficients in linear mixed effect and regression models and interpretation of CART and PCA analyses. 80

Table A-1. Yearly mean Tussock F_{CH4}, volumetric water content (VWC) and peat temperature (2 cm depth) with corresponding standard error. Median F_{CH4} values are noted before mean values..... 91

Table A-2. Yearly mean lawn F_{CH4}, volumetric water content (VWC) and peat temperature (2 cm depth) with corresponding standard error. Median F_{CH4} values are noted before mean values..... 92

Table A-3. Yearly mean collapse scar F_{CH4}, volumetric water content (VWC) and peat temperature (2 cm depth) with corresponding standard error. Median F_{CH4} values are noted before mean values. 93

Table A-4. Yearly mean palsa F_{CH4}, volumetric water content (VWC) and peat temperature (2 cm depth) with corresponding standard error. Median F_{CH4} values are noted before mean values. 93

Table A-5. July and August mean EC F_{CH4}, net radiation, WT, air and peat temperature (20-cm depth) with corresponding standard deviation for 2015-2017 growing seasons. Median F_{CH4} values are noted before mean values. 94

Table A-6. Linear mixed model results testing for differences in porewater samples between microform, depth and time where plot was treated as a random effect. 95

List of Figures

Figure 1. Daring Lake Tundra Ecosystem Research Station location in the Northwest Territories, relative to several Tłı̨chǫ communities and northern Canada (inset). 26

Figure 2. Extent of the wet sedge meadow at Daring Lake with adjacent uplands. The site includes 16 permanent collars; 10 near the EC tower and 6 collars within an area defined by collapse scars and palsas. 29

Figure 3. Aerial view of palsas extending across the wet sedge meadow (top left). Palsa and collapse scar features (top right), EC station looking E (bottom right) and view of the eddy covariance tripod looking NE (bottom left) (Photos: E. Humphreys). 30

Figure 4. Peat (0-40 cm) from the area surrounding the EC tower (left) and underlying sediment core from an area defined by palsas and collapse scars (right) with segregated ice lenses (photos: E. Humphreys). 31

Figure 5. Emma Riley and Caitlyn Proctor perform chamber measurements on lawn and tussock plots (left) and a view of lawn and tussock plots along boardwalks at the main fen area (right). 33

Figure 6. Mean daily F_{CH4} measured using chamber and eddy covariance techniques (top panel) and WT relative to the lawn surface and air temperature (bottom panel) from May-September, 2008-2018 (excluding 2011). May and July are indicated as 'M' and 'J' on the x-axis. Each chamber F_{CH4} point is the mean of 3–5 daytime chamber measurements depending on microform and year. Daily EC F_{CH4} are averaged on days with at least 8 half hourly measurements that met quality criteria. Short gaps of 5 days or less are linearly interpolated. 44

Figure 7. Across lawn plots, 2017 chamber F_{CH4} increased with increasing peak growing season percent cover of *Carex/Eriophorum* spp. 49

Figure 8. Loadings from PC1 and PC2 from PCA analysis of environmental variables and 2017 chamber F_{CH4}. (L=Lawn, T=Tussock, C=Collapse scar, P=Palsa). TD=Thaw depth, tencm=Soil temperature at a depth of 10 cm, Persedge = % cover of *Carex/Eriophorum* spp., logch = chamber F_{CH4}, VWC = percent volumetric water content. 50

Figure 9. Regression tree where predictor variables for 2017 chamber F_{CH4} are microform (C = Collapse scar and P = Palsa vs. T = tussock and L = lawn), and VWC. Complexity parameters for the first and second split are 0.70 and 0.08, respectively. 51

Figure 10. Right: the magnitude of F_{CH4} (scale across center in nmol m^{-2} s^{-1}) from July and August 2017 plotted with wind direction (angle from N noted around the perimeter) when 70% of the flux footprint was within 80 m of the flux tower. Left: the map of the wet sedge meadow (see Figure 2 for legend) with the area within 80 m of the tower circled. 54

Figure 11. The magnitude of F_{CH4} (nmol m^{-2} s^{-1}) from July and August 2017 plotted with wind direction when 70% of the flux footprint was within 80 m of the flux tower. The map of the wet sedge meadow from Figure 2 is next to the radial plot. 56

Figure 12. EC F_{CH4}, friction velocity, air temperature (Air T) and net radiation (Q*) over 4 days (July 8^{th} – 11^{th}, 2017) 57

Figure 13. Diel EC F_{CH4}, soil temperature and friction velocity (u_*) from July 10-11 (DOY 191-192), 2017. Soil temperature measurements are from the EC station (5 cm) and from the lawn collars (2 cm). The bottom two panels display a 24-hour set of F_{CH4} measurements using non-steady state chambers. Measurements were performed on two lawn plots, two tussock plots, and one collapse scar and palsa plot. The horizontal line marks where values become negative and therefore represent CH_4 uptake. 59

Figure 14. Daily mean lawn chamber F_{CH4} and site-level WT between 2009-2012 and 2017 (top) and from 2008, 2013-2016 (bottom). Years were separated based on significant coefficients for WT as an explanatory variable for chamber F_{CH4} with collar as a random effect. 63

Figure 15. Five-day moving averages using half hour measurements of EC F_{CH4}, WT and air temperature over the 2015, 2016 and 2017 growing seasons. 64

Figure 16. Dissolved CH_4 (ppm) and SUVA (L mg C^{-1} m^{-1}) for lawn and tussock plots at depths of up to 40 cm on three different dates in 2017. 68

Figure 17. TN (mg L^{-1}) and DOC (mg L^{-1}) for lawn and tussock plots at depths of up to 40 cm on three different dates in 2017. 69

Figure 18. Methane isotope composition from porewater CH_4 with increasing depth for lawn and tussock plots on three different dates in 2017. 71

Figure 19. Source isotopic signatures for CH_4 and CO_2 for lawn and tussock plots during the 2014 growing season. 74

List of Symbols and Abbreviations

Symbol	Definition	Symbol	Definition
C	carbon	OC	organic carbon
^{12}C	carbon-12	OM	organic matter
^{13}C	carbon-13	P	atmospheric pressure
$\delta^{13}C_{CH4}$	ratio of stable isotopes $^{13}C/^{12}C$ to a standard reference material	PAR	photosynthetically active radiation
$\delta^{13}C_{CO2}$		Pg	petagram
CO_2	carbon dioxide	POC	particulate organic carbon
CH_4	methane	ppmv	parts per million volume
DIC	dissolved inorganic C	R	ideal gas constant
DOC	dissolved organic C	SOM	soil organic matter
EC	eddy covariance	$SUVA_{254}$	specific absorbance at λ = 254 nm
F_{CH4}	methane flux	T_{air}	air temperature
F_{CO2}	carbon dioxide flux	T_2	soil temperature at 2 cm
H_2	hydrogen	T_5	soil temperature at 5 cm
H_2O	water	T_{10}	soil temperature at 10 cm
cm	centimeters	T_{20}	soil temperature at 20 cm
dx/dt	change in concentration over time	TD	thaw depth
°C	degrees Celsius	TN	total nitrogen
IRGA	infrared gas analyzer	V	chamber volume
LAI	leaf area index	VWC	volumetric water content
NPOC	non-purgeable OC	WMS	Wavelength modulation spectroscopy

1 Chapter: Introduction

Arctic terrestrial ecosystems play a large role in the global carbon (C) budget as permafrost soils contain approximately 1300 Pg of organic C (Hugelius *et al.,* 2014). With one third of the global terrestrial C pool in permafrost affected soils (McGuire *et al.*, 2009; Tarnocai *et al.,* 2009), Arctic terrestrial ecosystems have a great capacity to affect the global C cycle by contributing or mitigating emissions of carbon dioxide (CO_2) or methane (CH_4) to the atmosphere. Past studies have suggested that Arctic terrestrial ecosystems are an overall C sink, but the response of Arctic C dynamics to changes in climate and vegetation is uncertain (McGuire *et al.*, 2009). Shifts in Arctic environmental conditions could affect the balance between vegetation growth and decomposition such that Arctic ecosystems may become net sources of both CO_2 and CH_4 (Alm *et al.*, 1999; Lafleur *et al.*, 2001; Oechel *et al.*, 1995; Waddington & Roulet 1996).

Rising air temperatures in Arctic regions have been reported in recent decades (Chapman & Walsh, 1993; Overpeck *et al.*, 1997; Serreze *et al.*, 2000), demonstrating an enhanced greenhouse effect relative to other parts of the globe, otherwise known as Arctic amplification (Pachauri *et al.,* 2014), which has resulted in several climate-induced shifts in the biophysical environment. These include warmer soils and thawing permafrost (Schuur *et al.*, 2008), changes in winter snow cover (Welker *et al.*, 2000), tree (Danby & Hik, 2007) and shrub (Tape *et al.*, 2006) expansion, and earlier spring snowmelt and lengthening of the growing season (Høye *et al.*, 2007). These changes in ecological and abiotic characteristics influence the C cycle of Arctic environments with the potential to either enhance or mitigate climate change depending on the changes to

the relative rates of ecosystem sequestration vs emission of CO_2 and CH_4 (Pachauri *et al.,* 2014).

Wetlands are important contributors to terrestrial C cycles. They cover about 3% of land surface and contain one third of the global soil organic C (Frolking *et al.*, 2011; Limpens *et al.*, 2008; Page *et al.*, 2011). Arctic wetlands typically store a large amount of organic matter within their deep layers of water-logged peat, which decompose slowly due to cold and anoxic conditions. However, wetlands emit CH_4, a greenhouse gas 28.5 times more potent than CO_2 over a 100-year timeframe (Pachauri *et al.,* 2014). Wetlands account for 30% of global CH_4 emissions to the atmosphere with estimates of 142-208 Tg CH_4 yr^{-1} between 2000 and 2009 (Kirschke *et al.*, 2013). Of the 500-600 Tg CH_4 emitted annually on a global scale (Dlugokencky *et al.*, 2011), Arctic wetlands alone contribute an estimated 10-150 Tg CH_4 yr^{-1} (Gao *et al.*, 2013; McGuire *et al.*, 2012; Wik *et al.*, 2016). Wetlands with anaerobic conditions in saturated peat promote high rates of methanogenesis, the microbial production of CH_4 that occurs under reducing conditions (Joabsson *et al.*, 1999). Factors affecting the production, consumption, storage and transport of CH_4 in Arctic wetlands are important to consider when predicting future CH_4 fluxes (F_{CH4}) in a warming and wetting climate. With continued climate change, Arctic wetlands are expected to experience warming and changes in precipitation amount and timing (Houghton *et al.,* 2001). Some wetlands may experience drying due to greater rates of evapotranspiration and drainage due to permafrost thaw (Lafleur, 1993), while other landscapes may become wetter with subsidence of ice-rich permafrost (Jorgensen *et al.,* 2008; Smith *et al.,* 2005), all of which can potentially influence C cycling and CH_4 emissions. Arctic wetlands are likely to change in their structure, composition and

function (Pachauri *et al.,* 2014) and the combined effect of all these changes on CH_4 emissions is uncertain.

The soil-vegetation-climate interactions controlling F_{CH4} can vary over temporal and spatial scales (Moore *et al.*, 2011; Treat *et al.,* 2007; Turetsky *et al.*, 2014). Comparing F_{CH4} over multiple temporal and spatial scales can reveal underlying mechanisms that influence CH_4 production, storage and transport. Both emergent F_{CH4} patterns and processes are necessary to better understand the sensitivity of F_{CH4} to current and future climate and environmental change. Practically, this will provide insight into the transferability of relationships for predicting change in F_{CH4} in space and over time. This study will employ the eddy covariance (EC) method and the manual chamber method to assess ecosystem- and plot-scale F_{CH4} over 3 and 9 growing seasons, respectively within a Southern Arctic wetland at the Daring Lake Tundra Ecosystem Research Station. The main research objectives of this study are:

1) To characterize the temporal variability of F_{CH4} at the Daring Lake wetland site over several growing seasons using both EC and chamber measurements and identify relationships between F_{CH4} and environmental variables such as temperature, moisture, and vegetation.
2) To characterize the spatial variability of F_{CH4} among plots and within the EC footprint and compare EC and chamber-derived F_{CH4}.
3) To assess if the relationships between F_{CH4} and environmental variables are similar across different time periods (half hourly, seasonally, interannually) and suggest the mechanisms of F_{CH4} production, transport and storage that may explain variability in these relationships.

The organization of this thesis is as follows: Chapter 2 describes in detail some of the processes important to F_{CH4} in the context of similar studies; Chapter 3 outlines the two methods of F_{CH4} measurement, peat porewater sampling and ancillary measurements; Chapter 4 presents the results of this study; Chapter 5 discusses the processes driving F_{CH4} based on the evidence and their dependence on scale; and finally the conclusion, Chapter 6, summarizes key considerations when interpreting similar research and predicting future F_{CH4} from Arctic wetlands.

2 Chapter: Background

2.1 Carbon budgets

The C budget of an ecosystem is a result of the balance between vegetation growth (primary production) and respiration by heterotrophic and autotrophic organisms. Primary production consumes atmospheric CO_2 as it is sequestered through photosynthesis. Carbon is then reduced by plant metabolic processes and is both stored as energy for the plant and provides infrastructure for plant growth. Plant material makes its way into the soil through root growth, plant-animal interactions, and seasonal abscission events and may be stored in the soil as organic matter for short or long periods of time depending on rates of decomposition. Microbial decomposition releases several decomposition products including CH_4, CO_2, dissolved organic carbon (DOC), particulate organic carbon (POC) and dissolved inorganic carbon (DIC) (Davidson & Janssens, 2006). The gaseous exchange of C between the surface and the atmosphere includes fluxes of CO_2 (F_{CO2}), CH_4 and volatile hydrocarbons, while DOC, DIC and POC represent sub-surface C storage and aquatic fluxes. Conditions that favour the net increase of belowground C over time vs. conditions that promote net losses to the atmosphere are important to identify when quantifying feedback effects of climate change on atmospheric concentrations of C (Pachauri *et al.,* 2014).

Soil organic C accumulates in wetlands through a small but persistent imbalance between vegetation growth and its decomposition (Ström *et al.*, 2003). Soil organic C decomposition is restricted by cold and moist conditions and the presence of permafrost and other protection mechanisms. The highest densities of soil organic C are found in wet boreal and tundra ecosystems (Post *et al.*, 1982). Permafrost soils underlie roughly

24% of exposed land in the Northern hemisphere, where continuous permafrost is dominantly distributed between 66°N and 84°N (Zhang *et al.*, 1999). These frozen soils inhibit decomposition rates of organic material by physically and thermodynamically isolating C.

2.2 Arctic wetlands

Peat accumulating wetlands are wetlands with at least 40 cm of peat and are classified as either bogs or fens, where the influence of groundwater or surface water movement is the primary differentiating property (Warner & Rubec, 1997). Fens are minerotrophic and tend to have a fluctuating water table (WT) due to local groundwater and surface water dynamics, whereas the acidic, nutrient-poor bog water is unaffected by ground or surface water movement (Warner & Rubec, 1997). Peatlands are ecosystems with poorly drained soils and hydrophytic vegetation and that contain biological features adapted for wet conditions (Warner & Rubec, 1997). Arctic plant species suited to peatlands include both hydrophytic vascular plants such as *Carex* spp. (Christensen *et al.*, 1998; Emmerton *et al.,* 2014; Joabsson & Christensen, 2001; Moore & Knowles, 1987; Schimel, 1995)*, Eriophorum* spp. (Joabsson & Christensen, 2001; Nordstroem *et al.,* 2000; Schimel, 1995; Ström *et al.,* 2003) and non-vascular plants such as *Sphagnum* spp. and *Polytrichium* spp. (Christensen *et al.,* 1998; Emmerton *et al.,* 2014; Moore & Knowles, 1987; Nordstroem *et al.,* 2000). The presence of certain species is linked to the availability of nutrients. For example, with increasing *Sphagnum* moss coverage, wetlands tend to be more acidic due to the release of organic acids from decomposing *Sphagnum* material (Warner & Rubec, 1997). Vegetation associated with *Sphagnum* dominated wetlands in northern boreal and Arctic wetlands include Cotton grass

(*Eriophorum vaginatum*), ericaceous shrubs (*Kalmia, Ledum, Chamedaphne, Vaccinium* and *Gaylassacia* spp.) and black spruce (*Picea mariana*) (Batzer & Baldwin, 2012). Peatlands are typically characterized by microtopographic variation, where individual features are referred to as 'microforms'. These include shallow pools, low-lying, relatively wet and sparsely vegetated lawns, and raised, drier hummocks often densely packed with vascular plants (Sullivan *et al.,* 2008). In permafrost terrain, palsas are also possible. 'Palsa' is a Fennoscandian term that originally describes a raised hummock with a core of ice (Seppälä, 1972). More recently palsas have been defined as peat mounds with alternating layers of segregated ice and peat or mineral soil (ACGR-NRC, 1988). Palsas are often associated with the southern limits of discontinuous permafrost (Seppälä, 2011) due to the insulating property of dry peat, where otherwise conditions are too warm for perpetual ground ice. Palsas form in wet ecosystems and require at least 200-210 days a year with air temperatures below 0°C (Lundqvist, 1962). The segregation of ice into ice lenses (Berteaux *et al.,* 2016) results in heaving of soil and a raised surface. This surface supports plant communities less tolerant of saturated soils such as deciduous shrubs (Ackerman *et al.,* 2017; Myers-Smith *et al.,* 2015). Eventual collapse of the palsas results when moisture or warm air penetrates the ice core (Pissart, 2002), leaving a subsided, water-logged surface. These are known as collapse scars, where the standing dead remains of *Betula* or ericaceous shrubs indicate the former palsa microforms (Zuidhoff & Kolstrup, 2005). Other microforms or patterned ground that may occur in Arctic wetlands include frost or mudboils (Wilson and Humphreys, 2010), and low or

high-centered polygons with ice wedge margins degrading to wet troughs (Becker *et al.,* 2016; Mackay 2000).

Peatlands are a class of wetland where organic matter has accumulated based on geographic location and climatic conditions favouring peat growth over decomposition. Arctic peatlands developed during the Holocene around 8000-10000 years before present (BP) as determined using radiocarbon dating of basal peat (Tarnocai & Zoltai, 1988). Cool and moist conditions after the last deglaciation lead to the initial peat development of Arctic peatlands (Tarnocai, 1978). Peatland development may occur as a result of infilling and/or paludification (Tarnocai & Zoltai, 1988). Peatlands are distinguished by their geomorphology, chemistry, hydrology and vegetation. They may be patchy or extensive, fed by groundwater or perennial snowpack, coastal or within low-lying valleys, on ice wedge polygonal ground or underlain by glacial till (Woo & Young, 2006). Wet meadows in the Arctic are defined as wetlands receiving both overflow and subsurface flow and are thus often mineral rich. Meadows are covered in graminoid species (Woo & Young, 2006). Arctic wet sedge meadows as described by (Bliss and Matveyana, 1992; Christensen *et al.,* 2003; Christensen *et al.,* 1998; Christensen, 2001; Emmerton *et al.,* 2016; Emmerton *et al.,* 2014; Henry, 1998; Joabsson and Christensen, 2001; Joabsson *et al.,* 1999; Johnson et al., 2000; McEwing et al., 2015; Yu *et al.,* 2017) are usually characterized by sufficient peat accumulation to be classified as fens.

Canada contains one third of global peatlands (Rydin, 2006) with 16,000 km^2 of peatlands within the Arctic and most in the low Arctic (National Wetlands Working Group, 1986). The low Arctic, relative to the high Arctic, is comparatively warm and moist with higher mean annual temperatures, higher density of lakes and ponds (ECG,

2013) and longer growing seasons driven by latitudinal climatic gradients (Billings, 1973). In Canada, the Low Arctic is roughly defined as the region extending across the northern mainland between the Richardson Mountains in the Yukon to Ungava Bay in northern Quebec while the High Arctic includes the Canadian Arctic Archipelago and portions of the northeastern district of Keewatin and northern Quebec (ESWG, 1995). Low Arctic peatlands are abundant in the Mackenzie Delta and Yukon coast due to low lying, poorly drained topography densely packed with lakes (Tarnocai & Zoltai, 1988). On the Canadian shield, where this study takes place, peatlands are most common in the Keewatin district and southern Baffin Island but also occur throughout the region in low-lying areas such as shallow valleys, along drainage pathways, between bedrock outcrops, along the coast, within ponds, lakes or slow-flowing rivers or wherever high water table levels persist long enough for peat development through paludification or terrestrialization (Rydin, 2006). Wetlands and peatlands are scarcer in Canada's high Arctic/Arctic Archipelago due to an arid climate. But shallow peat accumulation occurs in lowlands sometimes fed by perennial snowpack and glacial meltwaters and along the coast (Emmerton *et al.* 2014; Tarnocai & Zoltai, 1988).

2.3 Methane fluxes

Methane fluxes span several orders of magnitude in northern wetlands (Emmerton *et al.*, 2014; Lai *et al.*, 2014; Moore *et al.*, 2011; Smemo & Yayitt, 2006), where wet sedge ecosystems are a dominant CH_4 source with an estimated average of 100 mg CH_4 $m^{-2}d^{-1}$ based on a meta-analysis of subarctic and Arctic sites in Alaska, Russia and Sweden (Vourlitis & Oechel, 1997) (Table 1). The large range in F_{CH4} reflects the large variability in environmental factors which affect methanogenesis and methanotrophy,

methane storage, and transport (Vourlitis & Oechel, 1997). Some of the environmental factors that correlate strongly with F_{CH4} are depth to water table (Christensen *et al.* 2000; McEwing *et al.* 2015; Moore & Knowles 1987; Moore *et al.* 2011; Ström & Christensen 2007; Torn & Chapin 1993; Waddington & Roulet, 1996), soil/peat temperature (Christensen *et al.* 1995; Moore *et al.* 2011; Ström *et al.* 2012), vegetation composition (Bubier *et al.*, 1995; Christensen *et al.* 2000; Joabsson & Christensen 2001; Lai *et al.* 2014; Moore et al 2011; Ström *et al.* 2012; Ström & Christensen 2007), net ecosystem exchange (NEE)/gross primary productivity (GPP) (Bubier *et al.*, 1995; Christensen *et al.*, 2000; Christensen *et al.*, 1996; Lai *et al.* 2014; McEwing *et al.* 2015; Ström *et al.* 2015; Waddington et al 1996), and thaw depth (Emmerton *et al.* 2014; Stuartevant & Oechel 2013; Verville *et al.* 2008; Zona *et al.* 2009). However, the degree to which these variables are important depends on the key mechanisms important in limiting or enhancing CH_4 fluxes and the temporal and spatial scale at which these mechanisms are important.

Table 1. Mean, median and ranges for F_{CH4} from wetlands, bogs, fens and wet sedge meadows. Units are converted to mg CH_4 m^{-2} d^{-1} and rounded to the nearest mg for comparisons across multiple datasets including the current study.

Region	Ecosystem	Method	Range	Mean	Median	Reference
Global	rich fen	chamber	-19 to 1328	93 ± 3	45	*Turetsky et al. (2014)*
High Arctic	wet sedge	EC	-8×10^{-1} to 3	$1 \pm 2 \times 10^{-1}$	-	*Emmerton et al. (2014)*
		chamber	-5×10^{-2} to $4 \times 10^{-}$	$2 \times 10^{-1} \pm 1 \times 10^{-1}$	-	
		chamber	n/a	64 ± 2*	-	*Strom et al. (2015)*
Arctic	wet sedge	chamber	30 to 142[#]	100	-	*Vourlitis & Oechel (1997)*
		EC	14 to 26[d]	21 ± 5	-	*Euskirchen et al. (2017)*
		EC	-1 to 105	52	-	*Friborg et al. (2000)*
		chamber	n/a	61	66	*Schimel (1995)*
		EC	-10 to166	54 ± 2	53	*current*
		chamber	-11 to 820	118 ± 3(112** ± 2)	108(98**)	
		chamber	6 to 638	144 ± 16, 70 ± 19***	-	*McEwing et al. (2015)*
Subarctic	wetland	chamber	-33 to 4114	112 ± 6	68	*Turetsky et al. (2014)*
	palsa fen	EC	42 to 180	-	-	*Hanis et al. (2013)*
Temperate	bog	chamber	-2 to >1000	-	-	*Moore et al. (2011)*
	treed rich fen	EC	0 to 111[d]	68	-	*Long et al. (2010)*

[d]daily mean values *2013 mean **weighted mean and median values ***mean values for wet and dry sites, respectively [#]values based on a meta-analysis of 10 publications documenting wet sedge sites across Alaska, Russia and Sweden.

2.3.1 CH_4 production

Methanogenic archaea cannot breakdown complex molecules, and thus require several bacterial communities to supply more easily decomposable substrates (Zinder, 1993). The production of CH_4 begins with the hydrolysis of organic polymers by fermenting bacterial enzymes, producing alcohols, fatty acids and H_2 (Conrad, 1999). These are then further broken down into acetate, H_2 and CO_2; the main substrates required for methanogenesis (Conrad, 1999). CH_4 production is classified based on the reaction substrate, where hydrogenotrophic and acetoclastic methanogenesis require H_2/CO_2 and acetate, respectively.

Acetoclastic methanogenesis, also referred to as acetate cleavage, produces both CO_2 and CH_4. Hydrogenotrophic methanogenesis involves the reduction of CO_2 with H_2 (Krohn *et al.*, 2017). The production of CH_4 can be dominated by either reaction pathway, usually dependent on the amounts of H_2/CO_2, acetate and the unique blend of methanogenic archaea within reducing environments (Kotsyurbenko *et al.*, 2004). Hydrogenotrophic methanogenesis becomes increasingly important relative to acetoclastic methanogenesis with decreasing supply of labile organic matter (OM), such as with depth in the peat/soil profile, where hydrogenotrophic methanogenesis accounts for 50-100% of the total CH_4 production (Chasar *et al.*, 2000; Hornibrook *et al.*, 1997; Nakagawa *et al.*, 2002). The rates of methanogenesis of both pathways can be affected by redox potential, the availability of nutrients, substrates and terminal electron acceptors (Whiticar, 1999) where methanogens can be outcompeted by other bacteria, such as sulphate-reducing bacteria (Whiticar, 1999). Acetate fermentation dominates 70% of methanogenesis in low-sulphate environments, with increasing rates of carbonate

reduction when acetate concentrations are low (Whiticar, 1999). Originating from fresh organic matter, acetate becomes less available with depth in the peat/soil profile (Chasar *et al.*, 2000; Hornibrook *et al.*, 2000) and over time within a growing season (Avery *et al.*, 2003). Methanogenesis is associated with highly reduced conditions, where both pathways are inhibited by redox potentials that are too high (Wang *et al.,* 1993). Methanogenesis generates less energy than the reduction of alternate electron acceptors such as Fe^{3+}, SO_4^{2-}, NO^{3-} and Mn^{4+}, and therefore is largely carried out once these electron acceptors have been reduced and sufficient substrate remains (Wang *et al.,* 1993). A soil redox potential of around -150 mV has been shown as the value below which methanogenesis may proceed (Masscheleyn *et al.,* 1993; Wang *et al.,* 1993).

When considering environmental controls on CH_4 production, soil temperature and depth of the water table are the most commonly mentioned variables (Dise *et al.*, 1993; Elberling *et al.*, 2008; Glaser & Chanton, 2009; Ström & Christensen 2007; Torn and Chapin 1993; Waddington *et al.*, 1996). Water table levels largely affect CH_4 production by controlling the location and depth of the anaerobic zone and the extent of the aerobic zone where CH_4 consumption occurs (Moore & Knowles, 1989). Increasing soil temperature increases reaction rates of both CH_4 production and CH_4 consumption (Dunfield *et al.*, 1993). Water table and soil temperature do not always correlate well with F_{CH4} at the plot-level (Strom *et al.*, 2015; Zhu *et al.*, 2014). The isolation of these variables neglects the influence of substrate availability (Amaral & Knowles, 1994; Bachoon & Jones, 1992; Valentine *et al.*, 1994; Williams & Crawford, 1984) and quality (Schimel, 1995) on CH_4 production rates. Further, Schimel (1995) found that plant community structure that promotes plant-mediated transport, which allows CH_4 to bypass

aerobic zones where methanotrophic microbes consume CH_4 and reduce CH_4 emissions (described further below), was a strong predictor of F_{CH4}.

2.3.2 CH_4 consumption

Low-affinity methanotrophy is the microbial consumption of CH_4 occurring at CH_4 concentrations higher than 40 ppm (Le Mer & Roger, 2001), and is characteristic of methanogenic ecosystems such as rice fields and wetlands (Le Mer & Roger, 2001). High-affinity oxidation of CH_4, occurring at near-atmospheric (2 ppm) CH_4 concentrations, contributes very little to overall consumption rates (Topp & Pattey, 1997). Methanotrophy can occur both aerobically and anaerobically, although the anaerobic mechanism is reported only for marine sediments (Alperin & Reeburg, 1985) and flooded rice fields (Chowdhury & Dick, 2013; Murase & Kimura, 1994). Variations in F_{CH4} are sometimes exclusively attributed to variations in methanotrophy (Sass *et al.*, 1990; Schütz *et al.*, 1989), making it an important process to understand when considering CH_4 emissions from Arctic wetlands. Methanotrophy is highly dependent on soil oxygen and CH_4 concentrations (Segers, 1998), therefore in water-logged peat layers this is largely dependent on root respiration; transporting oxygen from the atmosphere to the rhizosphere (Hanson & Hanson, 1996). If the water table is below the surface, or surface soil moisture is low, a large aerobic layer is formed between the water table and the atmosphere. CH_4 travelling towards the surface via diffusion can then be oxidized to CO_2 by methanotrophs before reaching the soil surface. Similar to CH_4 production, CH_4 consumption reaction rates are dependent on soil temperature (Dunfield *et al.*, 1993), although methanotrophy has a wider range of optimal temperatures (Dunfield *et al.*,

1993).

2.3.3 CH_4 transport

CH_4 is transported to the atmosphere via three main pathways; diffusion, ebullition and plant-mediated transport. Diffusion of CH_4 is proportional to the concentration gradient of CH_4 between the peat and the atmosphere, which drives a slow upward movement of CH_4 in soils where CH_4 production exceeds consumption, at least at depth. Diffusion coefficients and subsequently, diffusion rates, are much higher for unsaturated peat layers than those below the WT (Walter & Heimann, 2000). This has to do with differences in molecule size, temperature and pressure of a given substance where dissolved gasses are slower-moving compared to those in gaseous states due to the higher viscosity of liquid (Motinsky, 2011). Ebullition is the release of CH_4 in the form of gas bubbles from deep, anaerobic layers of peat. Methane release as ebullition is comparatively much faster, as fluxes greater than 40 g CH_4 m^{-2} can be released in short periods of time (Glaser *et al.*, 2004; Rosenberry *et al.*, 2013). If CH_4 concentrations are supersaturated in peat porewater, the pressure of the CH_4 will exceed hydrostatic pressure and bubbles are formed (Lai, 2009). These bubbles remain within the peat pores until a threshold pressure is reached and they are released to the atmosphere (Lai, 2009). This rapid ejection allows the CH_4 to bypass the methanotrophs within the aerobic zone.

Plant-mediated transport of methane release to the atmosphere has been documented in various Arctic wetlands (Andresen *et al.*, 2017; King *et al.*, 1998; Schimel, 1995; Ström & Christensen, 2012). Methane is transported by aerenchymatous tissues present in some hydrophytic vascular plants. These tissues allow for both diffusion of oxygen to the rhizosphere in water-logged environments and the transport of

CH_4 directly to the atmosphere. Aerenchymatous tissue transport is driven by pressure gradients between the plant and the atmosphere or due to diffusional gradients enhanced by plant respiration (Lai, 2009). Wet sedge meadows, often dominated by *Eriophorum vaginatum, E. scheuchzeri* and *Carex aquatilis,* can have enhanced F_{CH4} due to both plant-mediated transport and plant productivity whereby labile C and substrates are produced at depth and exuded from plant roots. Waddington *et al.* (1996) found that vascular plant transport of CH_4 through aerenchymous tissues was positively correlated to the position of the water table throughout the growing season, suggesting that plant-mediated transport of CH_4 is dependent on high water table levels. The average contribution of plant-mediated CH_4 release is reported as high as 75% of total wetland CH_4 emissions (Schimel, 1995). The effect on F_{CH4} is highly dependent on plant species type (Joabsson & Christensen, 2002; Schimel, 1995). Plant species that have shown significant effects on overall F_{CH4} from Arctic wetlands include *Eriophorum* spp. (Frenzel & Rudolph, 1998; King *et al.*, 1998; Ström *et al.,* 2012; Schimel 1995), *Carex aquatilis* (Andresen *et al.,* 2017; King *et al.,* 1998; Schimel, 1995), and *Arctophila fulva* (Andresen *et al.,* 2017). Although plant-mediated methane release can be a dominant pathway for CH_4 release, the overall effect of vascular plant abundance is dependent on the competing process of plant CH_4 consumption. Methanotrophic microorganisms within the plant and in the rhizosphere can oxidize CH_4 before its release to the atmosphere (Bosse and Frenzel, 1997; Gibert and Frenzel, 1995).

2.4 Scale dependence

The relationships between environmental variables and F_{CH4} can differ when considered at a range of spatial and temporal scales. At large spatial and temporal scales,

such as among ecosystems (Turetsky *et al.,* 2014) or among years (Smemo & Yavitt, 2006), the influence of water table depth is an important control on F_{CH4} with wetter conditions resulting in greater CH_4 emissions. Over shorter time scales, such as within a single summer season, this relationship is less clear when CH_4 emissions may show hysteresis or even negative correlations with water table depth (Brown *et al.* 2014). At finer spatial scales, such as 1 x 1 m plot-scale measurements at a given site, microtopography (and its close relationship with water table position) and vegetation characteristics are associated with variations in F_{CH4} (Fox *et al.* 2008; Sachs *et al.* 2010; Wickland *et al.* 2006). A study by Moore *et al.* (2011) examined scale-dependent CH_4 flux relationships at the Mer Bleue bog in eastern Ontario, Canada. Monthly mean F_{CH4} were highly correlated with peat temperature (within season effect), seasonal means were correlated to water table (interannual effect) and multi-year spatial variation correlated best with vegetation characteristics, followed by peat temperature and water table levels (spatial effect). Moore *et al.* (2011) suggested that the relative importance of these variables is affected by their spatial and temporal range, where large ranges of temperature, water table levels, or vegetation composition explain a greater proportion of variance in F_{CH4}.

2.5 Methods of measuring F_{CH4}

Measurements of C fluxes between the surface and the atmosphere are determined using 'top-down' and 'bottom-up' approaches to the system (McGuire *et al.*, 2009). The 'top-down' approach considers the atmospheric concentration of either CO_2 or CH_4 as representative of the dynamic surface it overlies. The 'bottom-up' approach measures surface concentrations of CO_2 and CH_4 at micro- and ecosystem scales. These

measurements can be integrated to represent the surface-atmosphere C cycle for various scales of interest (McGuire *et al.*, 2009). The bottom-up approach is often used for C budget studies as it captures the spatial and temporal variation of processes that are driving the C cycle. The most commonly used techniques of measuring site-specific CH_4 fluxes from the 'bottom-up' perspective are the eddy covariance method and the chamber method.

Eddy covariance measures vertical turbulent fluxes based on the covariance of vertical wind speed and concentrations of gases of interest. Studies that have examined CH_4 ecosystem-atmosphere exchange in Arctic wetlands have used the eddy covariance technique to measure hectare-sized areas upwind of the towers/masts upon which the measurement systems are installed. These studies have examined wet sedge meadows in the High Arctic (Emmerton *et al.*, 2014), in Alaska (Johnson *et al.*, 2000; Euskirchen *et al.*, 2016), and Greenland (Joabsson & Christensen, 2001; Soegaard & Nordstroem, 1999; Ström *et al.*, 2003; Sullivan *et al.*, 2008). Chamber measurements of F_{CH4} represent relatively small spatial scales. Chamber measurements F_{CH4} have also been made in Arctic peatlands (Billings *et al.*, 1982; Christensen *et al.*, 1998; Joabsson & Christensen, 2001; Moore & Knowles 1987; Roulet *et al.*, 2007; Schimel *et al.*, 1995; Ström *et al.*, 2015).

The chamber method encloses a surface and monitors the gas of interest either manually or automatically over a given period of time. Non-steady state chambers are typically closed loop and the concentration change within the volume is proportional to the flux. This is contrasted by the steady state chamber method, where air is passed through the chamber and the difference in CH_4 between the inlet and outlet is monitored. The manual or static chamber technique has been used in many recent studies (Lai *et al.*, 2014; Moore *et al.*, 2011; Ström *et al.*, 2015) where remote field locations restrict the use of on-

site gas analyzers. Instead, discrete samples are collected for analysis later and there is typically no circulation within the chamber between measurements. The plots encompassed by the chambers typically cover 0.05-0.07 m^2. The non-steady state chamber technique can be criticized due to a lack of spatial representation of an ecosystem and due to 'chamber effects' (Mosier, 1990). During the time required to sample a given area, a minimum of 20 minutes, the chamber creates its own microclimate that has a different temperature and humidity than the surrounding area. It affects the gas concentration gradients required to drive F_{CH4} and it negates the effect of wind turbulence on gas transport (Davidson *et al.*, 2002; Livingston & Hutchinson 1995; Lund *et al.*, 1999). When chambers are not automated, relatively few F_{CH4} measurements are made and are unable to capture the temporal variability in F_{CH4}. The discontinuity of temporal and spatial coverage of the chamber method is contrasted by the eddy covariance (EC) method, where vertical wind speed and gas concentrations are measured at high frequency (10 to 20 Hz) and a F_{CH4} is obtained typically every 30 minutes. The EC method is most applicable when the terrain is flat and homogeneous and extensive such that environmental conditions and the vegetation cover vary little within the area of measurements and beyond (Baldocchi, 2003). The EC technique correlates vertical fluctuations in turbulent wind with fluctuations in gas concentrations and assuming no advection or storage, the surface-atmosphere exchange of the gas is representative of the source/sink strength of an upwind area known as the footprint (Baldocchi, 2003). A systematic bias often presented by the EC method is the underestimation of effluxes at night during low wind speeds and limited atmospheric

turbulence (Aubinet *et al.*, 2000; Baldocchi *et al.*, 2000; Black *et al.*, 1996; Goulden *et al.*, 1996).

Due to the advantages and limitations of both methods, a number of studies have compared EC and chamber F_{CH4} from different ecosystems, including wetlands (Hendriks *et al.*, 2010; Meijide *et al.*, 2011; Sachs *et al.*, 2010; Schiler-Uijl *et al.*, 2010; Yu *et al.*, 2013). Yu *et al.* (2013) found the seasonal patterns of daily mean F_{CH4} at an alpine wetland were similar across manual chamber, automated chamber and EC methods. There were also comparable correlations for all methods between hourly mean F_{CH4} and soil temperature despite differences in diurnal patterns, where continuous chamber F_{CH4} peaked between 22:00 and 24:00 with peak soil temperature and EC F_{CH4} peaked around 13:30 with peak solar radiation (Yu *et al.*, 2013).

2.6 Methods to assess other factors influencing F_{CH4}

There are several below-ground indices that provide insight on CH_4 production pathways, CH_4 transport and OM structure and composition. Peat porewater may be sampled and analysed for DOC, total nitrogen (TN: the sum of organic nitrogen, ammonia, nitrates and nitrites) (Chasar *et al.*, 2000; King *et al.*, 1998; Strack *et al.*, 2006), $SUVA_{254}$ (the specific UV absorbance at a wavelength of 254 nm divided by the concentration of DOC) (Herndon *et al.*, 2015), dissolved CH_4 and CO_2, and their hydrogen (Chasar *et al.*, 2000; Hornibrook *et al*., 1997; Whiticar *et al.*, 1986) and C isotope composition (Chasar *et al.*, 2000; Kotsyurbenko *et al.*, 2004). Dissolved organic and inorganic C represent subsurface C reservoirs (Kayranli *et al.,* 2009) along with soil organic matter. Nitrogen is a limiting nutrient to both plant and microbial growth. Therefore, TN can affect primary production and litter quality and can favour growth of

vascular plants over bryophytes (Berendse *et al.*, 2001; Heijmans *et al.*, 2002). The form of nitrogen is also important as nitrate can act as an alternative electron acceptor and limit methanogenesis. $SUVA_{254}$ is a proxy for aromaticity (Weishaar *et al.*, 2003), due to the light absorbance of aromatic compounds. The sp^2 hybridized C-C bonds, those that mix both s and p electron orbitals before sharing electrons, are more abundant in aromatic compounds relative to simpler, long chain C compounds with sp^3 bonds. The sp^2 bonds absorb a higher frequency of radiation (smaller wavelength) than the sp^3 bonds (Peacock *et al.*, 2014). The molecular aromaticity of the DOC is of interest in that lower weights or decreased aromaticity (lower $SUVA_{254}$) typically indicates fresh C, whereas higher $SUVA_{254}$ values are linked to the preferential removal of labile DOC and the associated increase in relative abundance of less labile compounds (Pinney *et al.,* 2000).

The conversion of C from parent organic material to CH_4 or CO_2 and transport to the atmosphere can be tracked using C isotope ratios ($^{13}C/^{12}C$). $\delta^{13}C$ values indicate the difference in $^{13}C/^{12}C$ of the sample to a Cretaceous marine fossil, Pee Dee Belemnite (PDB) equivalent standard used when characterizing isotopic signatures in parts per mil. Most natural C compounds have lighter or negative $\delta^{13}C$ values relative to the PDB standard. Because lighter C is preferentially used in many biological processes, CH_4 signatures are very light. Differences in these isotope signatures can help identify the dominant CH_4 production pathway, the relative rates of methanogenesis and methanotrophy, and CH_4 transport. Methane has a $\delta^{13}C_{CH4}$ range of -110 ‰ to -50 ‰, with hydrogenotrophic methanogenesis ranging from -110‰ to -60‰ and acetate fermentation from -65‰ to -50‰ (Whiticar, 1999). Reaction pathways can also be differentiated by the ratios of $\delta^{13}C$ values between CO_2 and CH_4. The difference between

$\delta^{13}C_{CO2}$ and $\delta^{13}C_{CH4}$ is significantly greater for carbonate reduction (49-95‰) than for acetate fermentation (39-58‰) (Whiticar, 1999), the result of different kinetic isotope effects of the two pathways (Mach *et al.,* 2015). For both reaction pathways, molecules with a lighter isotopic weight react and diffuse more rapidly, resulting in an increasing concentration of ^{12}C relative to ^{13}C in microbial decomposition products of CO_2 and CH_4 (Whiticar, 1999). As these reactions continue to occur, there is an ongoing removal of ^{12}C, leaving behind increasingly heavy C molecules. If fresh OM is not continuously introduced belowground, CH_4 and CO_2 isotopic signatures can become ^{13}C enriched, nearing the signatures of the original organic matter (Whiticar, 1999).

Processes of CH_4 transport also result in fractionation where isotopically lighter $^{12}CO_2$ and $^{12}CH_4$ are both consumed and transported faster compared to $^{13}CO_2$ and $^{13}CH_4$ (Chanton, 2005; Whiticar, 1999). The result is F_{CH4} and F_{CO2} with $\delta^{13}C$ depleted signatures relative to dissolved CH_4 or CO_2 in the porewater. This fractionation occurs for plant-mediated transport, ebullition and diffusion. Chasar *et al.* (2000) found that CH_4 emitted from a mid-latitude, sedge-dominated fen was ^{13}C depleted by 3-8‰ compared to porewater $^{13}C_{CH4}$ whereas a bog site emitted CH_4 that was ^{13}C enriched by 5-8‰ compared to porewater CH_4. Chasar *et al.* (2000) suggested that these enriched ^{13}C values could be due to decreased transport of CH_4 or increased rates of methanotrophy. Methanotrophs preferentially use lighter CH_4 isotopes, leaving behind ^{13}C enriched CH_4. Methanotrophy can also result in lighter CO_2 as the ^{13}C of the CH_4 substrate is more

depleted than soil organic matter substrates. The fractionation of both CO_2 and CH_4 are important measures providing insight to rates of CH_4 transport and consumption.

Source $\delta^{13}C_{CO2}$ and $\delta^{13}C_{CH4}$ values can be determined using the 'Keeling plot' approach, based on a mass balance calculation using atmospheric and sample gas concentrations and isotope signatures (Keeling 1958; Keeling 1961). The method uses linear regression to solve a 2 member mixing model;

$$\delta^{13}C_a = c_b(\delta^{13}C_b-\delta^{13}C_s)(1/c_a) + \delta^{13}C_s \quad \text{[Eq. 1]}$$

where c_a, c_b and c_s represent the atmospheric concentration of CO_2 or CH_4, the background concentration of CO_2 or CH_4 and the source concentration of CO_2 or CH_4, respectively (Pataki *et al.*, 2003). Using measurements of atmospheric (from within the chamber enclosure at the end of a flux measurement) and background CO_2 or CH_4 concentrations, the resulting y-intercept ($\delta^{13}C_s$) is interpreted as the source isotope signature (Pataki *et al.*, 2003). The source isotope signature can then be used to suggest the production pathway of both CH_4 and CO_2, providing insight on possible production, consumption or transport limitations on F_{CH4}.

3 Chapter: Methods

To characterize the temporal variability of F_{CH4} at the Daring Lake wetland, measurements were conducted using both the chamber and EC technique over a variety of time periods. To characterize the spatial variability of F_{CH4}, fluxes and variables were compared among plots (chamber) and by wind direction (EC). Chamber measurements were performed by the author on the same collars (e.g. plots) 8 times over the 2017 growing season, including a 24-hour period in mid-July. Various research assistants and graduate students (Hayne 2009; Vandewint 2010) performed chamber measurements on these and other plots within the fen during the growing seasons of 2008 through 2016 excluding 2011. Environmental variables which were measured at the collars included soil temperature and moisture for all seasons, and thaw depth, vegetation composition and water table depth for the 2017 growing season only. LAI measurements were also performed on five permanent plots along the boardwalk leading to the EC tower from 2008-2017. EC instrumentation measured half-hourly F_{CH4} during the growing seasons of 2015-2017. Ancillary measurements at the same time step at the EC tower included water table depth, air and soil temperatures, net radiation, upwelling and downwelling photosynthetically active radiation (PAR) and atmospheric humidity. Linear regressions and mixed effect models were used to examine the relationships between F_{CH4} and the fore mentioned variables. Relationships between F_{CH4} and environmental variables were compared across multiple scales based on the coefficients resulting from linear regressions and mixed effect models. Temporal scales included diel, seasonal and multi-year periods and spatial scale was compared using the chamber (plot-level) and EC

(ecosystem-level) method. All measurements are described in detail in the following sections.

3.1 Site description

The field site is located at the Daring Lake Tundra Ecosystem Research Station (TERS), which is operated by the Government of Northwest Territories, Department of Environment and Natural Resources. TERS is located within the Southern Arctic ecozone, 300 km north east of Yellowknife and 100 km from the nearest Tłı̨chǫ community, Wekweètì (Figure 1). TERS is a research and monitoring facility established in 1995. The station also holds a tundra science and culture camp for youth in the area every year in August. The camp approaches learning from both scientific and Tłı̨chǫ traditional knowledge perspectives and showcases current Arctic research.

The Daring Lake fen is located at 64.965°N, 111.567°W, approximately 2 km south-east of TERS (Figure 1). The fen is described as a 48 ha Arctic wet sedge meadow and lies at the bottom of a shallow valley between an esker to the north and bedrock outcrops to the south. The fen receives overland and subsurface flow from approximately 1.5 km^2 of the surrounding area.

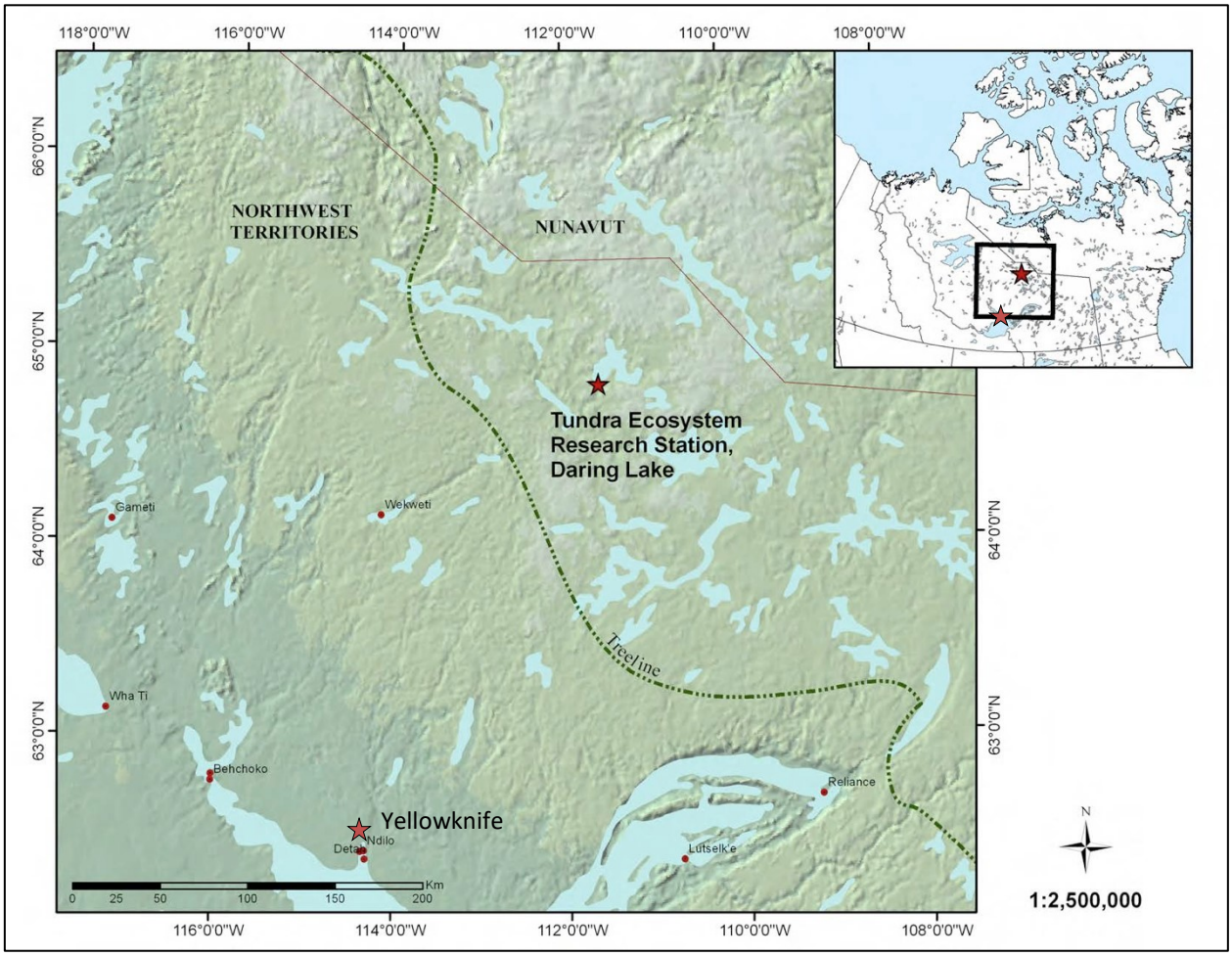

Figure 1. Daring Lake Tundra Ecosystem Research Station location in the Northwest Territories, relative to several Tłı̨chǫ communities and northern Canada (inset).

In the region, continuous permafrost extends to a depth of over 160 m (Dredge *et al.*, 1999). The peat soils in the fen have an active layer of approximately 0.70 m (Humphreys & Lafleur, 2011) while other areas within the valley have active layers ranging from 0.3-1.2 m as a result of varying soil texture, drainage and vegetation characteristics (Dredge *et al.,* 2012). The mineral soil underlying the fen peat is a fine-

textured silty loam while elsewhere in the research valley, soils are coarser with sand and sandy loam textures (Humphreys & Lafleur, 2011).

Using data from the Daring Lake weather station between 1995-2014, mean annual air temperature is -7.9°C, with mean January and July air temperatures of -29.1°C and 13.5°C, respectively. Mean summer precipitation is 141 mm (Skaarup, 2017).

The fen is characterized by different microforms (Figures 2 & 3). The lawns are flat and relatively low-lying, where the peat is almost always completely saturated. *Sphagnum* mosses dominate surface cover with sparse sedge cover. Within the lawns are tussocks, elevated mounds with drier conditions that have resulted in an increased growth of vascular plants such as sedges, bog rosemary and dwarf birch (Figure 3). Within the wetland small palsas, which are approximately 3-35 m wide and up to 70 m long and have peat soils approximately 30-50 cm above the water table due to ice lens development below within the finer-textured silty loam (Figure 4). This drier peat is dominated by *Betula nana*, *Ledum palustre, Vaccinium vitis-idea* and *Rubus chamaemorus* along with various sedges, lichen and moss underlain by a shallow active layer (Figure 3). Adjacent to the palsas are areas once populated with birch that have subsided, with dead birch stems and Sphagnum moss cover referred to here as 'collapse scars' in some locations fully saturated and in others, the surface is still above the water table (Figure 3).

The peat soils of the fen are mainly composed of sedge and *Sphagnum* plant materials (Figure 4), have a relatively low bulk density of 0.04 ± 0.01 g cm^{-3} between 0-10 cm (Piquette, 2009), the layer within which the water table usually remains, and a greater bulk density of 0.19 ± 0.01 g cm^{-3} for the 10-40 cm layer. The basal date is 1910

± 80 years BP with a long-term C accumulation rate of 17.3 g C m^{-2} yr^{-1} based on radiocarbon dating of a 40 cm peat core (Okolo, 2008).

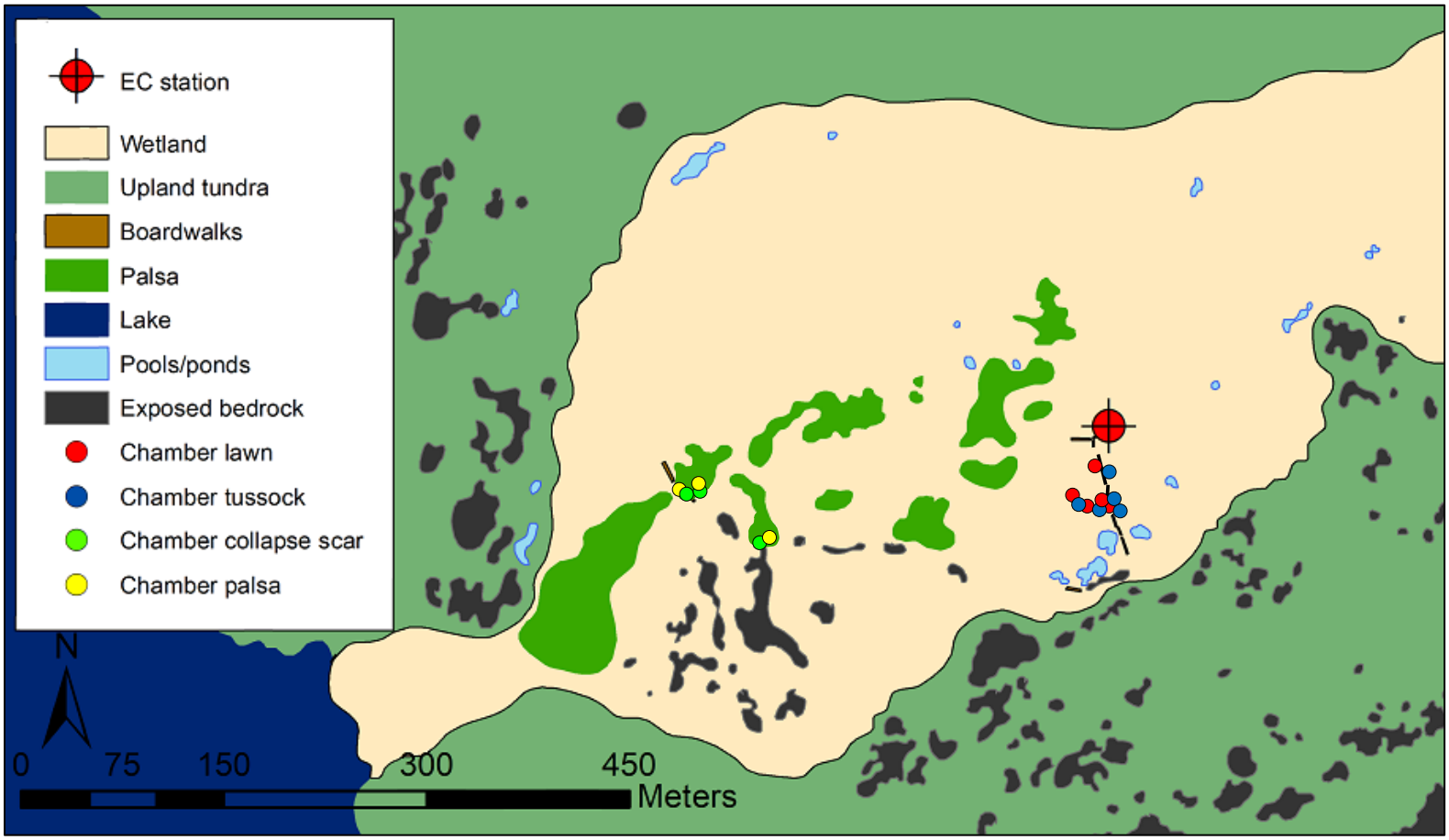

Figure 2. Extent of the wet sedge meadow at Daring Lake with adjacent uplands. The site includes 16 collars for F_{CH4} measurements; 10 near the EC tower and 6 collars within an area defined by collapse scars and palsas.

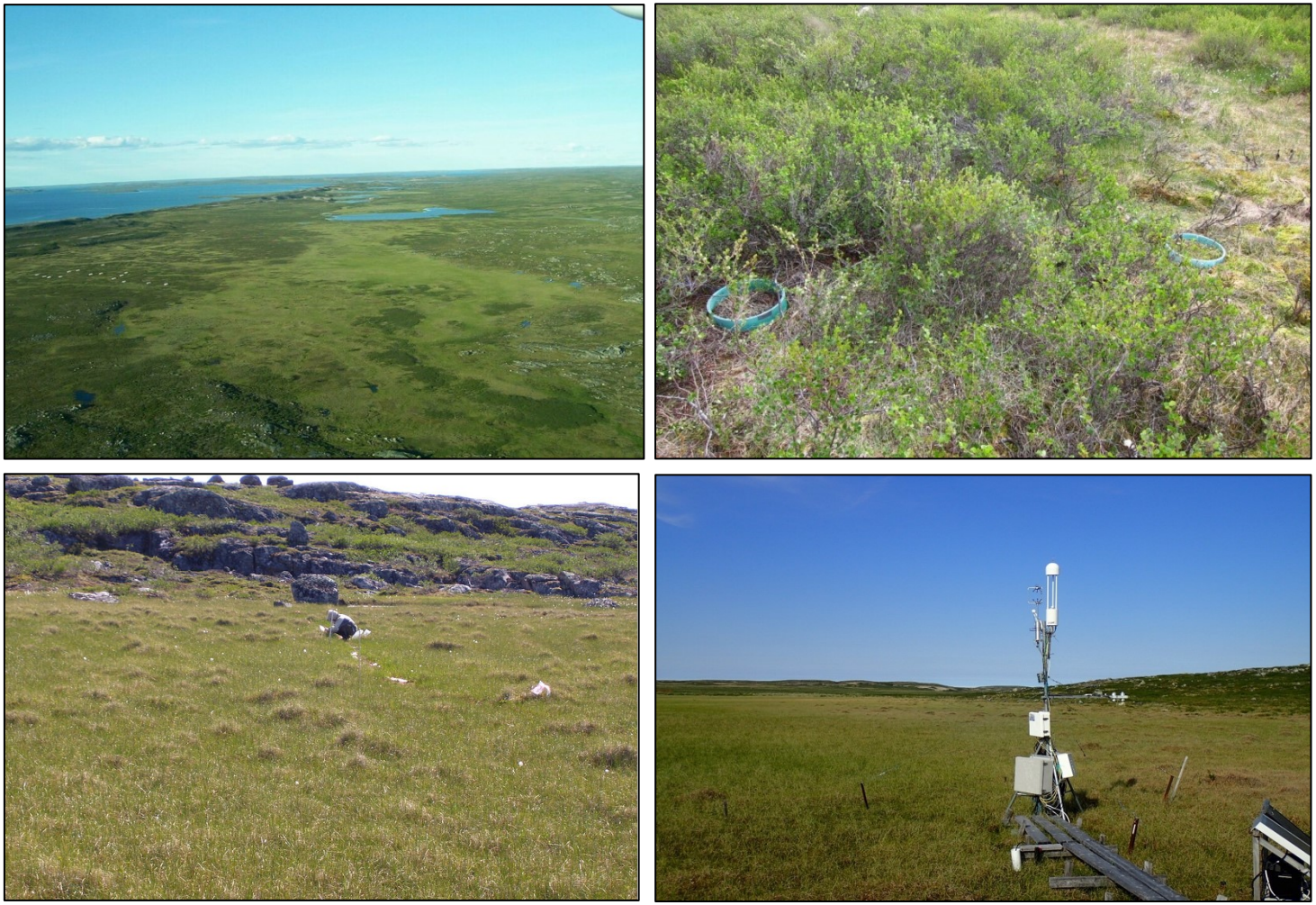

Figure 3. Aerial view of palsas extending across the wet sedge meadow (top left). Palsa and collapse scar features including two collars for F_{CH4} measurements (top right), EC station looking east (bottom right) and view from the EC tripod looking south toward the lawn and tussock collars (bottom left) (Photos: E. Humphreys).

Figure 4. Peat (0-40 cm) from the area surrounding the EC tower (left) and underlying sediment core from an area defined by palsas and collapse scars (right) with segregated ice lenses (photos: E. Humphreys).

3.2 Chamber measurements

The static non-steady state chamber method was used to measure F_{CH4} during the growing seasons of 2008-2017. Ten permanent collars were set up at plots characterized by both hummock and lawn microtopography from 2008-2017. Six collars were located to areas characterized by palsas and collapse scar features (2009-2010 and 2015-2017). Although the palsa and collapse scar collars did not all remain at exactly the same locations over all the years, the microform characteristics were relatively consistent within the 4 microform categories. Opaque chambers were sealed to each collar and measured F_{CH4} over 20-minute periods as described by Wilson and Humphreys (2010). At the beginning of each measurement and every 5 minutes after, air was mixed inside the chamber by pumping an attached 60 mL syringe to ensure a homogenous sample and 24 mL of air was sampled and transferred to an evacuated 12 mL vial. All vials were analyzed on a gas chromatograph equipped with a flame ionization detector (GC-FID) (CP 3800, Varian, CA, USA) at Carleton University's Biometeorology lab. The GC-FID was operated at 300°C with He as the carrier gas at a flow rate of 30 mL min^{-1}. Five standards of increasing CH_4 concentration ranging from 1 to 47 ppm along with He were used to develop the linear relationship between concentration and the integrated area under the chromatogram.

Figure 5. Emma Riley and Caitlyn Proctor perform chamber measurements on lawn and tussock plots (left) and a view of lawn and tussock plots along boardwalks at the main fen area (right).

Chamber F_{CH4} was calculated using the following equation:

$$F_{CH4} = \frac{V}{A}\frac{P}{RT}\frac{dx}{dt} \quad \text{[Eq. 2]}$$

where F_{CH4} in nmol m^{-2} s^{-1} is proportional to the rate of change of CH_4 over time (dx/dt). R is the gas constant of 8.314 J K^{-1} mol^{-1}, T is the temperature in the chamber in Kelvin approximated using a thermocouple buried 2 cm below the moss surface beside each collar, P is the barometric pressure in Pa measured at the EC station, and V and A are the chamber volume and area of 31.6 cm^3 and 70.2 cm^2, respectively. The rate of change of CH_4 was determined by the linear regression of five CH_4 concentrations over the 20-minute sampling interval. Up to two anomalous CH_4 concentration were removed from the time series due to sampling or analysis error, precipitation or ebullition events. The rejection of 1 point from a series occurred 32 times and rejection of 2 points from the series occurred twice over 1010 measurements. Regressions with R^2 values of < 0.85 were rejected for quality control purposes except in cases where fluxes were near-zero. Measurements where ebullition or other situations where a single concentration in the time series was inconsistent with a diffusive flux (e.g. non-monotonic relationships), that data point was excluded from the regression analysis. In total 3.4% of the flux measurements were rejected from 1010 measurements. Positive values represent F_{CH4} losses from the surface whereas negative fluxes represent CH_4 uptake by the ecosystem. To compare results to other studies, F_{CH4} were converted to mg CH_4 m^{-2} d^{-1} or mg CH_4 m^{-2} hr^{-1} from nmol m^{-2} s^{-1} using the molecular weight of CH_4 and assuming no diel variation in F_{CH4}.

For plot-level chamber F_{CH4}, several environmental variables were measured adjacent to collars, in an area with similar microtopography, vegetation and apparent moisture status. Soil/peat temperature at 2, 5 and 10 cm depths were read from installed thermocouples using a

digital thermometer (HH91 Portable digital thermocouple, Omega, Laval, QC, Canada). Thaw depth was determined by inserting a 1 cm diameter steel rod vertically into the peat to the depth of resistance. Water table depth (WT) was measured in a well beside each collar using a 'bubbler' (a steel tube with plastic tubing in which air was blown until bubbles were heard and the depth to the water surface was noted). The WT measurements were always performed after chamber F_{CH4} measurements, assuming that the bubbler may introduce CO_2 below the peat surface. Surface volumetric water content (VWC) was measured using a probe (Hydrosense II, Campbell Scientific Inc., Logan, UT, USA) equipped with 20 cm rods inserted vertically into the peat. The default calibration was used and extended linearly on the wet end of the calibration resulting in maximum VWC values of 92%. The Hydrosense II (soil moisture probe) has an accuracy of 3% assuming an electrical conductivity of < 4 dS/m. However, soil moisture measurements are most accurate over space within short time spans. Over multiple years with measurements taken by different people and using an earlier model of the Hydrosense probe, relationships between VWC, period and WT were not consistent. Linear regressions were performed on VWC when greater than 50%, and period readings for each year to gap-fill VWC values when the default calibration range was exceeded. For 2008, VWC and WT did not correlate consistently as VWC values were up to 20% greater than what was possible given the peat bulk density (approximately 0.04 – 0.12 g cm^{-3}) and porosity (approximately 99% - 92%) (calculated using a peat particle density of 1.5 g cm^{-3}, measured using a pycnometer by Silins

and Rothwell (1998)). VWC values for 2008 were thus approximated using the linear relationship between WT and VWC from 2009-2017.

3.3 Eddy covariance measurements

The EC instrumentation was mounted on a 2.5 m tripod and consisted of a 3-D sonic anemometer (R3-50, Gill Institute, Lymington, UK), a CO_2/H_2O open-path infrared gas analyzer (LI-7500, LI-COR Inc., Lincoln, NE, USA) and an open-path low-power CH_4 analyzer (LI-7700, LI-COR Inc., Lincoln, NE, USA). The LI-7500 measures CO_2 and H_2O densities using IR spectroscopy, measuring radiation absorbed by CO_2/H_2O molecules and corresponding concentrations. The LI-7700 measures CH_4 densities using Wavelength Modulation Spectroscopy (WMS), where light emitted from the laser is modulated to a frequency of 1.6 μm, corresponding to a methane absorption band (LI-COR, 2011). The resulting signal is demodulated and compared to a reference signal shape to determine CH_4 concentrations (LI-COR Inc., 2011). Wind speed in three dimensions, CH_4, CO_2 and H_2O concentrations were measured at a rate of 10 Hz and stored on a datalogger (CR3000, Campbell Scientific, Logon, UT, USA).

EC-derived F_{CH4} was measured during the growing seasons of 2015, 2016 and 2017. Mean flux densities of CH_4 were calculated using the EC technique for a 30 min period from the covariance of high frequency vertical velocity and CH_4 density fluctuations (Baldocchi, 2003). Fluctuations were determined as the difference from the 30 min mean after two axis coordinate rotation was applied to account for any sensor tilt. To correct for underestimation of F_{CH4} due to sensor separation, path averaging and other instrumentation characteristics, high frequency spectral corrections were applied following Massman (2000) and low frequency corrections

following Moncreiff *et al.* (2004)). Corrections to account for thermal expansion and dilution by water vapour were applied to 30-minute means following the equations derived by Webb *et al.* (1980) (LI-COR Inc., 2011). An equivalent pressure was calculated to account for the impact of temperature, pressure and water vapour on spectroscopic measurements (LI-COR Inc., 2011). Friction velocity, a measure of turbulence, was determined using the square root of the covariance of vertical (w) and horizontal (u) wind components as described by Aubinet *et al.* (2012). Fluxes were computed using EddyPro v6.2.1 software package (LI-COR Inc., Lincoln NE).

Measurements of F_{CH4} were removed from further analyses when the CH_4 open-path sensor windows were obscured (due to rain, dew, dirt, or during manual or automated cleaning intervals indicated when the analyzer's RSSI, relative signal strength indicator, was less than 20), when the CH_4 analyzer or other EC instruments malfunctioned, and during power failures. Friction velocity thresholds of 0.1 m s^{-1} were applied to remove nighttime measurements with insufficient vertical transport of CH_4. Daily F_{CH4} values were determined as the mean of all retained F_{CH4} when there were at least 8 half hour quality measurements available.

3.4 Environmental variables

Environmental variables were measured continuously at a rate of 5 s and stored as 30-minute averages on two dataloggers (CR21X and CR3000, Campbell Scientific) on the fen tripod. Water table depth was recorded continuously using a float and potentiometer apparatus relative to the peat surface until 2014, after which a pressure level sensor (OTT PLS, OTT Hydromet, Kempton, Germany) was used. Soil temperatures at 5, 10, 20 and 40 cm depths were measured using copper-constantan thermocouples and soil moisture was measured using two

probes (CS616, Campbell Scientific, Edmonton, Canada) (Lafleur & Humphreys, 2008). Upwelling and downwelling PAR were measured using quantum sensors (LI-190SA, LI-COR Inc., Lincoln, NB, USA), 4-component net radiation was measured using solarimeters and pyrgeometers (CNR1, Kipp & Zonen, Delft, The Netherlands), while air temperature and humidity was measured using an HMP45C probe (VaisalaOyj, Helsinki, Finland). Atmospheric pressure and wind speed were measured using a barometer (PTB101B, Vaisala Oyj, Helsinki, Finland) and anemometer and vane (Wind Monitor, R.M. Young, Traverse City, IM, USA), respectively at a weather station approximately 560 m to the NW (Lafleur & Humphreys, 2008).

3.5 Porewater sampling

Porewater samples were taken at three depths at four hummock and four lawn plots 3 times throughout the 2017 growing season. A sipper was constructed using a hollow 0.5 cm diameter steel tube with inlet holes at the bottom 5 cm of the rod. The sipper was inserted into the peat at 5-10, 15-20, 30-35 and 40-45 cm below the surface. A 60 mL Luer-Lok syringe and three-way stopcock was used to withdraw 60 mL of pore water, which was discarded before sampling 25 mL of pore water. The syringe was then filled with 35 mL of ambient air and shaken for two minutes to equilibrate the dissolved gases with the headspace air. The air was stored in an evacuated 100 mL Wheaton serum bottle and later analyzed for CH_4 and CH_4 isotopic signatures described below. The pore water was filtered through a 0.45 μm filter and kept cool until later analysis of DOC, $SUVA_{254}$, and TN.

3.5.1 Dissolved Organic Carbon

Porewater samples were analyzed for TN, DOC and specific UV absorbance ($SUVA_{254}$). Porewater samples of approximately 20 mL were filtered using vacuum filtration with a 0.45 μm

filter paper. They were then acidified with 1M HCl to a pH of 2-3. DOC was measured as 'non-purgeable' organic carbon (NPOC) on a total organic carbon analyzer (Schimadzu TOC-5000A, Schimadzu, Kyoto, Japan) at McGill University. After purging inorganic carbon fractions, OC was combusted to CO_2 and its concentration determined using IR absorption spectroscopy. The samples were then run individually on a UV-Vis spectrophotometer (Cary 60, Agilent, Santa Clara, CA).

3.5.2 Dissolved CH_4 and $\delta^{13}C$

Dissolved CH_4 concentrations were determined using a GC-FID/TCD (GC-2010, Shimadzu, Kyoto, Japan) with a 30 m capillary column (Carboxen PLOT 1010, Supelco, Bellefonte, PA). The GC was calibrated with certified CH_4 standards of 5, 1000, 10000 and 50000 ppm. $\delta\,^{13}C$ was determined using a ^{13}C-CH_4 analyzer (G2201i, Picarro Inc., CA, USA). Samples were first analyzed for dissolved CH_4 on the GC and then diluted using high purity synthetic air (Air Liquide). Sample aliquots of 20 mL were then injected into the G2201i within 1-3 days. These analyses were carried out at the University of Münster by the Ecohydrology and Biogeochemistry Group.

3.6 Vegetation survey

Vegetation characteristics were monitored during the growing season. Leaf area index (LAI) measurements were made using the point frame method (Wilson, 1959) and a handheld plant canopy analyzer (LAI-2200C, LI-COR Inc., Lincoln, NE, USA) at 5 plots on a transect south of the EC station. LAI measurements were taken weekly over the course of seven weeks from late June to August. The point frame method uses a 50 × 50 cm frame with interlacing fishing line to form 25 equal sized 4 x 4 cm grids. The frame was suspended above the

vegetation surface using four bamboo sticks marking the four corners of each plot. At each grid intersection, a thin wire pin was dropped to the surface. The number of times individual species touched the pin was recorded for each plot. A measure of leaf area for each species was calculated based on the number of hits and the plot area. The LAI-2200C calculates LAI from above and below canopy measurements of incoming radiation detected by a fisheye optical sensor. A light scattering correction was applied to each LAI value based on open sky measurements to account for the proportion of radiation not absorbed by the vegetation, which particularly important under direct sun (LI-COR Inc., 2016).

At each flux collar, percent cover was estimated for each species coverage by eye. The percentages were broken down into three broad categories; vascular, non-vascular and sedges.

3.7 Data Analysis

Statistical analysis was performed using R (R 3.3.2, The R Foundation for Statistical Computing, 2016). Each chamber plot was characterized during the 2017 growing season and was used to investigate factors influencing spatial and temporal variations in chamber F_{CH4} using linear mixed effect models with categorical variables (microform), vegetation characteristics (% cover *Carex /Eriophorum* spp.) and environmental variables (air/peat temperature, VWC, WT and thaw depth). Over all years, spatial and temporal variations in chamber F_{CH4} were analyzed using multiple linear regressions. Logarithmic transformations to F_{CH4} were applied when necessary to meet the assumptions of parametric tests. When F_{CH4} included negative values, F_{CH4} were translated before transformation based on minimum values. To investigate spatial effects, models were performed using values from all plots and then with plots separated by microform. To isolate the spatial components driving F_{CH4} variability, a model was run with values averaged

by microform. To investigate the temporal effects on F_{CH4} variability, data were investigated over multiple years and included year and microform as fixed effects when all data were combined. Repeat measures at a given location were accounted for by setting collar as a random effect.

Regression trees and principle component analysis (PCA) were used to identify the variables associated with spatial and temporal variations in 2017 chamber F_{CH4} using 'rpart' and 'party' packages for tree construction and design, respectively (R, R Core Team, 2016). Default settings in rpart [v. 4.1-13] were used. CART is a non-parametric analysis that splits data using recursive partitioning. CART analyzes the divisions in explanatory variables that best reduces variance in the response variable (Lawrence & Wright, 2001). The result is a hierarchical tree where each branch is defined by the conditions that will likely produce certain response variable values based on the dataset. The results of the CART were then compared with a principle components analysis (PCA) and multiple linear regression models.

The EC footprint determines the surface area measured by the gas analyzer and is defined as the contribution of each surficial feature to the vertical flux (Aubinet *et al.*, 2012). The distance of the footprint from the tower depends on atmospheric stability and surface roughness, where unstable conditions and increased turbulence results in shorter distances (Aubinet *et al.*, 2012). An analysis of the EC flux footprint was performed following Kljun *et al.* (2004) in EddyPro v6.2.1. The 70% cumulative flux distance sometimes extended beyond 150 m from the EC tower. These F_{CH4} data points as well as those when the distance was greater than 115 m in the SE direction were filtered as they extended beyond the wetland. The 70% cumulative flux distance and peak flux distance were plotted using a circular plot frame, so that these values could be visualized relative to the EC tower. They were then compared to a simplified vegetation

map of the wetland and the surrounding area. Using the same plot and map, F_{CH4} and wind direction were plotted when air temperature was greater than 15°C to relate source area to F_{CH4} during relatively warm periods (and to remove the potential bias of early growing season F_{CH4} when plants were still developing and soil thaw was minimal).

4 Chapter: Results

4.1 Spatial variability in F_{CH4}

The microforms differed considerably in their vegetation, edaphic and microclimate characteristics and F_{CH4} (Figure 6, Table 1). The palsas were much drier with no WT above the frost table through the growing season and near-zero F_{CH4}. There was less soil thaw at the palsa locations despite warmer near surface peat soil temperatures. Collapse scars had comparable VWC, thaw depth and WT values to tussock plots while mean F_{CH4} were substantially lower for all years. Collapse scars also had the lowest percent cover of both vascular plants and sedges, and highest percent cover of *Sphagnum*. Lawns had the highest WT, VWC and largest mean F_{CH4} from both the 2017 growing season and all years combined. Temperatures at all depths were relatively consistent between lawns and tussocks, with similar thaw at lawns and tussock plots with differences in depth reflecting the ~5 – 10 cm difference in tussock surface height relative to lawns. Details of F_{CH4} from each year are given in Appendix A.

At the ecosystem scale, EC F_{CH4} was roughly half the magnitude of emissions observed at lawns and tussocks and similar at times to collapse scar F_{CH4} (Figure 6). In 2017, daily mean EC F_{CH4} (± 1 standard error, SE) on the dates chamber measurements were made was 52 ± 4 nmol m^{-2} s^{-1}. In all three years on all dates when EC F_{CH4} were available in July and August, mean daily EC F_{CH4} was 39 ± 1 nmol m^{-2} s^{-1} (54 ± 2 mg CH_4 m^{-2} day^{-1}). In 2016, average May and June EC F_{CH4} was 13 ± 2 nmol m^{-2} s^{-1} (18 ± 2 mg CH_4 m^{-2} day^{-1}) and 28 ± 2 nmol m^{-2} s^{-1} (39 ± 2 mg CH_4 m^{-2} day^{-1}), respectively.

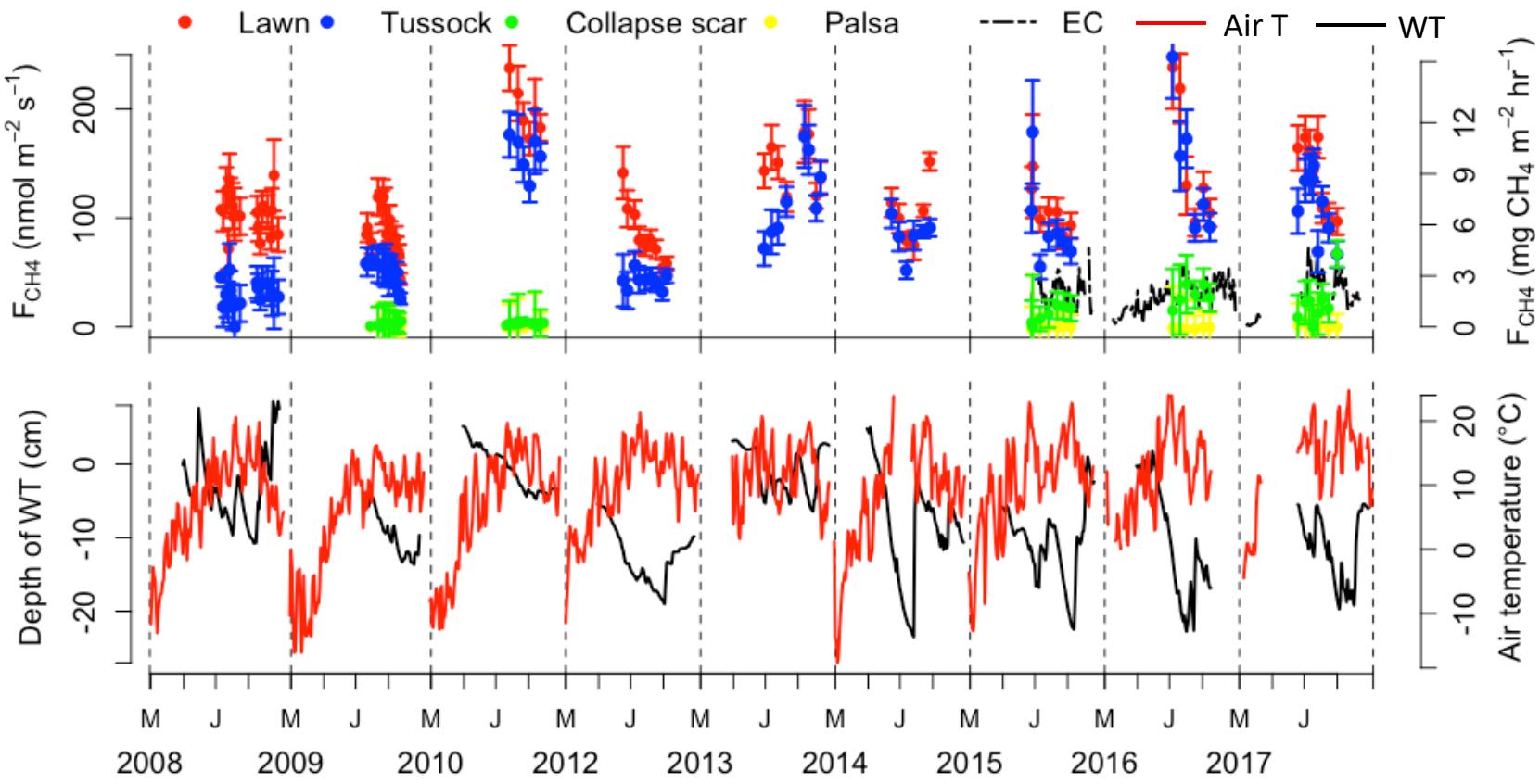

Figure 6. Mean daily F_{CH4} measured using chamber and eddy covariance techniques (top panel) and WT relative to the lawn surface and air temperature (bottom panel) from May-September, 2008-2017 (excluding 2011). May and July are indicated as 'M' and 'J' on the x-axis. Each chamber F_{CH4} point is the mean of 3–5 daytime chamber measurements depending on microform and year. Daily EC F_{CH4} are averaged on days with at least 8 half hourly measurements that met quality criteria. Short gaps of 5 days or less are linearly interpolated.

Table 2. Chamber F_{CH4}, vegetation and environmental characteristics classified by lawn, tussock, collapse scar and palsa microform. Median and/or mean ± 1 standard error are from 8 sampling days during the 2017 growing season and 5 collars each for lawn and tussock microforms and 3 collars each for collapse scars and palsas. Over the 9 years, 408, 404, 63, and 63 F_{CH4} measurements were used to compute means for the lawn, tussock, collapse scar, and palsa microforms, respectively.

	Lawns	Tussocks	Collapse scar	Palsa
Median, mean 2008 – 2017 F_{CH4} (nmol m^{-2} s^{-1})	105, 118 ± 4	64, 77 ± 5	1, 10 ± 2	0, 0± 0
Median, mean 2017 F_{CH4} (nmol m^{-2} s^{-1})	130, 141 ± 10	96, 112 ± 10	2, 20 ± 7	0, 2 ± 2
0-20 cm VWC (%)	86 ± 0	61 ± 2	63 ± 2	34 ± 2
WT (cm)	-7 ± 1	-19 ±1	-14 ± 2	n/a
thaw depth (cm)	41 ± 1	47 ± 1	48 ± 3	38 ± 2
T_{2cm} (°C)	13 ± 1	13 ± 1	17 ± 1	20 ± 1
T_{5cm} (°C)	11 ± 1	11 ±0	13 ± 1	14 ± 1
T_{10cm} (°C)	10 ± 0	10 ±0	9 ± 1	8 ± 1
Vascular plant cover (%)	34 ± 4	54 ±6	12 ± 9	49 ± 14
Carex/Eriophorum spp. cover (%)	30 ± 9	38 ± 4	12 ± 4	20 ± 10
Andromeda polifolia cover (%)	3 ± 2	15 ± 2	n/a	n/a
Sphagnum spp. cover (%)	66 ± 4	46 ± 6	88 ± 9	47 ± 12
0-10 cm bulk density (g soil cm^{-3})*	0.04 ± 0.01	0.04 ± 0.01	0.08 ±0.04	0.08 ± 0.01
12-40 cm bulk density (g soil cm^{-3})#	0.19 ± 0.01	0.19 ± 0.01	n/a	n/a
pH^	5.0± 0.1	4.9 ± 0.1	4.9± 0.1	4.9± 0.01

The following variables are not from the exact 2017 collar locations: *Bulk density values taken from analyses by Piquette (2009).
#Bulk density values taken from analyses of a 40-cm peat core overlain by lawn and tussock microforms by Okolo (Figure 3 in 2008).
^6 samples/microform (A Sarno, personal communication).

Spatial trends in F_{CH4} were investigated using plot-level measurements (Table 2) and mixed linear models (with collar as a random effect) over the 2017 growing season. With all plots combined, microform, specifically lawns and tussocks, explained 75% of the variance in F_{CH4} along with VWC (Table 3). Within the lawn plots, 5-cm soil temperature, percent cover of *Carex/Eriophorum* spp. and VWC explained 61% of F_{CH4} variability (Table 3, Figure 7). For collapse scar plots, although there is an apparent effect of percent cover of *Carex/Eriophorum* spp. (Figure 7), the use of a mixed effect model resulted in significant coefficients for VWC and 10-cm soil temperature only. This model explained 81% of the variance of F_{CH4} for collapse scar plots (Table 3). For tussock plots, thaw depth alone explained 28% of F_{CH4} variability. None of the measured variables were significant for palsa plot F_{CH4}.

PCA was run with four components based on the eigenvalues of each component, where a fifth did not significantly increase the proportion of variance explained. The first principle component (PC1) explained 30% of the variance within the dataset, where the loadings indicated an increase in F_{CH4} with a simultaneous increase in VWC and PC2 explained 28% of the variance within the dataset and loadings indicated an increase in F_{CH4} with increasing percent cover of *Carex/Eriophorum* spp. Loadings on PC3 and PC4 explained less than 25% of the variance within the dataset and did not have obvious relationships with any of the variables.

According to the biplot created with PCA loadings, F_{CH4} correlated most with VWC followed by percent cover of *Carex/Eriophorum* spp. These interpretations were based on the size and direction of the loadings, where arrows of greater length and of similar direction

represent a strong positive correlation. Microform clustered on the biplot due to the strength of these relationships in lawn and tussock plots relative to palsa and collapse scar plots (Figure 8).

The results from the CART were somewhat similar to those of PCA, where microform and VWC were both important in determining differences in chamber F_{CH4}. Percent cover of *Carex/Eriophorum* spp. was not a resultant variable within the tree, likely as percent cover of *Carex/Eriophorum* spp. was statistically significant as an explanatory variable across lawn plots only (Figure 9). Soil temperature (10 cm) and thaw depth also did not appear within the tree (Figure 9).

For the 9-year record of chamber F_{CH4} with all plots combined, 78% of the variability in log transformed F_{CH4} was described using a linear mixed effect model with collar as a random effect and microform, specifically lawn, tussock and palsa, year, 2-cm soil temperature and VWC as fixed effects (Table 3).

Table 3. Linear mixed effect models describing significant spatial and temporal trends in F_{CH4} both among and between lawn, tussock, collapse scar and palsa plots. T_5 and T_{10} are 5 and 10 cm soil temperatures, VWC is soil moisture, TD is thaw depth, %Carex is the percent cover of Carex/Eriophorum *spp*., WT is water table, and lawn, tussock and collapse scars are referred to in equations as the fixed effects of each microform. Collar is set as a random effect in each model with the exception of the model for the 2017 seasonal means where microform was not set as a fixed effect in order to highlight abiotic and biotic variable effects.

Year	Plot type	Equation	R^2	p	RMSE
All	All	$Log(F_{CH4}) = 1.7(Lawn) + 1.5(Tussock) - 0.5(Palsa) + 0.03(Year) + 0.01(T_{10}) + 0.01(VWC) - 69$ nmol m^{-2} s^{-1}	0.76	<0.001	0.4
2017	All	$F_{CH4} = 116(Lawn) + 84(Tussock) + 0.6(VWC) -12$ nmol m^{-2} s^{-1}	0.75	<0.001	34
	Lawn	$F_{CH4} = 7.8(T_5) + 3.8(\%Carex) + 1.7(VWC) – 178$ nmol m^{-2} s^{-1}	0.61	<0.001	31
	Tussock	$F_{CH4} = -2.9(TD) + 238$ nmol m^{-2} s^{-1}	0.28	<0.01	32
	Collapse scar	$Log(F_{CH4}) = -0.3(T_{10}) – 0.1(VWC) + 9$ nmol m^{-2} s^{-1}	0.81	<0.001	0.7
	Mean microform	$F_{CH4} = 3.4(WT) + 3.1(\%Carex) – 4.2(TD) + 249$ nmol m^{-2} s^{-1}	0.77	<0.001	23

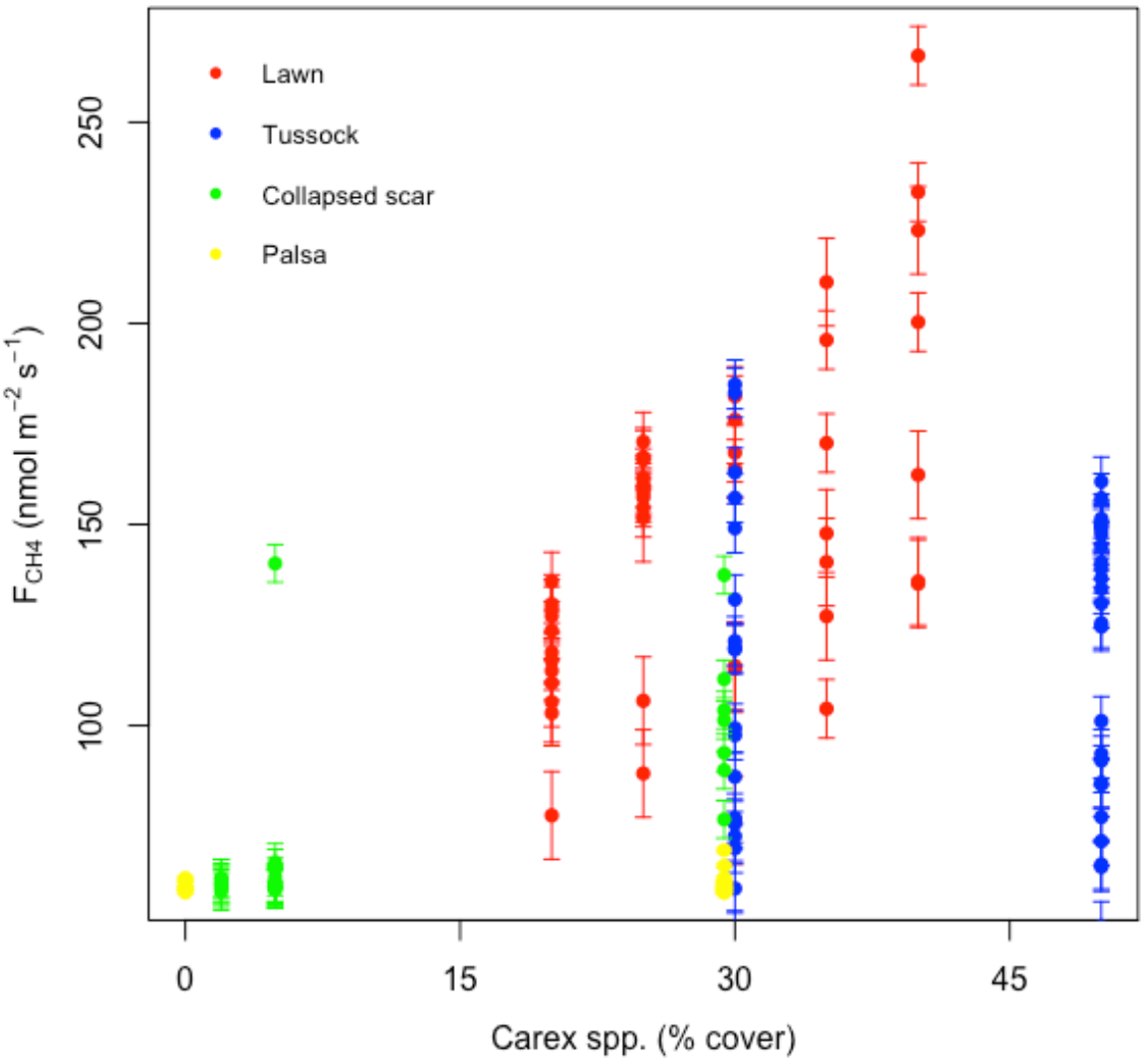

Figure 7. Across lawn plots, 2017 chamber F_{CH4} increased with increasing peak growing season percent cover of *Carex/Eriophorum* spp.

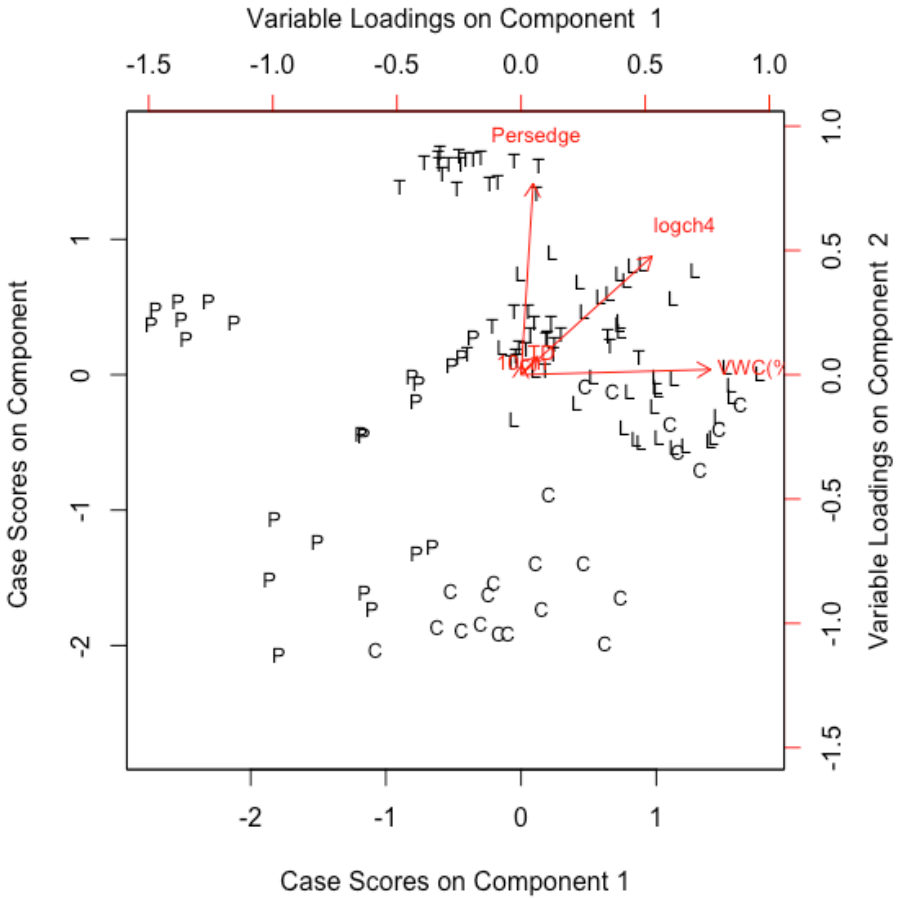

Figure 8. Loadings from PC1 and PC2 from PCA analysis of environmental variables and 2017 chamber F_{CH4}. (L=Lawn, T=Tussock, C=Collapse scar, P=Palsa). TD=Thaw depth, tencm=Soil temperature at a depth of 10 cm, Persedge = % cover of *Carex/Eriophorum* spp., logch = chamber F_{CH4}, VWC = percent volumetric water content.

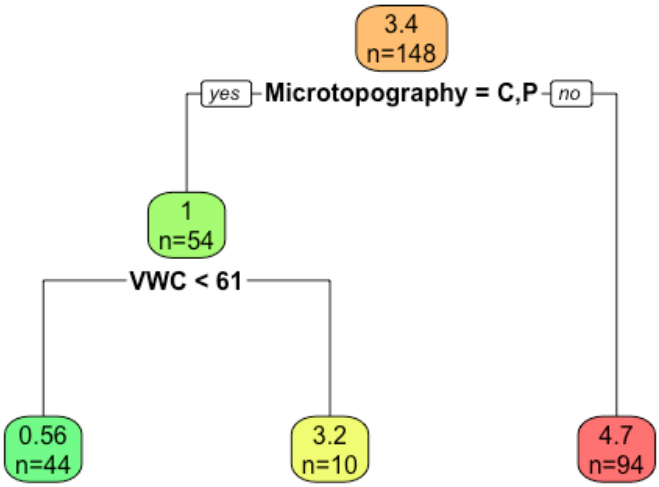

Figure 9. Regression tree where predictor variables for 2017 chamber F_{CH4} are microform (C = Collapse scar and P = Palsa vs. T = tussock and L = lawn), and VWC. Complexity parameters for the first and second split are 0.70 and 0.08, respectively.

4.2 EC footprint analysis

A footprint analysis was performed for the growing season of 2017 to assess the influence of source area on EC F_{CH4}. When the nighttime atmosphere was adequately turbulent ($u_* > 0.1$), the 70% cumulative flux distance (the distance from the tower where 70% of the F_{CH4} originated) was on average 103.4 ± 1.7 m. When the footprint extended beyond the measurement area (> 150 m), EC F_{CH4} were rejected. The peak flux distance (distance upwind from the EC station at which the greatest proportion of the F_{CH4} originated) was on average 36.5 ± 0.2 m.

To examine the spatial variation of EC F_{CH4}, July and August measurements were used when the 70% footprint distances were within 80 m of the flux tower (Figure 10). Lower CH_4 emissions originated from upwind areas between 100° and 290° (approximately SE to NW) which included some of the palsa area. South of the flux tower was an area characterized by lawns and tussocks but also included small ponds at the margins of the fen (pond F_{CH4} was not surveyed). The largest F_{CH4} originated from upwind areas between 300°-60° which largely coincided with an area dominated by lawns and tussocks (Figure 10). The heterogeneity of the surface type surrounding the flux tower resulted in significantly different F_{CH4} ($F=130$, $p<0.001$) as well as significant differences in air temperature, friction velocity, vapour pressure and net radiation (Table 4).

Based on the map in Figure 10, palsas covered 24% and lawns/tussocks 65% of the area within 80 m of the flux tower. It was roughly estimated that collapse scars made up 3% of the palsa area and tussocks made up 30% of the lawn/tussock areas. Ponds, which were not surveyed for F_{CH4}, made up 11% of the area but in this case was assumed to have fluxes similar to lawns. Therefore, lawn, tussock, collapse scar, and palsa area was set to 53, 23, 1 and 23 % of the area, respectively. The average daytime July and August 2017 mean (± SD) F_{CH4} was 51 ±

$2x10^{-2}$ nmol m^{-2} s^{-1} when the daytime 70% flux footprint was within 80 m of the tower (87% of the daytime measurements that met quality control criteria). Weighting the chamber F_{CH4} by the source areas listed above resulted in an average F_{CH4} of 100 ± 4 nmol m^{-2} s^{-1}.

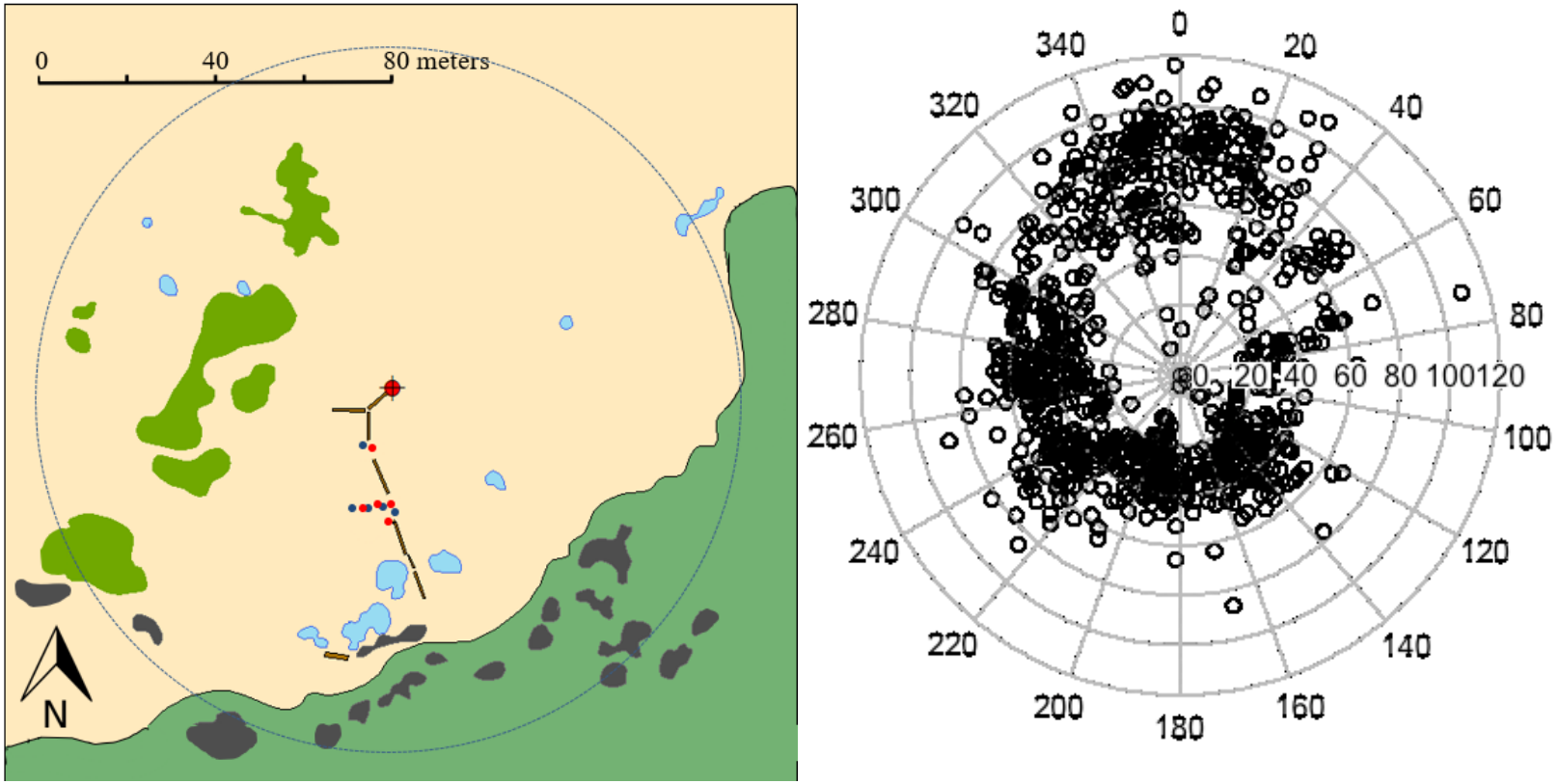

Figure 10. Right: the magnitude of F_{CH4} (scale across center in nmol m^{-2} s^{-1}) from July and August 2017 plotted with wind direction (angle from N noted around the perimeter) when 70% of the flux footprint was within 80 m of the flux tower. Left: the map of the wet sedge meadow (see Figure 2 for legend) with the area within 80 m of the tower circled.

Table 4. Differences in F_{CH4} and climatic variables including air temperature, friction velocity (u_*), vapour pressure (VP), net radiation (Q*) and water table depth (WT) based on source area relative to the EC tower with corresponding standard error. Median F_{CH4} values are noted before mean values. Significant differences ($p < 0.05$) in variables among source areas were determined using an ANOVA and Tukey HSD post-hoc test and are noted by different subscript letters within a column.

Surface type	F_{CH4} (nmol m^{-2} s^{-1})	Air temp. (°C)	u_* (m s^{-1})	VP (kPa)	Q* (W m^{-2})	WT (cm)	Wind direction (°)
Lawn/Tussock	61.1, 60.2 ± 1.28x10^{-4} ^{a}	15.2 ± 0.2^{a}	0.34 ± 0.01^{a}	1.1 ± 0.0^{a}	254 ± 7^{a}	-12.0 ± 0.2	200-236, 320-120
Lawn/Tussock/ Pond	32.2, 33.0 ± 8.18x10^{-4} ^{b}	18.7 ± 0.2^{b}	0.39 ± 0.01^{b}	1.3 ± 0.0^{b}	227 ± 9^{b}	-13.4 ± 0.3	120-200
Palsa	50.0, 50.1 ± 8.8x10^{-4} ^{c}	17.3 ± 0.3^{c}	0.36 ± 0.01^{c}	1.0 ± 0.0^{c}	294 ± 9^{a}	-13.1 ± 0.3	236-320

4.3 Temporal variability

4.3.1 Diel patterns

Half hour daytime EC F_{CH4} varied with radiation driven variables, such as 20-cm soil temperature, air temperature, net radiation and friction velocity, as well as vapour pressure (Figure 11, Table 5). Other variables including wind direction, relative humidity, and other soil temperature depths did not improve the model. The relationship between daytime EC F_{CH4} and these variables differed based on year, where friction velocity explained a significant proportion of variability across all three years (Table 5). The log transform of EC F_{CH4} was used in the models for years where data was positively skewed from large yet infrequent F_{CH}, which increased both the normality of the data distribution and the R^2 of resultant models.

Nighttime EC F_{CH4} was typically lower (22.6 ± 0.8 nmol m^{-2} s^{-1}) than daytime F_{CH4} (50.8 ± 2.9 nmol m^{-2} s^{-1}) and was associated with relatively low near-surface soil temperatures and/or low friction velocity and net radiation values. In contrast, chamber F_{CH4} collected over a 24-hour period showed little diel variation (Figure 12). Both air and 2-cm soil temperature explained a significant proportion of variance of EC F_{CH4} during this period ($R^2 = 0.45$, $p<0.001$).

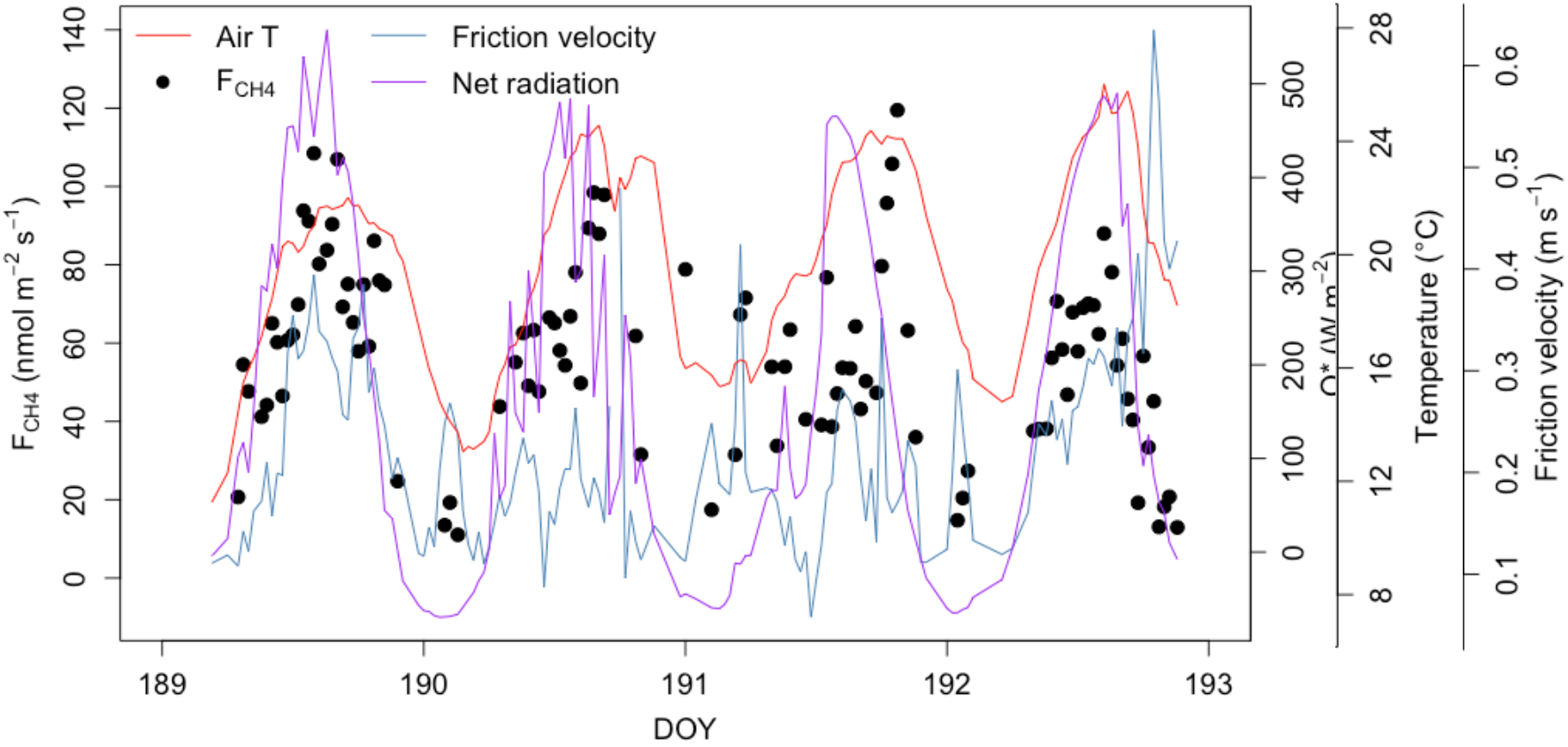

Figure 12. EC F_{CH4}, friction velocity, air temperature (Air T) and net radiation (Q*) over 4 days (July 8th – 11th, 2017)

Table 5. Linear regression equations for daytime (8:00-17:00) EC F_{CH4} and for 24 hr values July 10-11, 2017, coinciding with the dates with 24 hr chamber F_{CH4}. T_{air}, T_5, T_{10}, T_{20} are air, 5, 10 and 20-cm soil temperature, respectively, VP is vapour pressure, Q* is net radiation and u_* is friction velocity.

Year	Equation	R^2	p
2015	$\log(\text{daytime } F_{CH4}) = 0.0014(Q^*) - 0.9(u_*) - 0.5(VP) + 4.3$ nmol m^{-2} s^{-1}	0.43	<0.001
2016	$\log(\text{daytime } F_{CH4}) = 0.13(T_{20}) - 0.1(u_*:T_{20}) + 3.3$ nmol m^{-2} s^{-1}	0.39	<0.001
2017	$\log(\text{daytime } F_{CH4}) = 0.5(u_*) + 0.05(T_{air}) + 0.001(Q^*) + 2.6$ nmol m^{-2} s^{-1}	0.50	<0.001
2017 (July 10-11)	$\log(24\text{hr } F_{CH4}) = 0.17(T_{air}) - 0.11(T_2) + 1.7$ nmol m^{-2} s^{-1}	0.45	<0.001

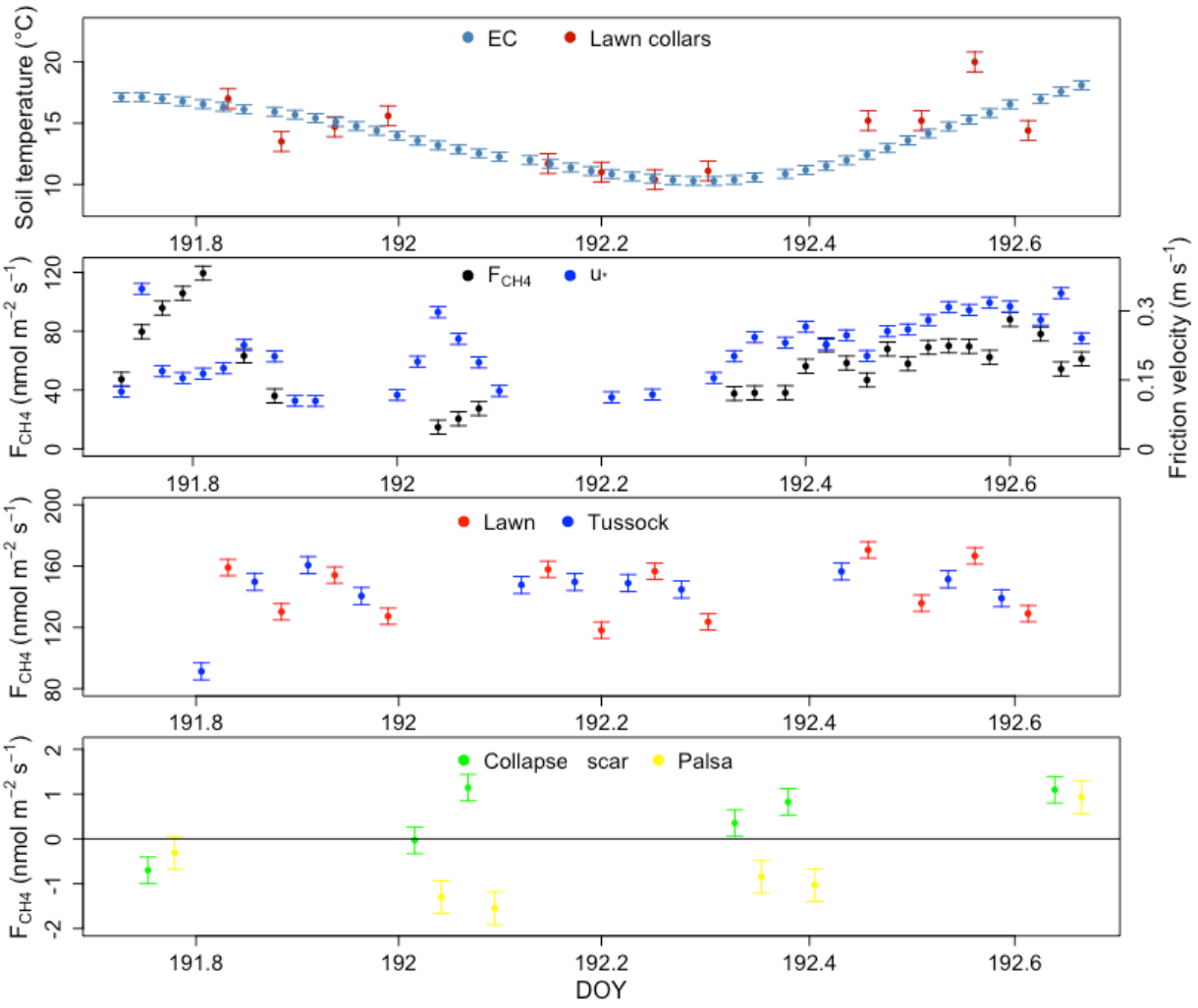

Figure 13. Diel EC F_{CH4}, soil temperature and friction velocity (u_*) from July 10-11 (DOY 191-192), 2017. Soil temperature measurements are from the EC station (5 cm) and from the lawn collars (2 cm). The bottom two panels display a 24-hour set of F_{CH4} measurements using non-steady state chambers. Measurements were performed on two lawn plots, two tussock plots, and one collapse scar and palsa plot. The horizontal line marks where values become negative and therefore represent CH_4 uptake.

4.3.2 Seasonal patterns

Both EC and chamber F_{CH4} varied within a growing season (Figure 6) as well as among years. In most years, EC and chamber F_{CH4} was greatest in late June/early July (Figure 6). Generally, soil temperatures and WT were negatively correlated for all depths, with the greatest correlations at depths of 40 and 60 cm (r = 0.50-0.90). The EC F_{CH4} record was near continuous from May through September 2016. In that year, the model with the greatest coefficient of determination included 20 cm soil temperature and WT (Table 6, Figure 14). No other variables (e.g. air temperature, vapour pressure, relative humidity, etc.) improved the model. Combining the two variables and adding interaction terms did not improve the models. In 2015 and 2017, only July and August EC F_{CH4} measurements were available. The models with highest R^2 differed among all three years (Table 6).

All 9 growing seasons between 2008 and 2017 were analyzed to investigate seasonal trends in chamber F_{CH4}. VWC and 10-cm soil temperature explained a significant proportion of seasonal variance in chamber F_{CH4} for all growing seasons combined (2008-2017). A linear mixed effect model predicted that a 5 % increase in VWC and a 5 °C increase in air temperature would result in an F_{CH4} increase of 14 nmol m^{-2} s^{-1} where collar and year were input as random effects. When chamber F_{CH4} were separated by year, relationships between soil or air temperature, VWC, WT and F_{CH4} varied (Table 6). Several growing seasons displayed relationships between F_{CH4} and site-level WT. These relationships were most pronounced in 2009, 2010, 2012 and 2017 (Table 6, Figure 13), where a linear mixed effect model resulted in significant coefficients for WT for the four growing seasons combined. During the 2013 growing

season, variability in F_{CH4} was explained by soil temperature alone. This year was particularly wet and cold (Figure 6) with mean air temperature and WT of 12.6°C and -2.5 cm, respectively on measurement days. LAI values determined using both the point frame method and the handheld canopy analyzer peaked mid-growing season during all years but did not explain seasonal F_{CH4} variability from 2008-2017.

Table 6. Linear regressions and mixed effect models for mean daily EC F_{CH4} and chamber F_{CH4}, respectively across multiple growing seasons. MEMs were performed using collar as a random effect from 2008-2017 and year when all years were combined. T_{air}, T_5, T_{10}, T_{20} are air, 5, 10 and 20-cm soil temperature, respectively, VWC is soil moisture, WT is water table depth, VP is vapour pressure, Q* is net radiation, u_* is friction velocity, TD is thaw depth, %Carex is percent cover of *Carex/Eriophorum* spp. and m is microform.

	Year	Model	R^2	p
EC	2015	$F_{CH4} = -52.5(u_*) - 22.4(VP) + 0.07(Q^*) + 67.3$ nmol m^{-2} s^{-1}	0.37	<0.001
	2016	$F_{CH4} = 1.3(T_{20}) - 0.61(WT) + 18.3$ nmol m^{-2} s^{-1}	0.41	<0.001
	2017	$\log(F_{CH4}) = 0.16(T_{20}) - 4.6$ nmol m^{-2} s^{-1}	0.54	<0.001
	all	$F_{CH4} = 2.7(T_{20}) + 2.3(year) + 0.06(Q^*) - 4.7$ nmol m^{-2} s^{-1}	0.36	<0.001
Chamber	2008	$F_{CH4} = 1.8(T_{air}) + 1.3(VWC) - 55.3$ nmol m^{-2} s^{-1}	0.39	<0.001
	2009	$F_{CH4} = 2.6(WT) + 1.8(T_{10}) + 78.0$ nmol m^{-2} s^{-1}	0.70	<0.001
	2010	$F_{CH4} = 11.7(WT) + 214$ nmol m^{-2} s^{-1}	0.41	<0.05
	2012	$\log(F_{CH4}) = 0.09(WT) + 5.8$ nmol m^{-2} s^{-1}	0.45	<0.01
	2013	$F_{CH4} = 3.6(T_5) + 90.5$ nmol m^{-2} s^{-1}	0.25	<0.05
	2014	$F_{CH4} = 4.4(T_5) + 2.8(VWC) - 134$ nmol m^{-2} s^{-1}	0.38	<0.05
	2015	$F_{CH4} = 4.6(T_{10}) + 2.1(VWC) - 92.8$ nmol m^{-2} s^{-1}	0.79	<0.01
	2016	$F_{CH4} = 3.0(VWC) - 82.4$ nmol m^{-2} s^{-1}	0.42	<0.01
	2017	$F_{CH4} = 2.3(\%Carex) - 3.5(TD) + 2.0(WT) + 222$ nmol m^{-2} s^{-1}	0.64	<0.001
	all	$\log(F_{CH4}) = 0.01(T_2) + 0.01(VWC) + 0.04(m{:}year) + 67$ nmol m^{-2} s^{-1}	0.76	<0.001
	2009-2012, 2017	$F_{CH4} = 3.4(WT) + 110.0$ nmol m^{-2} s^{-1}	0.45	<0.001

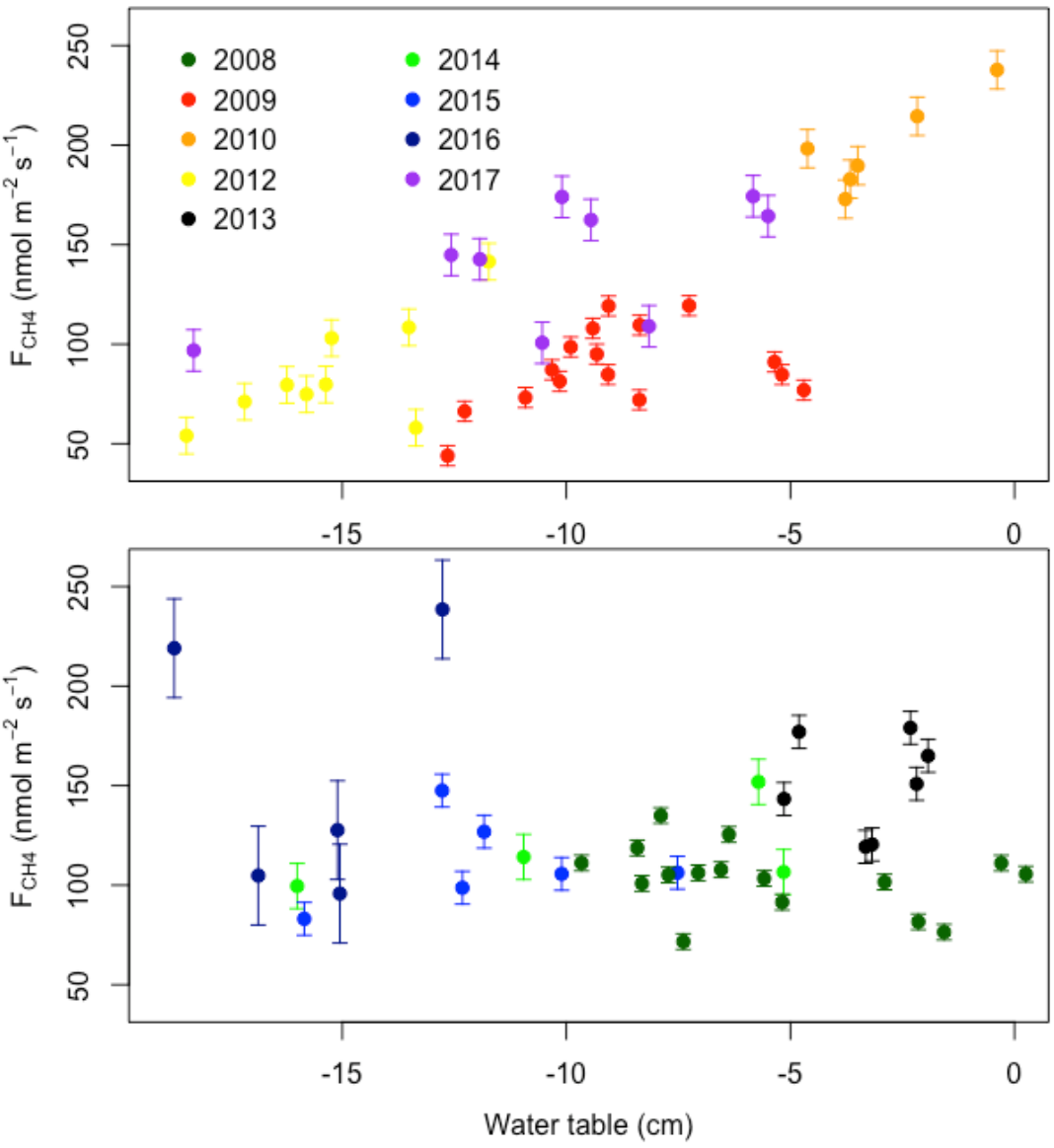

Figure 14. Daily mean lawn chamber F_{CH4} and site-level WT between 2009-2012 and 2017 (top) and from 2008, 2013-2016 (bottom). Years were separated based on significant coefficients for WT as an explanatory variable for chamber F_{CH4} with collar as a random effect.

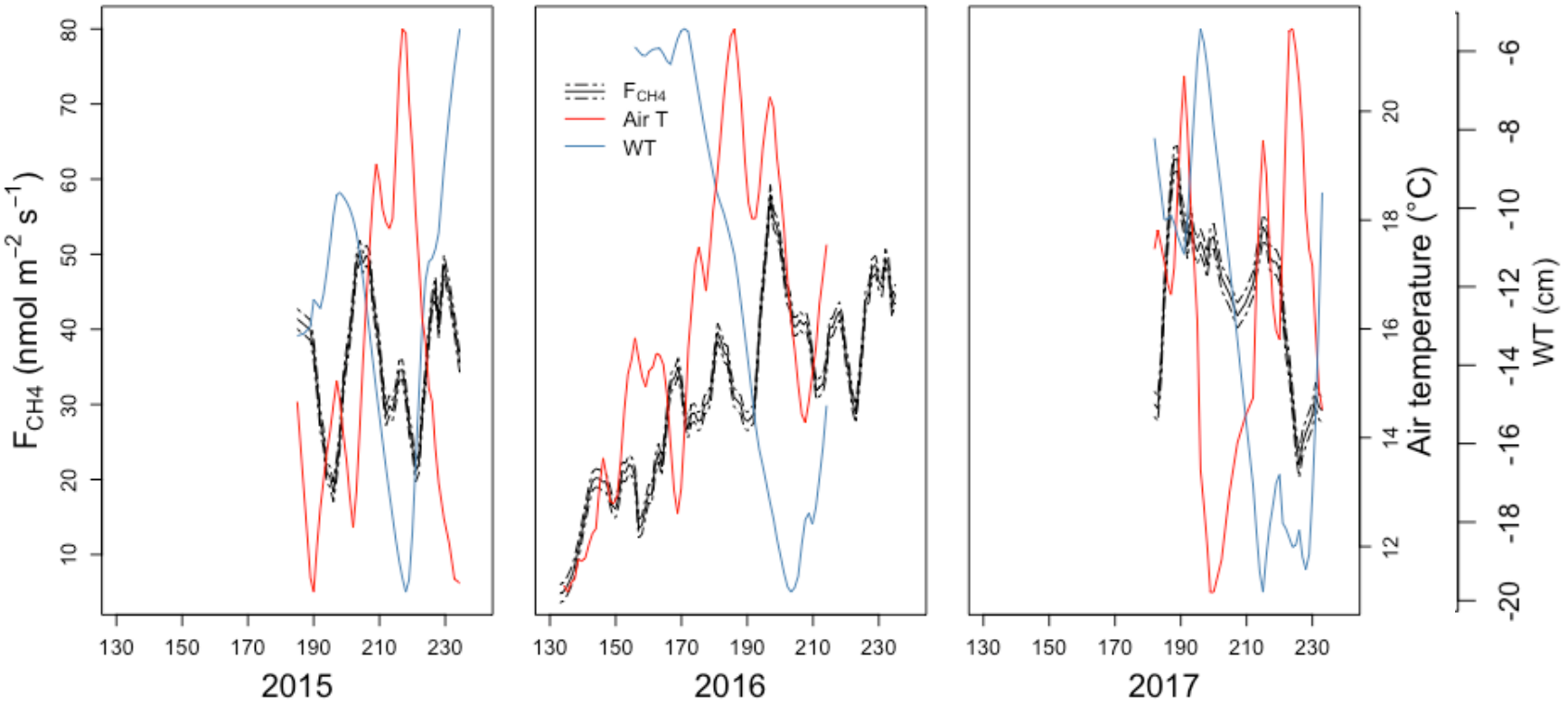

Figure 15. Five-day moving averages using half hour measurements of EC F_{CH4}, WT and air temperature over the 2015, 2016 and 2017 growing seasons.

4.3.3 Interannual trends

As noted earlier, year was a significant variable in a mixed effects model describing spatial and temporal variations in chamber F_{CH4} (Table 6). Large year-to-year variations in F_{CH4} are best highlighted by tussock and lawn chamber F_{CH4} which varied from 40 ± 2 nmol m^2 s^{-1} (average in 2008) to 159 ± 11 nmol m^2 s^{-1} (average in 2010) and 86 ± 6 nmol m^2 s^{-1} (average in 2012) to 200 ± 11 nmol m^2 s^{-1} (average in 2010), respectively. Year-to-year variation in F_{CH4} was smaller for collapse scars (3 ± 1 nmol m^2 s^{-1} in 2009 and 29 ± 10 nmol m^2 s^{-1} in 2016), and negligible for palsas (-1 ± 0.3 nmol m^2 s^{-1} in 2016 and 3 ± 0.3 nmol m^2 s^{-1} in 2010) (Figure 6). Greatest emissions from lawn and tussock microforms were during the 2010 growing season when mean VWC values were 86 ± 2 % and 92 ± 1 % for tussocks and lawns, respectively (Figure 6, Appendix 1, Table A-1&A-2) and the water table was on average 0.7 cm below the lawn surface and never dropped below 7 cm of the surface (Figure 6). Lowest emissions from lawn microforms and the second lowest emissions from tussock microforms were both during the 2012 growing season, when mean VWC was the lowest (or second lowest) of all years and the average water table was 12.4 ± 0.4 cm below the peat surface. The water table dropped further below the surface in other years (e.g. 2014 through 2017) but did not remain as consistently low (Figure 6).

Mean July and August EC F_{CH4} varied by only 3 to 9 nmol m^{-2} s^{-1} among the three years. Mean July and August EC F_{CH4} were largest in 2017, coinciding with the highest July and August soil and air temperatures of the three growing seasons (Appendix 1, Table A-3). As noted above, models describing seasonal variation in EC F_{CH4} varied

among the three years (Table 6). The only variables that consistently explained temporal variations in EC F_{CH4} were 20-cm soil temperature and net radiation (Table 6).

4.4 DOC, TN, SUVA

Porewater samples were taken on three days throughout the 2017 growing season; July 6th, 22nd and August 6th. Due to spatial differences in WT depth, porewater was extracted from a minimum depth of 5 cm for lawn plots and 15 cm for tussock plots. Porewater was extracted from only one of the collapse scar plots on one day where the WT was within 5 cm of the peat surface. Otherwise WT levels were too low to obtain samples from respective depths from the peat surface. This collapse scar plot had low DOC, TN, dissolved CH_4 and high $SUVA_{254}$ (mean values from 3 depths between 5 and 40 cm below the surface of 19.1 ± 1.4 mg L^{-1}, 0.97 ± 0.23 mg L^{-1}, 1132 ± 439 ppm and 6.8 ± 0.2 L mgC^{-1} m^{-1}, respectively) indicative of lower rates of microbial activity and relatively aromatic DOC. At the 15 and 30 cm depths where DOC, TN, and dissolved CH_4 were measured regularly at both depths, there were no significant differences associated with depth, date or microform (Appendix, Table A-6). Only $SUVA_{254}$ was significantly lower in lawns at these two depths (Appendix, Table A-6).

Within the tussock and lawn plots, trends in concentrations of DOC, TN and dissolved CH_4 and $SUVA_{254}$ were not always consistent across the three sampling dates and at various depths. For tussocks, DOC increased with depth (R^2=0.39, $p<0.001$), $SUVA_{254}$ decreased (R^2=0.43, $p<0.001$) and TN increased (R^2=0.66, $p<0.001$). There were no statistically significant changes in dissolved CH_4 with depth at tussock plots. Similar trends were observed for lawns where DOC increased with depth (R^2=0.23,

$p<0.01$), $SUVA_{254}$ decreased ($R^2=0.20$, $p<0.05$), and TN increased ($R^2=0.47$, $p<0.001$) while dissolved CH_4 also increased ($R^2=0.19$, $p<0.05$).

There was a tendency for DOC to decrease (Figure 16) and $SUVA_{254}$ to increase over the growing season 15 cm below tussock surfaces (Figure 15). However, these temporal patterns were not statistically significant ($R^2=0.70$, $p=0.10$; $R^2=0.76$, $p=0.08$, respectively). Similarly, there was no significant change in TN while there was a significant decrease in dissolved CH_4 ($R^2=0.29$, $p<0.01$) at 15 cm for tussock surfaces and for all depths below lawn surfaces ($R^2=0.30$, $p<0.01$). There were no discernable differences over time at the lawns for any of the other porewater variables. Dissolved CH_4 correlated with F_{CH4} across locations (30-cm CH_4 $r=0.46$, $p < 0.05$; 40-cm CH_4 $r=0.81$ $p <0.05$) while there was no significant correlation for 5 and 15 cm depths.

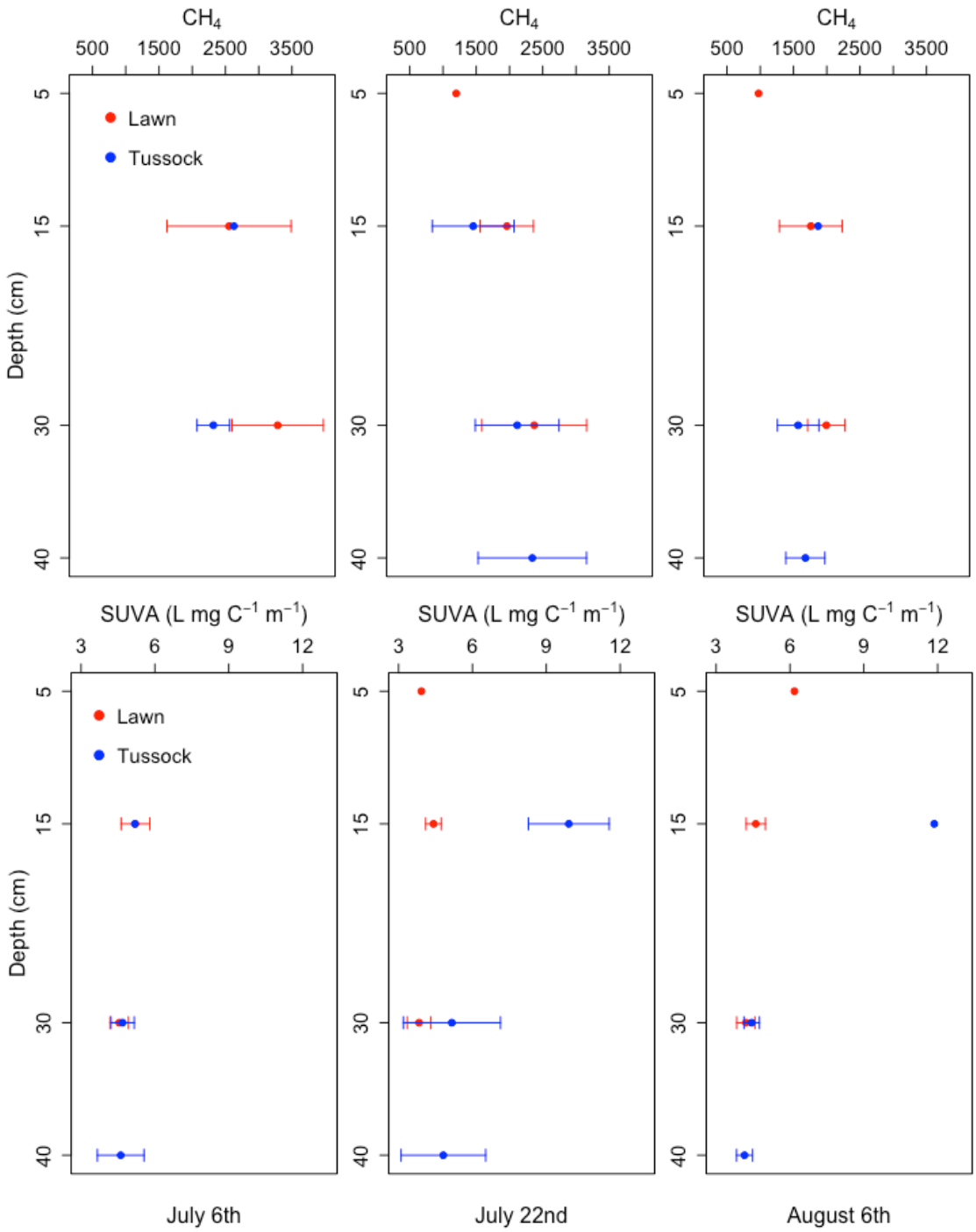

Figure 16. Dissolved CH_4 (ppm) and SUVA (L mg C^{-1} m^{-1}) for lawn and tussock plots at depths of up to 40 cm on three different dates in 2017.

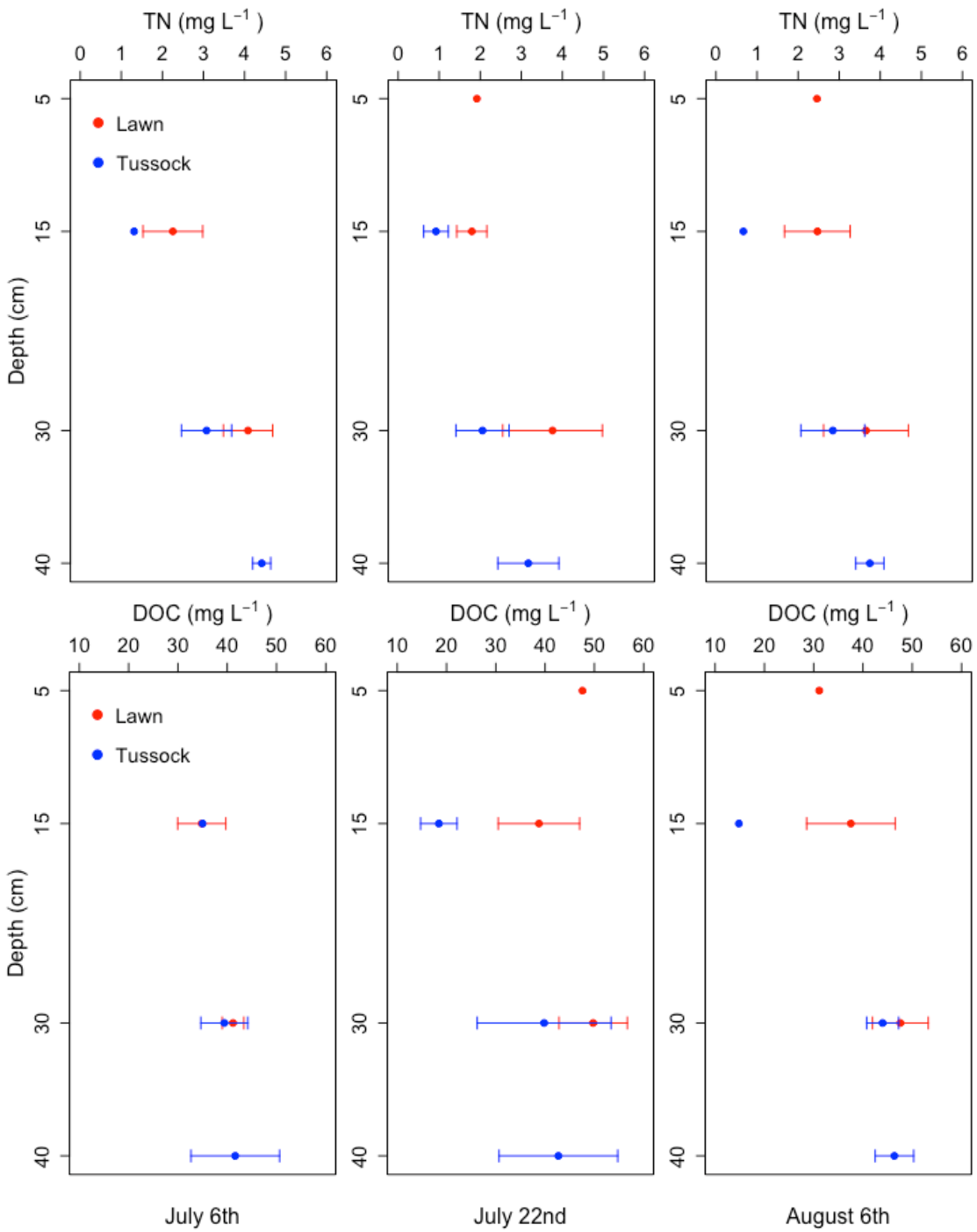

Figure 17. TN (mg L^{-1}) and DOC (mg L^{-1}) for lawn and tussock plots at depths of up to 40 cm on three different dates in 2017.

4.5 CH_4 and CO_2 isotope signatures

Delta ^{13}C-CH_4 in the 2017 porewater samples ranged from -53.6 ‰ to -77.2 ‰, with a mean of -64.9 ± 1.0 ‰ for all depths across all sample dates at lawns and -62.6 ± 1.0 ‰, at tussocks. The difference between tussock and lawns was more notable at a depth of 15 cm (Figure 17) where lawn CH_4 signatures were heavier (-57.1 ± 0.9 ‰) than tussocks (-65.7 ± 1.7 ‰), however this difference was not significant nor were the differences at 30 cm significant (Appendix, Table A-6). There was a tendency for depletion in $\delta^{13}C$-CH_4 with depth (model: $\delta^{13}C$-CH_4 = -0.29 (depth) – 52.8 ‰ (RMSE: 3.3, $p<0.01$)) and a negative relationship between $\delta^{13}C$-CH_4 and $\delta^{13}C$-CO_2 at 30-40 cm for tussock plots ($R^2=0.30$, $p<0.01$). There was also a significant depletion of $\delta^{13}C$-CH_4 with depth at lawns but only on July 6th (model: $\delta^{13}C$-CH_4 = -0.34 (depth) – 58.3 ‰ (RMSE=1.16, $p<0.001$). Porewater on this sampling date also had the highest dissolved CH_4 at 30 cm and the highest F_{CH4} for both tussock and lawn plots (Table 7). $\delta^{13}C$-CH_4 values became increasingly depleted over the growing season 15 cm below lawn surfaces (Table 7).

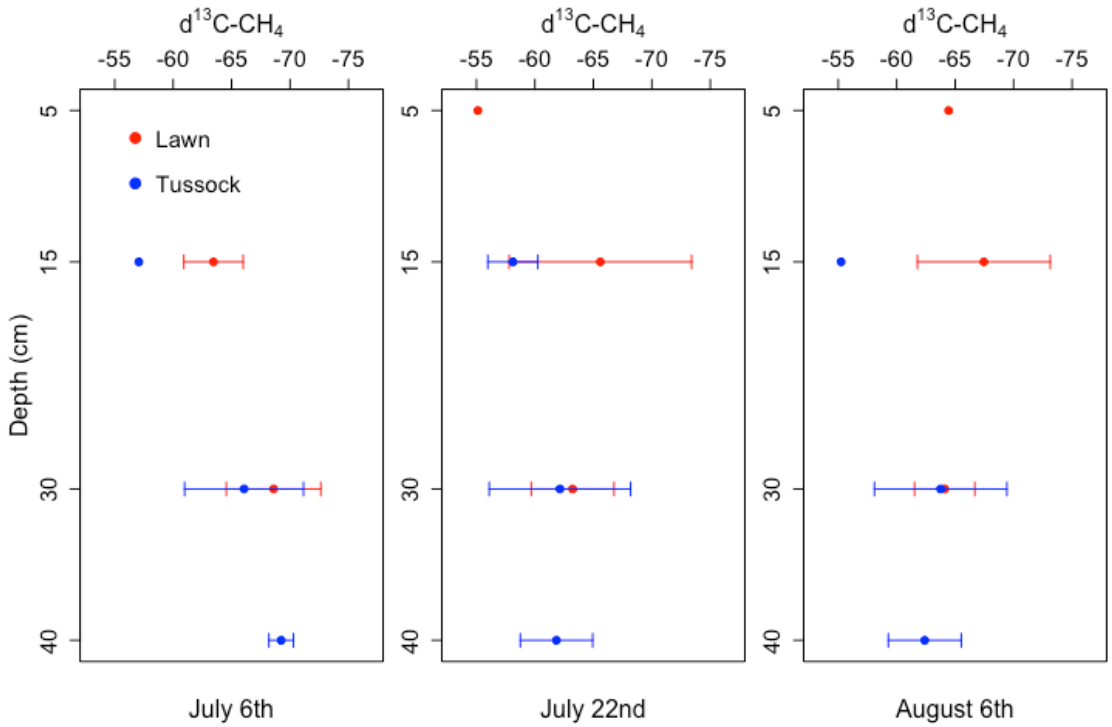

Figure 18. Methane isotope composition from porewater CH_4 with increasing depth for lawn and tussock plots on three different dates in 2017.

Table 7. Dissolved CH_4 concentrations and $\delta^{13}C$ values for CH_4 and CO_2 from porewater samples from 5 cm to a maximum depth of 40 cm from the peat surface. Standard error (SE) is listed for measurements with more than 1 replicate plot for the corresponding date.

Date	Microform/ Depth (cm)	$\delta^{13}C$-CH_4 (‰)				$\delta^{13}C$-CO_2 (‰)				$[CH_4]$ (ppm)				F_{CH4} (nmol m^{-2} s^{-1})	WT (cm)
		5	15	30	40	5	15	30	40	5	15	30	40		
July	Collapse scar	-65.1	-65.5	-71.3		-24	-21.4	-19.1		303.4	1293.4	1798.1		66.3	0.0
	Lawn		-63.5 ± 1.5	-68.6 ± 2.3			-11.3 ± 0.6	-10.3 ± 0.6			2552.5 ± 539.2	3285.3 ± 396.3		162.4 ± 14.0	-5.8 ± 0.9
	Tussock		-57.1	-66.1 ± 2.9	-69.2 ± 0.7		-12.7	-12 ± 0.2	-10.9 ± 0.9		2627.4	2317.2 ± 141.7	3537.0	140.1 ± 15.3	-19.4 ± 3.6
July 22nd	Lawn	-55.1	-65.6 ± 3.9	-63.2 ± 1.8		-13.1	-12.2 ± 0.8	-12.8 ± 1.3		1199.1	1959.7 ± 200.5	2372.1 ± 393.9		100.7 ± 19.6	-6.6 ± 1.0
	Tussock		-58.1 ± 1.5	-62.1 ± 3.0	-61.8 ± 1.5		-12.9 ± 0.7	-13.2 ± 0.9	-12.5 ± 0.5		1453.2 ± 434.6	2115.2 ± 314.5	2343.3 ± 407.5	90.9 ± 8.9	-15.2 ± 2.1
August 6th	Lawn	-64.4	-67.5 ± 2.8	-64.1 ± 1.3		-17.7	-11.8 ± 0.6	-13.6 ± 1.1		975.2	1758.8 ± 235.7	1994.2 ± 140.5		96.9 ± 17.8	-13.5 ± 1.5
	Tussock		-55.2	-63.8 ± 2.8	-62.4 ± 1.6		-13.8	-13.7 ± 1.0	-15.0 ± 1.0		1870.4	1569.6 ± 155.9	1678.5 ± 146.4	66.6 ± 14.8	-20.4 ± 1.3

4.6 Source CO_2 and CH_4 isotope signatures

Source isotopic signatures were roughly approximated using the Keeling plot approach. This method requires the isotope signatures of both emitted and atmospheric CH_4 and CO_2. Isotope signatures of emitted CH_4 were collected from tussock and lawn plots on August 7th and August 21st 2014 by leaving the chamber closed for 20 min and sampling at the end of this period. The source δ^{13}C-CH_4 values of both lawns and tussocks ranged from -89 ‰ and -69 ‰, while source δ^{13}C-CO_2 values range from -27 ‰ to -20 ‰. Mean source δ^{13}C-CH_4 values were -76.5 $\pm$ 1.9 ‰ and -71.6 $\pm$ 2.0 ‰ and mean source δ^{13}C-CO_2 values of -23.3 $\pm$ 0.7 and -26.1 $\pm$ 1.3 ‰ for lawn and tussock plots, respectively (Figure 18). There were no significant differences between lawn and tussock source isotopic signatures using both sampling dates combined. For lawn plots only, source δ^{13}C-CO_2 was significantly less negative on August 21st relative to August 7th ($t=3.01$, $p<0.01$). The source δ^{13}C-CH_4 was significantly more negative for lawn plots on August 21st relative to August 7th ($t=-2.8$, $p<0.04$) (Figure 18). The production pathway for both lawn and tussock CH_4 is likely carbonate reduction (e.g. hydrogenotrophic methanogenesis) as characteristic signatures range from 110‰ – 60‰ while acetate fermentation signatures range from 65‰ – 50‰ (Whiticar, 1999).

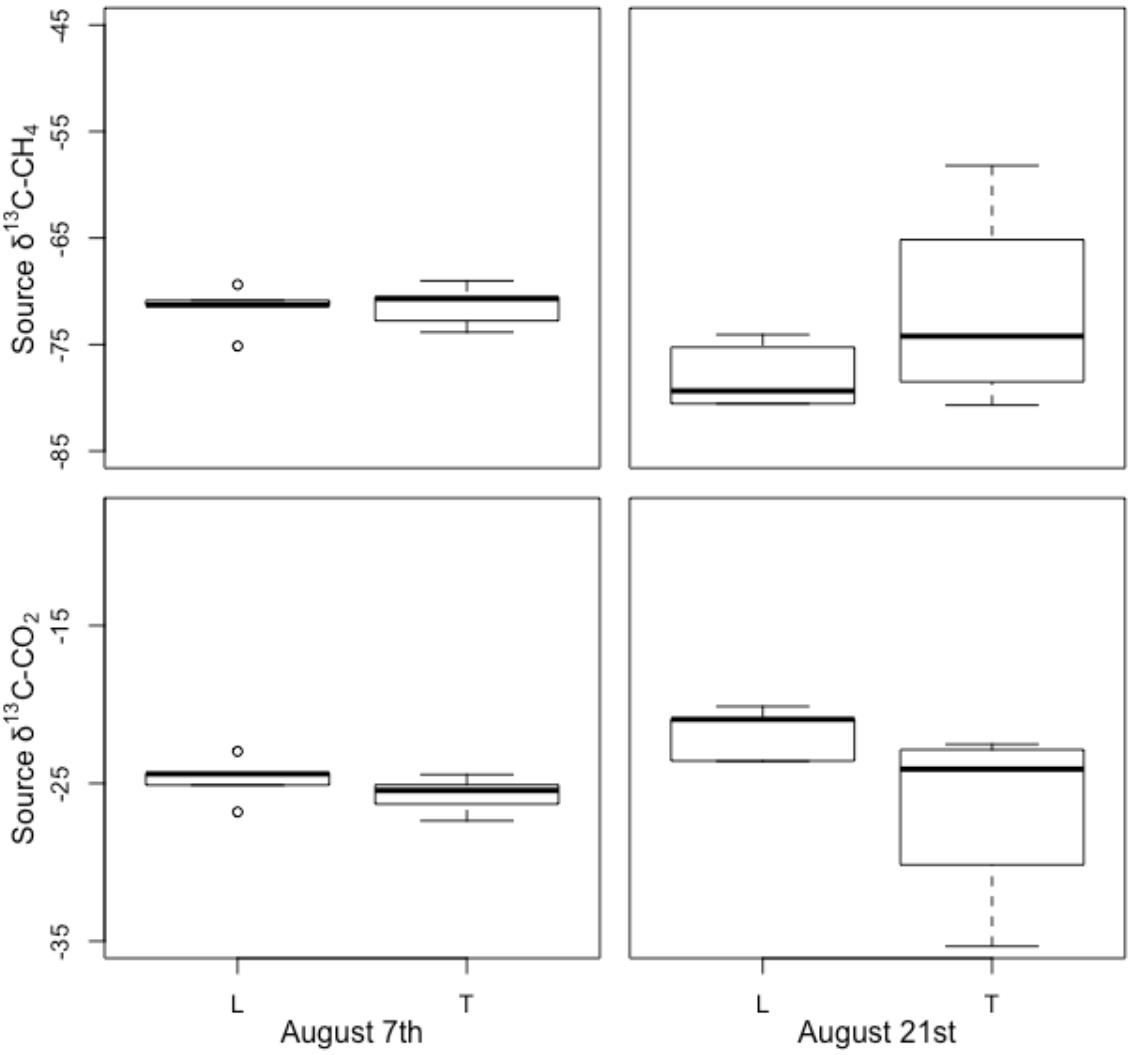

Figure 19. Source isotopic signatures for CH_4 and CO_2 for lawn and tussock plots during the 2014 growing season.

5 Chapter: Discussion

The results of this study highlight the importance of biotic and abiotic drivers of F_{CH4}, with the importance of different factors varying at several different spatial and temporal scales. This scale-dependence reveals the relative importance of CH_4 production, transportation and consumption processes on the rate of CH_4 released from the Arctic wet sedge meadow at Daring Lake. An understanding of scale-dependent emergent processes is important when predicting future rates of F_{CH4}. Similarly, the effect of measurement technique on F_{CH4} assessment is important to consider when monitoring the response of F_{CH4} to climate and landscape change and can help inform future studies on potential biases in sampling and research design.

5.1 Comparison to other wetland and Arctic sites

Daily mean and median chamber F_{CH4} from the Daring Lake fen for all years, and when weighted by surface area (111.6 ± 2.2 mg CH_4 m^{-2} day^{-1} and 97.6 mg CH_4 m^{-2} day^{-1}, respectively) and when arithmetically combined (118.5 ± 2.8 mg CH_4 m^{-2} day^{-1} and 108.0 mg CH_4 m^{-2} day^{-1}, respectively) were comparable to values from a meta-analysis of wetland F_{CH4} emissions around the world with mean and median fluxes ranging from 45 to 96 and 6 to 51 mg CH_4 m^{-2} day^{-1}, respectively where the largest mean and median values (112.2 ± 6.2 mg CH_4 m^{-2} day^{-1} and 68.4 mg CH_4 m^{-2} day^{-1}, respectively) were from nine wetland sites across Alaska and northern Europe (Turetsky *et al.* 2014). Weighted chamber F_{CH4} were comparable to those across four sites in the Alaskan Arctic coastal plain near Barrow and Ivotuk (McEwing *et al.*, 2015) but larger than multiple wetland sites, including an Alaskan wet meadow on the north slope of the Brooks

mountain range (Schimel, 1995) and both EC (Friborg *et al.,* 2000) and chamber (Strom *et al.,* 2015) values from fen sites in NE Greenland near the Zackenberg research station. The growing season at Daring Lake is longer and warmer than many of these sites but as noted by Turetsky *et al.* (2014), more southerly locations did not always have greater chamber F_{CH4} than these Arctic and subarctic sites.

Although mean summer (July & August) EC F_{CH4} were roughly 50% of the chamber F_{CH4} at Daring Lake, they were similar to those from a fen in NE Greenland (Friborg et al., 2000) and a subarctic fen in Churchill, Manitoba (Hanis *et al.*, 2013). EC F_{CH4} were much higher than a sedge/grass moss meadow wetland at Lake Hazen (Emmerton *et al.,* 2014) and an Alaskan wet sedge tundra site (Euskirchen *et al.*, 2017). Compared to non-Arctic sites, the Daring Lake EC F_{CH4} were slightly lower than a boreal rich treed fen in Northern Alberta (Long *et al.*, 2010), and a temperate restored wetland (Knox *et al.*, 2015) but larger than those from a boreal Finnish fen (Rinne *et al.*, 2007) and a temperate ombrotrophic bog (Brown *et al.*, 2014). As with the chamber F_{CH4}, EC F_{CH4} was highly variable among sites and more southerly locations did not always appear to have larger F_{CH4}.

5.2 Environmental variables influencing spatial and temporal F_{CH4} variability

Spatial and temporal F_{CH4} variability derived from both chamber and EC measurements was largely driven by moisture and/or temperature-related variables and microform classifications (Table 8). Moisture-related variables (WT, VWC) were important as drivers of chamber F_{CH4} variability across different microforms, between multiple lawn and collapse scar plots, and over multiple seasons. Highest values of WT/VWC coincided with the largest yearly mean chamber F_{CH4}. The importance of

VWC and WT has been identified by many other studies (Christensen *et al.,* 2000; McEwing *et al.*, 2015; Moore *et al.*, 2011; Moore & Knowles 1989; Olefeldt *et al.*, 2012; Strom & Christensen 2007; Torn & Chapin 1993; Waddington *et al.*, 1996), where saturated soils reduce rates of methanotrophy and high WT levels increase the depth of the anaerobic zone which may increase CH_4 production rates by increasing substrate availability and/or by promoting reducing conditions that favour methanogenesis (Kettunen *et al.*, 1999; Seybold *et al.*, 2002). F_{CH4} and dissolved CH_4 concentrations were correlated at 30 and 40-cm depths which suggests that rates of methanogenesis are important in determining resulting F_{CH4}.

The importance of microform on F_{CH4} variability was in part a result of differences in WT/VWC among microforms. Methanotrophy was likely higher at tussock plots, based on negative correlations between $\delta^{13}C_{CH4}$ and $\delta^{13}C_{CO2}$. The enrichment of $\delta^{13}C_{CH4}$ and simultaneous depletion in $\delta^{13}C_{CO2}$ is characteristic of methanotrophy, where methanotrophs preferentially use lighter ^{12}C molecules and leave behind the heavier ^{13}C (Whiticar, 1999). Using the ^{13}C depleted CH_4 as their substrate, CO_2 produced by methanotroph respiration also has a depleted $^{13}C_{CO2}$ signature relative to that of aerobic SOM decomposition. Although the isotopic signatures were only roughly derived using a two-point Keeling approach, $\delta^{13}C_{CH4}$ values of -76.5 $\pm$ 1.9 ‰ and -71.6 $\pm$ 2.0 ‰ for lawns and tussocks, respectively, were within the range observed using chambers in the Fennoscandian Arctic and close to the coherent signature of -71 ‰ observed above these wetlands (Fisher *et al.*, 2017). Carbonate reduction tends to become more important with decreasing availability of fresh OM, with increasing depth in the peat profile (Chasar *et al.*, 2000; Hornibrook *et al.*, 1997; Nakagawa *et al.*, 2002),

and has been linked to latitude, vegetation and pH (Holmes *et al.*, 2015). The dominance of carbonate reduction over acetate fermentation at the Daring Lake meadow is expected given the low pH at this site.

In the current study, neither WT nor VWC consistently explained variation in F_{CH4} across all temporal and spatial scales. VWC was an important driver when considering spatial variability of the entire wetland (e.g. among microforms), where there was a large range in VWC (coefficient of variation=27%) compared to that of soil temperature (coefficient of variation=16%), demonstrating the idea that variables with large ranges may have greater explanatory power (Moore *et al.*, 2011). At a temperate Canadian bog (Mer Bleue), Moore *et al.* (2011) consistently found an increase in average F_{CH4} with increasing WT among a) plots and b) among years (peat temperature was the best predictor of F_{CH4} among months) after averaging all plot F_{CH4}. The proportion of variation in temporal F_{CH4} to WT was relatively small in contrast. At Daring Lake, years when VWC or WT values were generally high throughout an entire growing season (e.g. 2013) and temperatures were relatively low, seasonal variations in F_{CH4} could be more sensitive to temperature-related variables. However, among years, higher WT levels were associated with larger F_{CH4} during the 2010, 2013, 2016, and 2017 chamber measurement periods. During these periods, WT was generally within 5 cm of the surface. The exceptions included 2008 when high WT occurred at the end of the summer when air was rapidly cooling. Also, in 2016, large F_{CH4} were observed as the WT dropped and temperatures rose steeply. Similar trends have been reported in several wetland C budget studies as 'episodic' fluxes (Bellisario *et al.*, 1990; Strack *et al.*, 2004; Treat *et al.*, 2007). The decrease in WT affects local pressure gradients such that CH_4 is released faster than

it can be consumed by methanotrophs in the overlying oxic peat layers (Windsor *et al.*, 1992). Decreasing WT is also often related to increases in soil and air temperature, enhancing bacterial production and consumption processes. An inverse relationship between EC F_{CH4} and WT and a positive relationship between EC F_{CH4} and temperature was observed during periods of both the 2015 and 2017 growing seasons (Figure 14). This was observed by Brown *et al.* (2014) and Goodrich *et al.* (2015) and described in terms of several potential mechanisms such as degassing, enhanced diffusivity and increased production rates as noted above. These studies also noted a lack of 'recovery' of F_{CH4} once WT increased after drawdown due to reduced methanogenesis as a result of a replenishment of alternate electron acceptors and/or reduced substrate availability after longer periods of aerobic decomposition. Moore *et al.* (2011) found that WT drawdown in the late summer had the most profound effect on inter-annual F_{CH4} as the largest emissions could occur at that time when peat was warmest. At Daring Lake, as at a northern Manitoba wetland (Bubier *et al.*, 2005), WT over the whole growing season had a strong effect on F_{CH4} and particularly during mid-summer rather than late summer. It is possible that the shorter growing seasons and typically cold weather during late summer at these more northerly peatlands may help explain the smaller importance of late summer (ie. August) WT. The relationship between F_{CH4} and WT and VWC is therefore dissimilar between spatial and temporal scales in part due to the various mechanisms involving F_{CH4} production, transport and consumption that are important across space and time.

Table 8. The importance of several abiotic and biotic variables in driving variation in chamber (plot-scale) and EC (ecosystem) F_{CH4}, represented by the occurrence of significant coefficients in linear mixed effect and regression models and interpretation of CART and PCA analyses.

Variable	Plot-scale	Ecosystem
Moisture-related	Spatial variation (among and within microforms)	Seasonal variation*
	Seasonal variation, Inter-annual variation**	
Temperature-related	Spatial variation (among and within microforms)	Diel variation, Seasonal variation
	Seasonal variation	Inter-annual EC F_{CH4}**
Vegetation-related	Spatial variation***	
Microform	Spatial variation	Spatial variation
Year	Seasonal variation****	

* inverse relationship with WT **Associations between the variable and the magnitude of yearly mean F_{CH4} ***Among lawn plots only ****Year:microform interaction drives variability chamber F_{CH4} (2008-2017)

Temperature-related variables (air temperature, 2, 5, 10 and 20-cm soil temperatures and TD) were important in models describing chamber F_{CH4} among and within different microforms and over multiple seasons. Temperature was an important driver for over EC-derived F_{CH4} at the diel scale, over multiple seasons and within seasons where increases in summer mean air and soil temperatures corresponded to increasingly large mean summer F_{CH4}. The temperature dependence of CH_4 production is well known through effects on microbial activity and on substrate production (through vegetation production), and even on dissolved CH_4 solubility. Although methanotrophy is also a temperature dependent process, this is likely not as important at this site as soil temperature and F_{CH4} were consistently positively correlated. Although temperature-related variables helped explain overall chamber F_{CH4} variability, its impact was more important temporally than spatially. For example, higher F_{CH4} from lawn compared to tussock plots was likely unrelated to increased CH_4 production with temperature as soil temperatures were significantly less at lawn plots. Similarly, negligible emissions from the palsa plots was more readily attributed to unsaturated soils rather than shallower thaw.

Using EC methods, we observed significant diel variation in F_{CH4}, where daytime F_{CH4} were associated net radiation and variables driven by radiation such as air temperature, friction velocity and soil temperature. In accordance to conclusions drawn by Moore et al. (2011), where the nature of the relationship between CH_4 and explanatory variables is related to the range of observations, diel variations are linked to radiation, the variable with the greatest possible range given the diel scale. Nighttime F_{CH4} were on

average 54% lower than daytime F_{CH4}. Diel variation in F_{CH4} is reported in several northern (Hanis *et al.*, 2013; Long *et al.*, 2010; Mikkelä *et al.*, 1995) and Arctic wetlands (Nakano *et al.* 2000), and is usually associated with temperature (Hanis *et al.*, 2013; Hendriks *et al.*, 2007; Long *et al.*, 2010), friction velocity (Kim *et al.*, 1998) or solar radiation (Kim & Verma, 1998; Kim *et al.*, 1998; Long *et al.*, 2010; Whiting & Chanton, 1996). EC measurements are only possible due to turbulent gas transfer, where lack thereof causes small or negligible F_{CH4} to be observed. This is unlikely the sole mechanism driving diel variation as the trend persisted when data points were filtered based on low u_* values. A possible mechanism driving diel variation in EC F_{CH4} is the plant mediated transport of CH_4 driven by convective flow. Soil/air temperature and solar radiation enhance the temperature and humidity gradients responsible for convective flow. Plant-mediated transport, as a mechanism likely contributing to F_{CH4} variability between multiple lawn plots, could be contributing to F_{CH4} over time through diel changes in convective flow and has been suggested for other studies (Kim *et al.*, 1998; Whiting & Chanton, 1996). The lack of comparable diel variation in chamber F_{CH4} is likely due to differences in methodology, as the chamber technique used in this study effectively eliminates turbulent air flow. The changes in microclimate created by the enclosing chamber can also affect temperature gradients related to plant-mediated convective flow. In an alpine wetland in the Tibetan Plateau, diel variations in F_{CH4} also differed based on the measurement technique (Yu *et al.* 2013). Diel variation existed for both chamber and EC values, but Yu *et al.* (2013) suggested that inhibition of plant-

mediated transport due to 'chamber effects', where turbulence and gradient-driven transport are diminished was responsible for differences in F_{CH4} patterns.

Vegetation characteristics, specifically the presence of vascular plants, can influence wetland F_{CH4} through increased organic substrate supply and increased transport through aerenchymatous tissues. At Daring Lake, the percent cover of sedges explained significant variation in F_{CH4} among lawn plots only. However, comparison of $SUVA_{254}$ between lawn and tussock plots indicate SOM quality differences (more readily decomposable organic matter at lawn plots) that could be in part a function of vegetation production and play a role in driving larger F_{CH4} from lawns. Relationships between vascular plant cover and F_{CH4} has been shown in many Arctic wetlands (Joabsson *et al.*, 1999; McEwing *et al.,* 2015; Schimel, 1995; Ström *et al.*, 2003). Contrary to the current study, CH_4 emissions from Alaskan wet sedge meadows were less dependent on vascular plant cover at wet sites compared to dry sites, and dry sites with substantial vascular plant cover had comparable F_{CH4} to wet sites (McEwing *et al.*, 2015). McEwing *et al.* (2015) defined their wet sites as those with WT levels at or above the surface during the measurement period. Lawn plots in the current study are likely more dependent on vascular plant transport of F_{CH4} due to WT levels that are consistently lower than 5 cm from the peat surface. Although this mechanism was only investigated in 2017, it likely introduces temporal F_{CH4} variability across the whole period (2008-2017) as it interacts with microform WT and soil moisture.

5.3 Microform as an integrated set of explanatory environmental variables

Microform emerged as an important driver of spatial variability of F_{CH4} at both the plot and ecosystem level as these pre-determined classifications have characteristic

differences in soil temperature, moisture, nutrient availability, plant composition and productivity and OM decomposition (Bubier *et al.*, 1993) which can be linked to small but important differences in elevation either driven by frost heave (palsas), ice lens degradation (collapse scars), or vegetation habit (tussocks). Such differences in climatic and ecological properties influence F_{CH4} through CH_4 productivity, transport and/or consumption. The emergence of microform as a variable driving F_{CH4} over space suggests that these plot classifications can characterize more F_{CH4} variability than multiple environmental variables combined. Microform has been linked to spatial variability in F_{CH4} in Canadian boreal peatlands (Bubier *et al.*, 1993), Alaskan wet sedge meadows (Whalen & Reeburgh, 1992) and Minnesota peatlands (Crill *et al.*, 1988), and is important for determining how peatland CH_4 cycling will respond to future climatic changes (Strack & Waddington, 2007). For example, F_{CH4} differ based on varying responses of microform to changes in WT, vegetation composition and air/soil temperature (Strack & Waddington, 2007), controlling the response of the wetland as a whole to climatic change. Following this idea, changes in percent cover of sedges will likely affect future F_{CH4} from the Daring Lake meadow due to the high spatial coverage of lawns.

EC F_{CH4} differed slightly based on upwind source area and the proportion of fen characterized by lawns tussocks and/or ponds or palsas. Despite negligible emissions/small uptake from plot-level palsas, upwind areas with palsas had similar EC CH_4 emissions than to areas dominated by lawns and tussocks and greater emissions than the areas with lawn and tussocks and pond areas. The similarity in F_{CH4} with direction, despite large microform F_{CH4} differences observed using chambers, may be due to the

contributions from further upwind. The flux footprint represented 70% of the flux source area such that an additional 30% of the flux may have included more upland terrain where F_{CH4} are negligible or even reflect small rates of CH_4 uptake (Hayne, 2009). Fluxes from areas with open water surfaces have been investigated by Spott (2003), where during calm conditions the water bodies emitted 2-10 mg CH_4 m^{-2} d^{-1} compared to 89 mg CH_4 m^{-2} day^{-1} from vegetated surfaces, where differences are largely related to available substrates for methanogenic activity. However, emissions from subarctic wetland ponds may also be much greater (1830 mg CH_4 m^{-2} day^{-1}; Laurion *et al.* 2010). In the current study, fluxes from ponds were not measured but are likely small in comparison to peatlands dating from pre-Holocene periods (Jones & Yu, 2010), where long term C accumulation results in larger reservoirs of stored CH_4.

In addition to distinct VWC, WT and vegetation differences, below-ground indices provided further explanation for microform-driven F_{CH4} variability. As previously stated, differences between lawn and tussock plots were related to SOM quality and rates of methanotrophy. With similar VWC, WT and vegetation characteristics, differences between collapse scar and lawn plots were greatest in their SOM quality, where collapse scars had much higher $SUVA_{254}$ values. The collapse scar plot also had lower dissolved CH_4 than any other plot throughout the 2017 growing season at 5, 15 and 30 cm depths. SOM quality differences at collapse scars could be due to their mechanism of formation, as subsided areas from former peat mounds with segregated layers of ice and mineral soil. Bubier *et al.* (1995) observed large and variable F_{CH4} from collapse scar sites, ranging from 19-108 mg CH_4 m^{-2} d^{-1} and higher than fen sites dominated by hummocks and hollows. Bubier *et al.* (1995) also point out that increased air temperatures and

subsequent peat plateau or palsa degradation can lead to increased F_{CH4} in discontinuous permafrost zones. Although the Daring Lake meadow is underlain by continuous permafrost, and collapse scar F_{CH4} were not as large, the dynamics of palsa degradation will likely play a role in long-term CH_4 cycling at the meadow.

Inter-annual variability of chamber F_{CH4} was large and dominated by changes in lawn and tussock F_{CH4} related to WT and VWC. As variability among years was highest for tussock plots, it is likely that rates of methanotrophy as affected by WT position was largely responsible for inter-annual variability in chamber F_{CH4}. Variability in EC F_{CH4} was comparatively small, although the measurement period represented fewer growing seasons. Mean EC F_{CH4} increased with increasing mean air and soil temperatures, suggesting that CH_4 productivity is driving inter-annual variation in EC F_{CH4}. This mechanism does not emerge for chamber F_{CH4} as both spatial and temporal components of variation are integrated over the multi-year period (2008-2017). This is shown by the significant interaction between year and microform driving variability in chamber F_{CH4} over all growing seasons.

5.4 Differences between and limitations of plot and ecosystem-scale F_{CH4} measurement methods

The results of this study indicate a substantial difference between F_{CH4} measured by EC and manual chamber methods. Weighting chamber F_{CH4} by area type did not greatly improve the comparison. Chamber fluxes also had much greater variability over space and time relative to those measured using EC, which is expected due to the spatial heterogeneity that is sampled using plot measurements. Relationships between F_{CH4} and climatic and abiotic variables differed based on methodology although seasonal variation

in both EC and chamber F_{CH4} was driven by a moisture and/or temperature-related variable, depending on the range and rate of change of both variables given the growing season. Differences between the two techniques are also partially due to the temporal representativeness of the half-hourly EC values compared to chamber measurements that are performed 1-2 times per week. Although Yu *et al.* (2013) showed no significant differences between F_{CH4} measured by either EC, manual or closed chamber techniques with similar seasonal variation in F_{CH4}, Sachs *et al.* (2010) found different seasonal variation, peak F_{CH4} and F_{CH4} controls using simultaneous EC and closed chamber techniques in Siberian Arctic tundra. EC F_{CH4} showed no clear seasonal variation while chamber F_{CH4} decreased towards the end of the growing season. Controls of EC F_{CH4} included near-surface turbulence, low atmospheric pressure and precipitation while chamber F_{CH4} were related to air temperature. At a high Arctic wetland meadow at Lake Hazen (Emmerton *et al.*, 2014), both F_{CH4} magnitudes and seasonal dynamics differed between EC and chamber measurements. The authors in that study suggested the differences were due to the EC measurements representing a much wetter surface compared to chambers which were situated at drier margins of the wetland.

Large uncertainties are introduced when up/down scaling F_{CH4} between plot and ecosystem levels. This is further aggravated by the difficulty in characterizing episodic flux (e.g. ebullition), which is an important method of CH_4 transport (Windsor *et al.*, 1992) but is not typically captured by chamber measurements. Ebullition measurements, the quantification of CH_4-containing bubbles from porewater and within the peat profile, were not performed as part of this study.

Another limitation of this study relates to the measurement methods. The EC

method requires steady-state atmospheric conditions, homogeneous surface characteristics and flat terrain for accurate measurements that allow for the comparison of turbulent exchange of an entity to biological consumption/production rates (Baldocchi, 2003). The underestimation of nighttime flux was addressed by filtering data with friction velocities less than 0.1 m s^{-1}, but anomalies related to the heterogeneous wetland surface and surrounding upland terrain remain an issue. Limitations of the chamber method include repeated measurements and soil/peat disturbances that may cause an over-estimation of fluxes which may help explain differences between EC and chamber values. Chamber measurements also represent a distinct moment in time throughout the daytime only. However, the lack of temporal variation in chamber F_{CH4} over a 24-hour period suggested that these discreet measurements could approximate daily average values. When comparing F_{CH4} between chamber and EC-derived values, challenges arose when representing the EC footprint with plot measurements. Much of the area of the footprint was not measured using the chamber technique and provides a potential explanation for the inconsistencies between EC and chamber F_{CH4}. Although F_{CH4} values were not comparable between methods, the use of both EC and chamber methods allowed for the identification of many important mechanisms driving F_{CH4} over both time and space.

Finally, the current study focused on growing season fluxes only. Although F_{CH4} is expected to be low throughout winter, there may be CH_4 bursts associated with active layer thaw and freeze in the spring and fall, respectively that are important to year-round estimates of CH_4 emissions (Mastepanov *et al.*, 2008; Pirk *et al.*, 2015).

6 Chapter: Conclusion

There was large F_{CH4} variability over time and space at the Daring Lake Arctic wet sedge meadow over the growing seasons of 2008 to 2017 attributed to differences in microform, VWC, WT, temperature, vegetation composition, radiation and year. Seasonal averages varied between 118-277 mg CH_4 m^{-2} d^{-1} and 40-52 mg CH_4 m^{-2} d^{-1} for chamber and EC values, respectively. Relationships between EC and chamber F_{CH4} and climatic and abiotic variables included some similar drivers over time and space. Both EC and chamber F_{CH4} variability was driven by microform over space, which could be linked to differences in vegetation (ie. presence of sedges) and moisture status. Over time, both EC and chamber F_{CH4} variability was driven by moisture and/or temperature-related variables. Chamber F_{CH4} variability was linked to variations in SOM quality and percent cover of sedges, through varying rates of methanotrophy, CH_4 production and plant-mediated transport, respectively.

The importance of moisture and/or temperature related variables in driving F_{CH4} variability was dependent on the range and rate of change of each variable given the scale, where varying rates of change can introduce confounding effects of multiple competing mechanisms. Variables with large ranges of values (VWC over space, radiation over 24 hours) explained larger proportions of variability in F_{CH4} than others. Inter-annual variability in F_{CH4} was related to VWC/WT and soil temperature for chamber and EC methods, respectively. Both moisture and temperature-related variables are important for driving F_{CH4} over large time scales, yet significant relationships vary based on methodology and the spatial and temporal representativeness of the method. The combination of chamber and EC methods allowed for an investigation of a variety of

mechanisms acting over time and space that would be difficult to assess with either method alone. Although chamber and EC measurements are integrating different sized areas, it is unclear if comparing these values is a true comparison of scale. Changes to the sampling design would improve the spatial representativeness of chamber measurements, potentially helping to identify if the discrepancies between chamber and EC F_{CH4} are related to scale or the method itself.

Temporal dynamics in microform across the wetland will likely play a role in long-term C cycling and CH_4 emissions, where larger F_{CH4} can be expected from continued palsa degradation at the Daring Lake wet sedge meadow once collapse scars develop into lawns. When predicting future F_{CH4} from Arctic wetlands, we can generally expect higher F_{CH4} with warmer and wetter conditions. Predictions of future F_{CH4} require accurate representation and integration of multiple, sometimes competing, processes that contribute to the spatial and temporal variability of wetland CH_4 emissions.

Appendices

Appendix A

Table A-1. Yearly mean Tussock F_{CH4}, volumetric water content (VWC) and peat temperature (2 cm depth) with corresponding standard error. Median F_{CH4} values are noted before mean values.

Year	**F_{CH4}** (nmol m^2 s^{-1})	**VWC** (%)	**T_{2cm}** (°C)
2008	38.5, 39.4 ± 2.5	63.3 ± 2.3	14.7 ± 0.6
2009	52.0, 46.0 ± 3.1	41.4 ± 1.8	14.1 ± 0.4
2010	161.0, 158.6 ± 11.2	85.9 ± 2.4	18.4 ± 1.0
2012	33.5, 42.6 ± 4.7	39.6 ± 2.9	19.1 ± 0.7
2013	107.2, 122.6 ± 10.5	85.3 ± 0.7	14.6 ± 0.9
2014	85.0, 85.1 ± 8.0	84.6 ± 0.9	15.5 ± 0.8
2015	75.3, 82.1 ± 7.3	84.8 ± 0.9	12.3 ± 0.5
2016	114.6, 132.1 ± 13.5	81.4 ± 0.7	12.6 ± 0.6
2017	119.2, 109.7 ± 6.1	55.2 ± 1.0	13.2 ± 0.4

Table A-2. Yearly mean lawn F_{CH4}, volumetric water content (VWC) and peat temperature (2 cm depth) with corresponding standard error. Median F_{CH4} values are noted before mean values.

Year	**F_{CH4}** (nmol m^2 s^{-1})	**VWC** (%)	**T_{2cm}** (°C)
2008	104.0, 104.3 ± 4.2	89.5 ± 1.3	14.7 ± 0.6
2009	83.6, 91.9 ± 4.6	88.6 ± 0.8	13.1 ± 0.4
2010	202.3, 199.3 ± 11.3	91.5 ± 1.3	18.3 ± 1.0
2012	82.1, 85.6 ± 5.8	75.9 ± 2.1	17.7 ± 0.5
2013	142.5, 152.0 ± 8.3	87.5 ± 0.5	13.3 ± 0.7
2014	97.6, 104.7 ± 6.0	86.9 ± 0.4	14.1 ± 0.6
2015	102.2, 103.0 ± 6.2	87.1 ± 0.5	11.8 ± 0.4
2016	120.8, 152.6 ± 21.0	81.6 ± 0.9	11.0 ± 0.4
2017	140.6, 142.8 ± 6.6	71.1 ± 1.5	12.5± 0.4

Table A-3. Yearly mean collapse scar F_{CH4}, volumetric water content (VWC) and peat temperature (2 cm depth) with corresponding standard error. Median F_{CH4} values are noted before mean values.

Year	**F_{CH4}** (nmol m^2 s^{-1})	**VWC** (%)	**T_{2cm}** (°C)
2009	2.8, 2.8 ± 0.8	73.2 ± 2.3	13.9 ± 0.5
2010	3.4, 3.3 ± 0.3	81.3 ± 1.1	19.6 ± 0.8
2015	11.9, 12.9 ± 4.8	62.3 ± 4.9	17.0 ± 1.1
2016	28.2, 29.1 ± 9.8	62.9 ± 4.2	15.2 ± 1.2
2017	17.2, 18.6 ± 6.0	63.5 ± 3.5	17.4 ± 0.8

Table A-4. Yearly mean palsa F_{CH4}, volumetric water content (VWC) and peat temperature (2 cm depth) with corresponding standard error. Median F_{CH4} values are noted before mean values.

Year	**F_{CH4}** (nmol m^2 s^{-1})	**VWC** (%)	**T_{2cm}** (°C)
2009	0.1, 0.8 ± 0.4	31.2 ± 1.4	13.5 ± 0.4
2010	0.2, 3.3 ± 0.3	27.7 ± 1.1	18.9 ± 1.1
2015	-0.3, -0.4 ± 0.2	32.4 ± 2.2	20.5 ± 1.5
2016	-1.2, -1.3 ± 0.3	37.8 ± 3.4	20.1 ± 1.3
2017	-0.3, 0.6 ± 0.6	32.7 ± 3.8	20.0 ± 1.0

Table A-5. July and August mean EC F_{CH4}, net radiation, WT, air and peat temperature (20-cm depth) with corresponding standard deviation for 2015-2017 growing seasons. Median F_{CH4} values are noted before mean values.

Year	F_{CH4} (nmol m^2 s^{-1})	T_{air} (°C)	T_{20cm} (°C)	Q*	WT (cm)
2015	28.4, 33.4 ± 2.4x10^{-2}	12.6 ± 7.1	7.1 ± 4.5	125 ± 177	-12.1 ± 6.0
2016	37.7, 39.1 ± 2.1x10^{-2}	13.9 ± 7.0	7.5 ± 3.6	154 ± 177	-15.9 ± 7.8
2017	37.6, 42.0 ± 2.6x10^{-2}	15.2 ± 6.9	7.6 ± 4.0	138 ± 174	-12.3 ± 4.5

Table A-6. Linear mixed model results testing for differences in porewater samples between microform, depth and time where plot was treated as a random effect.

Variable	Fixed effects	DF	t-value	p
TN	microform	6	1.9	>0.05
	depth	6	-1.7	>0.05
	date	5	-0.7	>0.05
	microform:date	5	2.2	>0.05
	microform:depth	5	-1.9	>0.05
	depth:date	5	1.7	>0.05
$[CH_4]$	microform	6	0.8	>0.05
	depth	6	-0.6	>0.05
	date	5	-0.2	>0.05
	microform:date	5	2.3	>0.05
	microform:depth	5	-0.8	>0.05
	depth:date	5	0.6	>0.05
DOC	microform	6	-0.4	>0.05
	depth	6	-0.1	>0.05
	date	5	-0.5	>0.05
	microform:date	5	1.6	>0.05
	microform:depth	5	0.4	>0.05
	depth:date	5	0.1	>0.05
$SUVA_{254}$	microform	6	0.6	>0.05
	depth	6	-1.1	>0.05
	date	5	-1.4	>0.05
	microform:date	5	-8.7	**<0.001**
	microform:depth	5	-0.6	>0.05
	depth:date	5	1.1	>0.05
$\delta^{13}C_{CH4}$	microform	6	-0.1	>0.05
	depth	6	0.2	>0.05
	date	5	-0.1	>0.05
	microform:date	5	-1.3	>0.05
	microform:depth	5	0.1	>0.05
	depth:date	5	-0.2	>0.05
$\delta^{13}C_{CO2}$	microform	6	-0.9	>0.05
	depth	6	0.8	>0.05
	date	5	-0.2	>0.05
	microform:date	5	1.7	>0.05
	microform:depth	5	0.9	>0.05
	depth:date	5	-0.8	>0.05

References

Ackerman D, D Griffin, SE Hobbie and JC Finlay. (2017). Arctic shrub growth trajectories differ across soil moisture levels. *Global change biology* 23(10): 4294-302.

Alm J, L Schulman, J Walden, H Nykanen, PJ Martikainen and J Silvola. (1999). Carbon balance of a boreal bog during a year with an exceptionally dry summer. *Ecology* 80(1): 161-174.

Alperin MJ and WS Reeburgh. (1985). Inhibition experiments on anaerobic methane oxidation. *Applied and Environmental Microbiology* 50(4): 940-5.

Amaral JA and R Knowles. (1994). Methane metabolism in a temperate swamp. *Applied and environmental microbiology* 60(11): 3945-51.

Andresen CG, MJ Lara, CE Tweedie and VL Lougheed. (2017). Rising plant-mediated methane emissions from arctic wetlands. *Global change biology* 23(3):1128-39.

Associate Committee on Geotechnical Research (A.C.G.R.-N.R.C.) 1988: Glossary of permafrost and related ground-ice terms. National Research Council of Canada, Ottawa, Permafrost Subcommittee, Technical memorandum 142, 156 pp.

Aubinet M, A Grelle, A Ibrom, Ü Rannik, J Moncrieff, T Foken, AS Kowalski, PH Martin, P Berbigier, CH Bernhofer, R Clement, J Elbers, A Granier, T Grünwald, K Morgenstern, K Pilegaard, C Rebmann, W Snijders, R Valentini, T Vesala. (2000). Estimates of the annual net carbon and water exchange of European forests: the EUROFLUX methodology. *Adv. Ecol. Res.* 30: 114–175.

Avery GB, RD Shannon, JR White, CS Martens and MJ Alperin. (2003). Controls on Methane Production in a Tidal Freshwater Estuary and a Peatland: Methane Production via Acetate Fermentation and CO_2 Reduction. *Biogeochemistry* 62(1):19-37.

Bachoon D and RD Jones. (1992). Potential rates of methanogenesis in sawgrass marshes with peat and marl soils in the Everglades. *Soil Biology and Biochemistry* 24(1):21-7.

Baldocchi DD. (2003). Assessing the eddy covariance technique for evaluating carbon dioxide exchange rates of ecosystems: past, present and future. *Global Change Biology* 9(4): 479-492.

Baldocchi DD, E Falge, L Gu *et al.* (2001b). FLUXNET: a new tool to study the temporal and spatial variability of ecosystem-scale carbon dioxide, water vapour and energy flux densities. *Bulletin of the American Meteorological Society* 82: 2415- 2434.

Batzer DP and AH Baldwin. (2012). Wetland habitats of North America: ecology and conservation concerns. University of California Press, CA.

Bellisario LM, JL Bubier, TR Moore and JP Chanton. (1999). Controls on CH_4 emissions from a northern peatland. *Global Biogeochemical cycles* 13(1): 81-91.

Becker MS, TJ Davies and WH Pollard. (2016). Ground ice melt in the high Arctic leads to greater ecological heterogeneity. *Journal of Ecology* 104(1): 114-24.

Berendse F, N Van Breemen, H Rydin, A Buttler, M Heijmans, MR Hoosbeek, JA Lee, E Mitchell, T Saarinen, H Vasander and B Wallén. (2001). Raised atmospheric CO_2 levels and increased N deposition cause shifts in plant species composition and production in Sphagnum bogs. *Global Change Biology* 7(5): 591-8.

Berteaux D, G Gauthier, F Domine, RA Ims, SF Lamoureux, E Lévesque E and N Yoccoz. (2016). Effects of changing permafrost and snow conditions on tundra wildlife: critical places and times. *Arctic Science* 3(2): 65-90.

Billings WD. (1973). Arctic and alpine vegetations: similarities, differences, and susceptibility to disturbance. *BioScience* 23(12):697-704.

Billings WD, JO Juken, DA Mortensen and KM Peterson. (1982). Arctic Tundra: A Source or Sink for Atmospheric Carbon Dioxide in a Changing Environment? *Oecologia* 53: 7-11.

Black TA, G Den Hartog, HH Neumann, PD Blanken, PC Yang, C Russell, Z Nesic, X Lee, SG Chen, R Staebler and MD Novak. (1996). Annual cycles of water vapour and carbon dioxide fluxes in and above a boreal aspen forest. *Global Change Biology* 2(3): 219-29.

Bliss LC and NV Matveyeva. (1992). Circumpolar arctic vegetation. *Arctic ecosystems in a changing climate: an ecophysiological perspective* 59-89.

Bosse U and P Frenzel. (1997). Activity and distribution of methane-oxidizing bacteria in flooded rice soil microcosms and in rice plants (Oryza sativa). *Applied and Environmental Microbiology* 63(4):1199-207.

Brown RJE. (1968). Permafrost investigation in northern Ontario and north-eastern Saskatchewan. Canada, National Research Council, Division of Building Research, Technical Paper 291.

Brown MG, ER Humphreys, TR Moore, NT Roulet and PM Lafleur. (2014). Evidence for a nonmonotonic relationship between ecosystem-scale peatland methane emissions and water table depth. *Journal of Geophysical Research: Biogeosciences* 119(5):826-35.

Bubier JL, G Bhatia, TR Moore, NT Roulet and PM Lafleur. (2003). Spatial and Temporal Variability in Growing Season Net Ecosystem Carbon Dioxide Exchange at a Large Peatland in Ontario, Canada. *Ecosystems* 6: 353-367.

Bubier J, A Costello and TR Moore. (2005). Microtopography and methane flux in boreal peatlands, northern Ontario, Canada. *Can. J. Bot.* 71: 1056 – 1063.

Bubier JL, PM Crill, TR Moore, K Savage and RK Varner. (1998). Seasonal patterns and

controls on net ecosystem CO_2 exchange in a boreal peatland complex. *Global Biogeochem. Cycles* 12: 703-714.

Bubier JL, TR Moore, L Bellisario, NT Comer and PM Crill. (1995). Ecological controls on methane emissions from a northern peatland complex in the zone of discontinuous permafrost, Manitoba, Canada. *Global Biogeochemical Cycles* 9(4): 455-70.

Bubier JL, TR Moore, NT Roulet. (1993). Methane emissions from wetlands in the mid-boreal region of northern Ontario, Canada. *Ecology* 74: 2240-2254.

Chapman WL and JE Walsh. (1993). Recent Variations of Sea Ice and Air Temperature in High Latitudes. *Bulletin American Meteorological Society* 74(1): 33-47.

Chanton JP. (2005). The effect of gas transport on the isotope signature of methane in wetlands. *Organic Geochemistry* 36(5): 753-68.

Chasar, LS, JP Chanton, PH Glaser, DI Siegel and JS Rivers (2000). Radiocarbon and stable carbon isotopic evidence for transport and transformation of dissolved organic carbon, dissolved inorganic carbon, and CH_4 in a northern Minnesota peatland. *Global Biogeochem. Cycles* 14(4): 1095–1108.

Chowdhury TR and RP Dick. (2013). Ecology of aerobic methanotrophs in controlling methane fluxes from wetlands. *Applied soil ecology* 65: 8-22.

Christensen TR, A Ekberg, L Ström, M Mastepanov, N Panikov, M Öquist, BH Svensson, H Nykänen, PJ Martikainen and H Oskarsson. (2003). Factors controlling large scale variations in methane emissions from wetlands. *Geophysical Research Letters* 30(7).

Christensen TR, T Friborg, M Sommerkorn *et al.* (2000). Trace gas exchange in a high Arctic valley 1. Variations in CO_2 and CH_4 flux between tundra vegetation types. *Global Biogeochemical Cycles* 14: 701–713.

Christensen TR, S Jonasson, TV Callaghan and M Havström. (1995). Spatial variation in high-latitude methane flux along a transect across Siberian and European tundra environments. *Journal of Geophysical Research: Atmospheres* 100(D10):21035-45.

Christensen TR, S Jonasson, A Michelsen, TV Callaghan and M Havstrom. (1998). Environmental controls on soil respiration in the Eurasian and Greenlandic Arctic. *J. Geophys. Res.* 103: 15–29.

Christensen TR, IC Prentice, J Kaplan, A Haxeltine and S Sitch. (1996). Methane flux from northern wetlands and tundra: an ecosystem source modelling approach. *Tellus B* 48(5): 652-61.Conrad R. (1999). Contribution of hydrogen to methane production and control of hydrogen concentrations in methanogenic soils and sediments. *FEMS Microbiology Ecology* 28(3): 193-202.

Crill PM, KB Bartlett, RC Harris *et al.* (1988). Methane flux from Minnesota peatlands. *Global Biogeochem. Cycles* 3: 371-384.

Danby RK and DS Hik. (2007). Variability, contingency and rapid change in recent subarctic alpine tree line dynamics. *Journal of Ecology* 95: 352-363.

Davidson EA and IA Janssens. (2006). Temperature sensitivity of soil carbon decomposition and feedbacks to climate change. *Nature* 440(7081): 165–173.

Davidson EA, KV Savage, LV Verchot and R Navarro. (2002). Minimizing artifacts and biases in chamber-based measurements of soil respiration. *Agricultural and Forest Meteorology* 113(1): 21-37.

Dise NB. (1993). Methane emission from Minnesota peatlands: spatial and seasonal variability. *Global Biogeochemical Cycles* 7: 123-142.

Dlugokencky EJ, EG Nisbet, R Fisher and D Lowry. (2011). Global atmospheric methane:

budget, changes and dangers. *Philosophical transactions. Series A, Mathematical, physical, and engineering sciences* 369: 2058–2072.

Dredge LA, DE Kerr and SA Wolfe. (1999) Surficial materials and related ground ice conditions, Slave Province, N.W.T., Canada. *Canadian Journal of Earth Science* 36: 1227–1238.

Dunfield P, R Dumont and TR Moore. (1993). Methane production and consumption in temperate and subarctic peat soils: response to temperature and pH. *Soil Biology and Biochemistry* 25(3): 321-6.

Ecosystem classification group (ECG). (2013). Ecological Regions of the Northwest Territories – Northern Arctic. Department of Environment and Natural Resources, Government of Northwest Territories, Yellowknife, NT, Canada.

Ecological Stratification Working Group. (1995). A National Ecological Framework for Canada. Agriculture and Agri-Food Canada, Research Branch, Centre for Land and Biological Resources Research and Environment Canada, State of the Environment Directorate, Ecozone Analysis Branch, Ottawa/Hull.

Elberling B, MP Tamstorf, A Michelsen, MF Arndal, C Sigsgaard, L Illeris, C Bay, BU Hansen, TR Christensen, ES Hansen and BH Jakobsen. (2008). Soil and plant community- characteristics and dynamics at Zackenberg. *Advances in ecological research* 40: 223-48.

Emmerton CA, VL St Louis, ER Humphreys, JA Gamon, JD Barker and GZ Pastorello. (2016). Net ecosystem exchange of CO_2 with rapidly changing high Arctic landscapes. *Global change biology* 22(3): 1185-1200.

Emmerton CA, VL St. Louis, I Lehnhern, ER Humphreys, E Rydz and HR Kosolofsk. (2014).

The net exchange of methane with high Arctic landscapes during the summer growing season. *Biogeosciences* 11: 3095-3106.

Euskirchen ES, MS Bret-Harte, GR Shaver, CW Edgar and VE Romanovsky. (2017). Long-term release of carbon dioxide from arctic tundra ecosystems in Alaska. *Ecosystems* 20(5): 960-974.

Fisher RE *et al.* (2017). Measurement of the ^{13}C isotopic signature of methane emissions from northern European wetlands. *Global Biogeochem. Cycles* 31: 605–623.

Fox AM, B Huntley, CR Lloyd, M Williams and R Baxter. (2008). Net ecosystem exchange over heterogeneous Arctic tundra: Scaling between chamber and eddy covariance measurements. *Global Biogeochem Cycles* 22 GB2027.

Frenzel P and J Rudolph. (1998). Methane emission from a wetland plant: the role of CH_4 oxidation in Eriophorum. *Plant and Soil* 202(1): 27-32.

Friborg T, TR Christensen, BU Hansen, C Nordstroem and H Soegaard. (2000). Trace gas exchange in a high-Arctic valley: 2. Landscape CH_4 fluxes measured and modeled using eddy correlation data. *Global Biogeochemical Cycles* 14(3): 715-23.Frolking S, J Talbot, MC Jones, CC Treat, JB Kauffman, ES Tuittila and NT Roulet. (2011). Peatlands in the Earth's 21st century climate system. *Environmental Reviews* 371-96.

Galand PE, K Yrjala and R Conrad. (2010). Stable carbon isotope fractionation during methanogenesis in three boreal peatland ecosystems. *Biogeosciences* 7: 3893–3900.

Gao X, CA Schlosser, A Sokolov, KW Anthony, Q Zhuang and D Kicklighter. (2013). Permafrost degradation and methane: low risk of biogeochemical climate-warming feedback. *Environmental Research Letters* 8: 035014.

Gilbert B and P Frenzel. (1995). Methanotrophic bacteria in the rhizosphere of rice microcosms

and their effect on porewater methane concentration and methane emission. *Biology and Fertility of Soils* 20(2): 93-100.

Glaser PH, JP Chanton, P Morin, DO Rosenberry, DI Siegel, O Ruud, LI Chasar and AS Reeves. (2004). Surface deformations as indicators of deep ebullition fluxes in a large northern peatland. *Global Biogeochemical Cycles* 18(1).

Glaser PH and JP Chanton. (2009). Methane accumulation and release from deep peat: measurements, conceptual models, and biogeochemical significance. *Carbon Cycling in Northern Peatlands* 184: 145-58.

Goulden ML, JW Munger, SM Fan, BC Daube and SC Wofsy. (1996). Measurements of carbon sequestration by long-term eddy covariance: Methods and a critical evaluation of accuracy. *Global change biology* 2(3):169-82.

Hanis KL, M Tenuta, BD Amiro and TN Papakriakou. (2013). Seasonal dynamics of methane emissions from a subarctic fen in the Hudson Bay Lowlands. *Biogeosciences* 10: 4465 – 4479.

Hanson RS and TE Hanson. (1996). Methanotrophic bacteria. *Microbiological reviews* 60(2): 439-71.

Hayne SL. (2009). Controls on Atmospheric Exchanges of Carbon Dioxide and Methane for a Variety of Arctic Tundra Types. Master of Science, Carleton University, Ottawa, Ontario, Canada.

Heijmans MM, H Klees, W De Visser, F Berendse. (2002). Effects of increased nitrogen deposition on the distribution of ^{15}N-labeled nitrogen between Sphagnum and vascular plants. *Ecosystems* 5(5):500-8.

Hendriks DM, J Van Huissteden and AJ Dolman. (2010). Multi-technique assessment of spatial

and temporal variability of methane fluxes in a peat meadow. *Agricultural and Forest Meteorology* 150(6): 757-74.

Henry GH. (1998). Environmental influences on the structure of sedge meadows in the Canadian High Arctic. *Plant Ecology* 134(1): 119-29.

Hendriks DMD, J Van Huissteden, AJ Dolman, MK Van Der Molen (2007). The full greenhouse gas balance of an abandoned peat meadow. *Biogeosciences Discussions, European Geosciences Union* 4(1): 277-316.

Herndon EM, Z Yang, J Bargar, N Janot, TZ Regier, DE Graham, SD Wullschleger, B Gu and L Liang. (2015). Geochemical drivers of organic matter decomposition in arctic tundra soils. *Biogeochemistry* 126(3): 397-414.

Holmes ME, JP Chanton, MM Tfaily and A Ogram. (2015). CO_2 and CH_4 isotope compositions and production pathways in a tropical peatland. *Global Biogeochemical Cycles* 29(1):1-18.

Horn MA, C Matthies, K Kusel, A Schramm and HL Drake. (2003). Hydrogenotrophic methanogenesis by moderately acid-tolerant methanogens of a methane-emitting acidic peat. *Appl Environ Microbiol* 69: 74–83

Hornibrook ER, FJ Longstaffe and WS Fyfe. (2000). Factors influencing stable isotope ratios in CH_4 and CO_2 within subenvironments of freshwater wetlands: implications for δ-signatures of emissions. *Isotopes in Environmental and Health Studies* 36(2): 151-76.Hornibrook ERC, WS Longstaffe and WS Fyfe. (1997). Spatial distribution of microbial methane production pathways in temperate zone wetland soils: stable carbon and hydrogen isotope evidence. *Geochimica et Cosmochimica Acta* 61: 745-753.

Houghton JT, DL Albritton, LG Meira Filho, U Cubasch, X Dai, Y Ding, DJ Griggs, B

Hewitson, I Isaksen, T Karl and M McFarland. (2001). Technical summary of working group 1. Cambridge University Press.

Høye TT, E Post, H Meltofte, NM Schmidt and MC Forchhammer. (2007). Rapid advancement of spring in the High Arctic. *Current Biology* 17(12): R449-51.

Hugelius G, J Strauss, S Zubrzycki, JW Haraden, EAG Schuur, C-L Ping, L Schirrmeister, G Grosse, GJ Michaelson, CD Koven, JA O'Donnell, B Elberling, U Mischra, P Camill, Z Yu, J Palmtag and P Kuhry. (2014). Estimated stocks of circumpolar permafrost carbon with quantified uncertainty ranges and identified data gaps. *Biogeosciences* 11: 6573–6593.

Humphreys ER and PM Lafleur. (2011). Does earlier snowmelt lead to greater CO_2 sequestration in two low Arctic tundra systems? *Geophysical Research Letters* 38: L09703.

Joabsson A and TR Christensen. (2001). Methane emissions from wetlands and their relationship with vascular plants: an Arctic example. *Glob Change Biol* 7: 919–32.

Joabsson A, TR Christensen and B Wallén. (1999). Vascular plant controls on methane emissions from northern peatforming wetlands. *Trends in Ecology & Evolution* 14(10): 385-388.

Johnson LC, GR Shower, DH Cades, E Rastetter, K NadelHogger, A Giblin, J Laundre and A Stanley. (2000). Plant Carbon-Nutrient Interactions Control CO_2 exchange in Alaskan Wet Sedge Tundra Ecosystems. *Ecology* 81(2): 453-469.

Jones MC and Z Yu. (2010). Rapid deglacial and early Holocene expansion of peatlands in Alaska. *PNAS* 107(16): 7347-7352.

Jørgensen AS, G Doré, É Voyer, Y Chataigner and L Gosselin. (2008). Assessment of the

effectiveness of two heat removal techniques for permafrost protection. *Cold Regions Science and Technology* 53(2): 179-92.

Kayranli B, M Scholz, A Mustafa and Å Hedmark. (2010). Carbon storage and fluxes within freshwater wetlands: a critical review. *Wetlands* 30(1): 111-24.

Keeling CD. (1958). The concentration and isotopic abundances of atmospheric carbon dioxide in rural areas. *Geochim Cosmochim Acta* 13: 322–334.

Keeling CD. (1961). The concentration and isotopic abundance of carbon dioxide in rural and marine air. *Geochim. Cosmochim. Acta* 24: 277–298.

Kettunen A, V Kaitala, A Lehtinen, A Lohila, J Alm, J Silvola and PJ Martikainen. (1999). Methane production and oxidation potentials in relation to water table fluctuations in two boreal mires. *Soil Biol. Biochem.* 31(12): 1741–1749.

Knox SH, C Sturtevant, JH Matthes, L Koteen, J Verfaillie and D Baldocchi. (2015). Agricultural peatland restoration: effects of land-use change on greenhouse gas (CO_2 and CH_4) fluxes in the Sacramento-San Joaquin Delta. *Global Change Biology* 21(2): 750-65.

Kotsyurbenko OR, KJ Chin, MV Glagolev, S Stubner, MV Simankova, AN Nozhevnikova and R Conrad. (2004). Acetoclastic and hydrogenotrophic methane production and methanogenic populations in an acidic West-Siberian peat bog. *Environmental microbiology* 6(11):1159-73.

Kim J and SB Verma. (1992). Soil surface CO_2 flux in a Minnesota peatland. *Biogeochemistry* 18: 37–51.

Kim J, SB Verma, DP Billesbach DP and RJ Clement. (1998). Diel variation in methane emission from a midlatitude prairie wetland: significance of convective throughflow in Phragmites australis. *Journal of Geophysical Research: Atmospheres* 103(D21): 28029-

39.

King JY, WS Reeburgh and SK Regli. (1998). Methane emission and transport by arctic sedges in Alaska: results of a vegetation removal experiment. *Journal of Geophysical Research: Atmospheres* 103(D22):29083-92.

Kirschke S, P Bousquet, P Ciais, M Saunois, JG Canadell, EJ Dlugokencky, P Bergamaschi, D Bergmann, DR Blake, L Bruhwiler and P Cameron-Smith. (2013). Three decades of global methane sources and sinks. *Nature geoscience* 6(10): 813.

Kljun N, P Calanca, MW Rotach and HP Schmid. (2004). A simple parameterisation for flux footprint predictions. *Boundary-Layer Meteorology* 112(3): 503-23.

Krohn J, I Lozanovska, Y Kuzyakov, S Parvin and M Dorodnikov. (2017). CH_4 and CO_2 production below two contrasting peatland micro-relief forms: An inhibitor and $\delta^{13}C$ study. *Science of The Total Environment* 586: 142-51.

Lafleur PM. (1993). Potential water balance response to climatic warming: The case of a coastal wetland ecosystem of the James Bay lowland. *Wetlands* 13(4): 270-6.

Lafleur PM and ER Humphreys. (2008). Spring warming and carbon dioxide exchange over low Arctic tundra. *Global Change Biol.* 14: 740–756.

Lafleur PM, NT Roulet and SW Admiral. (2001). Annual cycle of CO2 exchange at a bog peatland. *Journal of Geophysical Research* 106(D3): 3071-3081.

Lai DY. (2009). Methane dynamics in northern peatlands: a review. *Pedosphere* 19(4):409-21.

Lai DY, NT Roulet and TR Moore. (2014). The spatial and temporal relationships between CO2 and CH4 exchange in a temperate ombrotrophic bog. *Atmospheric Environment* 89: 249-259.

Laurion I, WF Vincent, S MacIntyre, L Retamal, C Dupont, P Francus and R Pienitz. (2010).

Variability in greenhouse gas emissions from permafrost thaw ponds. *Limnology and Oceanography* 55(1): 115-33.

Lawrence RL, A Wright. (2001). Rule-based classification systems using classification and regression tree (CART) analysis. *Photogrammetric engineering and remote* sensing 67(10):1137-42.

Le Mer J and P Roger. (2001). Production, oxidation, emission and consumption of methane by soils: a review. *European Journal of Soil Biology* 37(1): 25-50.

LI-COR Inc. (2011). LI-7700 Open path CH_4 analyzer: Instruction manual. LI-COR Biosciences, Lincoln, NE.

Limpens J, F Berendse, C Blodau, JG Canadell, C Freeman, J Holden, N Roulet, H Rydin and G Schaepman-Strub. (2008). Peatlands and the carbon cycle: from local processes to global implications-a synthesis. *Biogeosciences* 5: 1475-91.

Livingston GP and GL Hutchinson. (1995). Enclosure-based measurement of trace gas exchange: applications and sources of error. *Biogenic trace gases: measuring emissions from soil and water* 51: 14-51.

Long KD, LB Flanagan and T Cai. (2010). Diurnal and seasonal variation in methane emissions in a northern Canadian peatland measured by eddy covariance. Global change biology 16(9): 2420.

Lund CP, WJ Riley, LL Pierce LL and CB Field. (1999). The effects of chamber pressurization on soil-surface CO_2 flux and the implications for NEE measurements under elevated CO_2. *Global Change Biology* 5(3): 269-81.

Lundqvist, J. (1962). Patterned ground and related frost phenomena in Sweden. *Sver. Geol. Unders. Arsb.* 55(C): 583, 101 p.

Mach V, Blaser MB, Claus P, Chaudhary PP and Rulík M. (2015). Methane production potentials, pathways, and communities of methanogens in vertical sediment profiles of river Sitka. *Frontiers in Microbiology* 6: 506.

Mackay JR. (2000). Thermally induced movements in ice-wedge polygons, western arctic coast: a long-term study. *Géographie physique et Quaternaire* 54(1): 41-68.

Masscheleyn PH, RD DeLaune and WH Patrick Jr. (1993). Methane and nitrous oxide emissions from laboratory measurements of rice soil suspension: effect of soil oxidation-reduction status. *Chemosphere* 26(1-4): 251-60.

Massman WJ. (2000). A simple method for estimating frequency response corrections for eddy covariance systems. *Agricultural and Forest Meteorology* 104(3): 185-98.

Mastepanov M, C Sigsgaard, EJ Dlugokencky, S Houweling, L Ström, MP Tamstorf and TR Christensen. (2008). Large tundra methane burst dring onset of freezing. *Nature* 456(7222): 628.

McEwing KR, JP Fisher and D Zona. (2015). Environmental and vegetation controls on the spatial variability of CH_4 emission from wet-sedge and tussock tundra ecosystems in the Arctic. *Plant and soil* 388(1-2): 37-52.

McGuire AD, TR Christensen, D Hayes et al. (2012). An assessment of the carbon balance of Arctic tundra: Comparisons among observations, process models, and atmospheric inversions. *Biogeosciences* 9: 3185–3204.

McGuire AD, LG Anderson, TR Christensen, S Dallimore, L Guo, DJ Hayes, M Heimann, TD Lorenson, RW Macdonald and N Roulet. (2009). Sensitivity of the carbon cycle in the Arctic to climate change. *Ecol. Monogr.* 79: 523–555.

Meijide A, G Manca, I Goded, V Magliulo, PD Tommasi, G Seufert and A Cescatti. (2011).

Seasonal trends and environmental controls of methane emissions in a rice paddy field in Northern Italy. *Biogeosciences* 8(12): 3809-21.

Metje M and P Frenzel. (2005). The effect of temperature on anaerobic ethanol oxidation and methanogenesis in an acidic peat from a northern wetland. *Appl Environ Microbiol* 71: 8191–8200.

Miao Y, C Song, L Sun, X Wang, H Meng and R Mao. (2017). Growing season methane emission from a boreal peatland in the continuous permafrost zone of Northeast China: effects of active layer depth and vegetation. *Biogeosciences* 9(11): 4455-64.

Mikkelä C, I Sundh, BH Svensson and M Nilsson. (1995). Diurnal variation in methane emission in relation to the water table, soil temperature, climate and vegetation cover in a Swedish acid mire. *Biogeochemistry* 28(2): 93-114.

Moncrieff J, R Clement, J Finnigan and T Meyers. (2004). Averaging, detrending, and filtering of eddy covariance time series. In: *Handbook of micrometeorology* pp. 7-3. Springer, Dordrecht.

Moore TR, A De Young, JL Bubier, ER Humphreys, PM Lafleur and NT Roulet. (2011). A multi-year record of methane flux at the Mer Bleue bog, southern Canada. *Ecosystems* 14(4): 646.

Moore TR and R Knowles. (1989). The influence of water table levels on methane and carbon dioxide emissions from peatland soils. *Canadian Journal of Soil Science* 69(1): 33-8.

Moore TR and R Knowles. (1987). Methane and carbon dioxide evolution from subarctic fens. *Can. J. Soil Sci.* 67: 77-81.

Mosier AR. (1990). Gas flux measurement techniques with special reference to techniques suitable for measurements over large ecologically uniform areas. In: Bouwman, A.F.

(Ed.), Soils and the Greenhouse Effect. Wiley, Chichester, pp. 289–301.

Motinsky IL. (2011). Diffusion coefficient. In: Thermopedia: A-to-Z Guide to Thermodynamics, Heat and Mass Transfer, and Fluids Engineering. Thermopedia.

Murase J and M Kimura. (1994). Methane production and its fate in paddy fields: VI. Anaerobic oxidation of methane in plow layer soil. *Soil science and plant nutrition* 40(3): 505-14.

Myers-Smith IH and DS Hik. (2017). Climate warming as a driver of tundra shrubline advance. *Journal of Ecology* 106: 547-560.

Nakagawa F, N Yoshida, Y Nojiri, and VN Makarov. (2002). Production of methane from alasses in eastern Siberia: Implications from its 14C and stable isotopic compositions. *Global Biogeochem. Cycles* 16(3): 14.1-14.15.

Nakano T, S Kuniyoshi, and M Fukuda. (2000). Temporal variation in methane emission from tundra wetlands in a permafrost area, northeastern siberia. *Atmospheric Environment* 34 (8): 1205-13.

Oechel W, GL Vourlitis, SJ Hastings and SA Bochkarev. (1995). Change in Arctic CO_2 Flux Over Two Decades: Effects of Climate Change at Barrow, Alaska. *Ecological Applications* 5(3): 846-855.

Okolo I. (2008). Analysis of long term carbon accumulation in an Arctic fen. Undergraduate Thesis in Environmental Science, Carleton University, Ottawa, Ontario, Canada.

Olefeldt D, MR Turetsky, PM Crill and AD McGuire *et al.* (2013). Environmental and physical controls on northern terrestrial methane emissions across permafrost zones. *Global Change Biology* 19(2): 58.

Overpeck J, K Hughen, D Hardy, R Bradley, R Case, M Douglas, B Finney, K Gajewski, G

Jacoby, A Jennings, S Lamoureux, A Lasca, G MacDonald, J Moore, M Retelle, S Smith, A Wolfe and G Zielinski. (1997). Arctic Environmental Change of the Last Four Centuries. *Science* 278: 1251-1256.

Pachauri RK, MR Allen, VR Barros, J Broome, W Cramer, R Christ, JA Church, L Clarke, Q Dahe, P Dasgupta, NK Dubash, O Edenhofer... and JP van Ypserle. (2014): Climate Change 2014: Synthesis Report. Contribution of Working Groups I, II and III to the Fifth Assessment Report of the Intergovernmental Panel on Climate Change / R. Pachauri and L. Meyer (editors), Geneva, Switzerland, IPCC.

Page SE, JO Rieley and CJ Banks. (2011). Global and regional importance of the tropical peatland carbon pool. *Global Change Biology* 17(2): 798-818.

Pataki DE, JR Ehleringer, LB Flanagan, D Yakir, DR Bowling, CJ Still, N Buchmann, JO Kaplan and JA Berry. (2003). The application and interpretation of Keeling plots in terrestrial carbon cycle research. *Global Biogeochemical Cycles* 17(1).

Peacock M, CD Evans, N Fenner, C Freeman, R Gough, TG Jones and I Lebron. (2014). UV-visible absorbance spectroscopy as a proxy for peatland dissolved organic carbon (DOC) quantity and quality: considerations on wavelength and absorbance degradation. *Environmental Science: Processes & Impacts* 16(6): 1445-61.Pinney ML, PK Westerhoff and L Baker. (2000). Transformations in dissolved organic carbon through constructed wetlands. *Water Research* 34(6): 1897-911.

Piquette S. (2010). Quantification of Greenhouse Gas Flux and Net Ecosystem Exchange in Variable Ecosystems in the Daring Lake, NWT Area. Undergraduate Thesis in Physical Geography and Earth Science, Carleton University, Ottawa, Ontario, Canada.

Pirk N, T Santos, C Gustafson, AJ Johansson, F Tufvesson, FJ Parmentier, M Mastepanov and

TR Christensen. (2015). Methane emission bursts from permafrost environments during autumn freeze-in: New insights from ground-penetrating radar. *Geophysical Research Letters* 42(16):6732-8.

Pissart A. (2002). Palsas, lithalsas and remnants of these periglacial mounds. A progress report. *Progress in Physical Geography* 26(4): 605-21.

Post WM, WR Emanuel, PJ Zinke and AG Stangenberger. (1982). Soil carbon pools and world life zones. *Nature* 298: 156–159.

R Core Team (2016). R: A language and environment for statistical computing. R Foundation for Statistical Computing, Vienna, Austria. URL https://www.R- project.org/.

Reeburgh W and S Whalen. (1992). High-Latitude Ecosystems as CH_4 Sources. *Ecological Bulletins* 42: 62-70.

Rinne J, T Riutta, M Pihlatie, M Aurela, S Haapanala, J-P Tuovinen, E-S Tuittila and T Vesala. (2007). Annual cycle of methane emission from a boreal fen measured by the eddy covariance technique. *Tellus* 59B, 449-457.

Rosenberry DO, PH Glaser, DI Siegel and EP Weeks. (2003). Use of hydraulic head to estimate volumetric gas content and ebullition flux in northern peatlands. *Water Resources Research* 39(3).

Roulet NT, PM Lafleur, PJ Richard, TR Moore, ER Humphreys, and JL Bubier. (2007). Contemporary carbon balance and late Holocene carbon accumulation in a northern peatland. *Global Change Biology* 13(2): 397-411.

Rydin H, JK Jeglam, A Hooijer. (2006). *The biology of peatlands*. Oxford University Press.

Sachs T, M Giebels, J Boike and L Kutzbach. (2010). Environmental controls on CH4 emission from polygonal tundra on the microsite scale in the Lena river delta, Siberia. *Global*

Change Biology 16(11): 3096-110.

Sass RL, FM Fisher, PA Harcombe, FT Turner. (1990). Methane production and emission in a Texas rice field. *Global Biogeochemical Cycles* (1):47-68.

Schimel JP. (1995). Plant transport and methane production as controls on methane flux from arctic wet meadow tundra. *Biogeochemistry* 28(3):183-200.

Schleser GH. (1982). The Response of COSchrier-Uijl AP, PS Kroon, PA Leffelaar, JC Van Huissteden, F Berendse and EM Veenendaal. (2010). Methane emissions in two drained peat agro-ecosystems with high and low agricultural intensity. *Plant and soil* 329(1-2): 509-20.

Schütz H, A Holzapfel-Pschorn, R Conrad, H Rennenberg and W Seiler. (1989). A 3-year continuous record on the influence of daytime, season, and fertilizer treatment on methane emission rates from an Italian rice paddy. *Journal of Geophysical Research: Atmospheres* 94(D13): 16405-16.

Schuur EA, J Bockheim, JG Canadell, E Euskirchen, CB Field, SV Goryachkin, S Hagemann, P Kuhry, PM Lafleur, H Lee and G Mazhitova. (2008). Vulnerability of permafrost carbon to climate change: Implications for the global carbon cycle. *AIBS Bulletin* 58(8):701-14.

Segers R. (1998). Methane production and methane consumption: a review of processes underlying wetland methane fluxes. *Biogeochemistry* (1): 23-51.

Seppälä, M. (2011). Synthesis of studies of palsa formation underlining the importance of local environmental and physical characteristics. *Quaternary Res.* 75: 366–370.

Seppälä, M. 1972: Pingo-like remnants in the Peltojärvi area of Finnish Lapland. *Geografiska Annaler* 54(A): 37–45.

Serreze MC, JE Walsh, FS Chapin III, T Osterkamp, M Dyurgerov, V Romanovsky, WC Oechel, J Morison, T Zhang and RG Barry. (2000) *Climatic Change* 46: 159.

Seybold CA, W Mersie, J Huang and C McNamee. (2002). Soil redox, pH, temperature, and water-table patterns of a freshwater tidal wetland. *Wetlands* 22(1): 149–158.

Silins U and RL Rothwell. (1998). Forest peatland drainage and subsidence affect soil water retention and transport properties in an Alberta peatland. *Soil Science Society of America Journal* 62(4): 1048-1056.

Skaarup E. (2017). The impacts of shrub abundance on microclimate and decomposition in the Canadian Low Arctic.

Smemo KA and JB Yavitt. (2006). A multi-year perspective on methane cycling in a shallow peat fen in central New York State, USA. *Wetlands* 26(1): 20-29.

Smith LC, Y Sheng, GM MacDonald and LD Hinzman. (2005). Disappearing arctic lakes. *Science* 308(5727): 1429-1429.

Soegaard H and C Nordstroem (1999). Carbon dioxide exchange in a high-arctic fen estimated by eddy covariance measurements and modeling. *Global Biogeochem. Cycles* 5: 547–562.

Soegaard H, C Nordstroem, T Friborg, BU Hansen, TR Christensen and C Bay. (2000). Trace gas exchange in a high-Arctic valley: 3. Integrating and scaling CO_2 fluxes from canopy to landscape using flux data, footprint modeling, and remote sensing. *Global Biogeochemical Cycles* 14(3): 725-44.

Spott O. (2003). *Frostmusterbedingte Seen der Polygonalen Tundra und ihre Funktio als Quellen atmosparischen Methans.* Unpublished Diploma Thesis, University of Leipzig, Leipzig, Germany.

Strack M and JM Waddington. (2007). Response of peatland carbon dioxide and methane fluxes to a water table drawdown experiment. *Global Biogeochemical cycles* 21(1).

Strack M, JM Waddington, L Rochefort and ES Tuittila. (2006). Response of vegetation and net ecosystem carbon dioxide exchange at different peatland microforms following water table drawdown. Journal of Geophysical Research: *Biogeosciences* 111(G2).

Strack M, JM Waddington and ES Tuittila. (2004). Effect of water table drawdown on northern peatland methane dynamics: Implications for climate change. *Global Biogeochemical Cycles* 18(4).

Ström L and TR Christensen. (2007). Below ground carbon turnover and greenhouse gas exchanges in a sub-arctic wetland. *Soil Biology and Biochemistry* 39(7): 1689-1698.

Ström L, A Ekberg, M Mastepanov and TR Christensen. (2003). The effect of vascular plants on carbon turnover and methane emissions from a tundra wetland. *Glob. Change Biol.* 9: 1185– 92.

Ström L, JL Falk, K Skov, M Jackowicz-Korczynski, M Mastepanov, TR Christensen, M Lund and NM Schmidt. (2015). Controls of spatial and temporal variability in CH_4 flux in a high arctic fen over three years. *Biogeochemistry* 125: 21–35.

Ström L, T Tagesson, M Mastepanov, and TR Christensen. (2012). Presence of *Eriophorum scheuchzeri* enhances substrate availability and methane emission in an Arctic wetland. *Soil Biology and Biochemistry* 45: 61-70.

Sturtevant C, BL Ruddell, SH Knox, J Verfaillie, JH Matthes, PY Oikawa *et al.* (2016). Identifying scale-emergent, nonlinear, asynchronous processes of wetland methane exchange. *Journal of Geophysical Research: Biogeosciences* 121(1): 188-204.

Sturtevant CS and WC Oechel. (2013). Spatial variation in landscape-level CO_2 and CH_4 fluxes

from Arctic coastal tundra: Influence from vegetation, wetness, and the thaw lake cycle. *Global Change Biol.* 19: 2853–2866.

Sullivan PF, SJT Arens, RA Chimner and JM Welker. (2008). Temperature and Microtopography Interact to Control Carbon Cycling in a High Arctic Fen. *Ecosystems* 11: 61-76.

Tape KE, M Sturm and C Racine. (2006). The evidence for shrub expansion in northern Alaska and the Pan-Arctic. *Global Change Biology* 12(4): 686-702.

Tarnocai CJ, G Canadell, EAG Schuur, P Kuhry, G Mazhitova and S Zimov. (2009). Soil organic carbon pools in the northern circumpolar permafrost region. *Global Biogeochem. Cycles* 23: GB2023.

Tarnocai C. (1978). Genesis of organic soils in Manitoba and the Northwest Territories. In Proceedings, 3rd York University Symposium on Quaterary Research. *Geographical Abstracts* 453-470.

Tarnocai C and SC Zoltai. (1988). Wetlands of Arctic Canada. Pgs 29-53 In: Wetlands of Canada, by National Wetlands Working Group, Canada Committee on Ecological Classification. Polyscience Publications Inc., Montreal, Quebec.

Topp E and E Pattey. (1997). Soils as sources and sinks for atmospheric methane. *Canadian Journal of Soil Science* 77(2):167-77.

Torn MS and FS III Chapin. (1993). Environmental and biotic controls over methane flux from arctic tundra. *Chemosphere* (1-4): 357-68.

Treat CC, JL Bubier, RK Varner and PM Crill. (2007). Timescale dependence of environmental and plant-mediated controls on CH4 flux in a temperate fen. *J. Geophy. Res. Biogeosci.* 112: G01014.

Treat ND, JAN Malik, O Reid, L Yu, CG Shuttle, G Rumbles et al. (2013). Modelling the effects of climate change and disturbance on permafrost stability in northern organic soils. *Nature Mater* 12:1-6.

Turetsky MR, A Kotowska, J Bubier, NB Dise, P Crill, ER Hornibrook, K Minkkinen K, TR Moore, IH Myers-Smith, H Nykänen and D Olefeldt. (2014). A synthesis of methane emissions from 71 northern, temperate, and subtropical wetlands. *Global change biology* 20(7): 2183-97.

Valentine DW, EA Holland and DS Schimel. (1994). Ecosystem and physiological controls over methane production in northern wetlands. *Journal of Geophysical Research: Atmospheres* 99(D1): 1563-71.

Verville JH, SE Hobbie, FS Chapin and DU Hooper. (2008). Response of tundra CH_4 and CO_2 flux to manipulation of temperature and vegetation. *Biogeochemistry* 41(3):215-35.

Vourlitis GL and Oechel WC. (1997). The Role of Northern Ecosystems in the Global Methane Budget. In: Global Change and Arctic Terrestrial Ecosystems, Oechel WC (editor), Global Change Research Group, San Diego, CA.

Vourlitis GL, WC Oechel, SJ Hastings and MA Jenkins. (1993). The effect of soil moisture and thaw depth of CH_4 flux from wet coastal tundra ecosystems on the north slope of Alaska. *Chemosphere* 28(12): 1-4.

Waddington JM and NT Roulet. (1996). Atmosphere-wetland carbon exchanges: Scale dependency of CO2 and CH4 exchange on the developmental topography of a peatland. *Global biogeochemical Cycles* 10(2): 233-245.

Waddington JM, NT Roulet, RV Swanson. (1996). Water table control of CH_4 emission enhancement by vascular plants in boreal peatlands. *Journal of Geophysical Research:*

Atmospheres 101(D17): 22775-85.

Walter BP and Heimann M. (2000). A process-based, climate-sensitive model to derive methane emissions from natural wetlands: Application to five wetland sites, sensitivity to model parameters, and climate. *Global Biogeochemical Cycles* 14(3):745-65.

Wang ZP, RD Delaune, WH Patrick and PH Masscheleyn. (1993). Soil redox and pH effects on methane production in a flooded rice soil. *Soil Science Society of America Journal* 57(2): 382-5.

Warner BC and CDA Rubec. (1997). The Canadian wetland classification system. National Wetlands Working Group, Wetlands Research Centre, University of Waterloo, Waterloo, Ontario.

Webb EK, GI Pearman, R Leuning. (1980). Correction of flux measurements for density effects due to heat and water vapour transfer. *Quart. J. Roy. Meteorol. Soc.* 106: 85-100.

Weishaar JL, GR Aiken, BA Bergamaschi, MS Fram, R Fujii and K Mopper. (2003). Evaluation of specific ultraviolet absorbance as an indicator of the chemical composition and reactivity of dissolved organic carbon. *Environmental science & technology* 37(20): 4702-8.

Welker JM, JT Fanhnestock and MH Jones (2000). Annual CO_2 flux in dry and moist arctic tundra: Field responses to increases in summer temperatures and winter snow depth. *Clim. Change* 44: 139–150.

Whalen SC and WS Reeburgh. (1992). Interannual variations in tundra methane emission: a 4-year time series at fixed sites. *Global Biogeochemical Cycles* 6: 139 – 159.

Whiticar MJ. (1999). Carbon and hydrogen isotope systematics of bacterial formation and oxidation of methane. *Chemical Geology* 161(1-3): 291-314.

Whiticar MJ, Faber E, Schoell M. (1986). Biogenic methane formation in marine and freshwater environments: CO_2 reduction vs. acetate fermentation-isotope evidence. *Geochimica et Cosmochimica Acta* 50: 693-709.

Whiting GJ and JP Chanton. (1996). Control of the diurnal pattern of methane emission from emergent aquatic macrophytes by gas transport mechanisms. *Aquatic Botany* 54(2-3): 237-53.

Wickland KP, RG Striegl, JC Neff and T Sachs. (2006). Effects of permafrost melting on CO_2 and CH_4 exchange of a poorly drained black spruce lowland. *Journal of Geophysical Research: Biogeosciences* 111(G2).

Wieder RK. (2001). Past, Present and Future Peatland Carbon Balance: An Empirical Model Based on 210Pb-Dated Cores. Ecological Applications 11: 327–342.

Wik M, RK Varner, KW Anthony, S MacIntyre and D Bastviken. (2016). Climate-sensitive northern lakes and ponds are critical components of methane release. *Nature Geoscience* 9(2): 99.

Williams RT and RL Crawford. (1984). Methane production in Minnesota peatlands. *Applied and Environmental Microbiology* 47(6): 1266-71.

Windsor J, TR Moore and NT Roulet. (1992). Episodic fluxes of methane from subarctic fens. *Can J. Soil Sci.* 72: 441-452.

Woo MK and KL Young. (2006). High Arctic wetlands: their occurrence, hydrological characteristics and sustainability. *Journal of Hydrology* 320(3-4): 432-50.

Yu L, H Wang, G Wang, W Song, Y Huang, SG Li, N Liang, Y Tang and JS He. (2013). A comparison of methane emission measurements using eddy covariance and manual and automated chamber-based techniques in Tibetan Plateau alpine wetland. *Environmental*

pollution 181: 81-90.

Wilson JW. (1959). Analysis of the Spatial Distribution of Foliage by Two-Dimentional Point Quadrants. *The New Phytologist* 58(1): 92-99.

Wilson KS and ER Humphreys. (2010). Carbon dioxide and methane fluxes from Arctic mudboils. *Can. J. Soil Sci.* 90: 441-449.

Zhang T, RG Barry, K Knowles, JA Heginbottom and J Brown. (1999). Statistics and characteristics of permafrost and ground-ice distribution in the Northern Hemisphere. *Polar Geography* 23(2):132-54.

Zhu Q, J Liu, C Peng, H Chen, X Fang, H Jiang, G Yang, D Zhu, W Wang and X Zhou. (2014). Modelling methane emissions from natural wetlands by development and application of the TRIPLEX-GHG model. *Geoscientific Model Development* 7(3): 981-99.

Zinder SH. (1993). Physiological ecology of methanogens. In: Methanogenesis (pp. 128-206). Springer, Boston, MA.

Zona D, WC Oechel, JU Kochendorfer, U Paw, AN Salyuk, PC Olivas, SF Oberbauer and DA Lipson (2009). Methane fluxes during the initiation of a large-scale water table manipulation experiment in the Alaskan Arctic tundra. *Global Biogeochemical Cycles* 23(2).

Zuidhoff FS and E Kolstrap. Palsa Development and Associated Vegetation in Northern Sweden. *Arctic, Antarctic and Alpine Research* 37(1): 49-60.